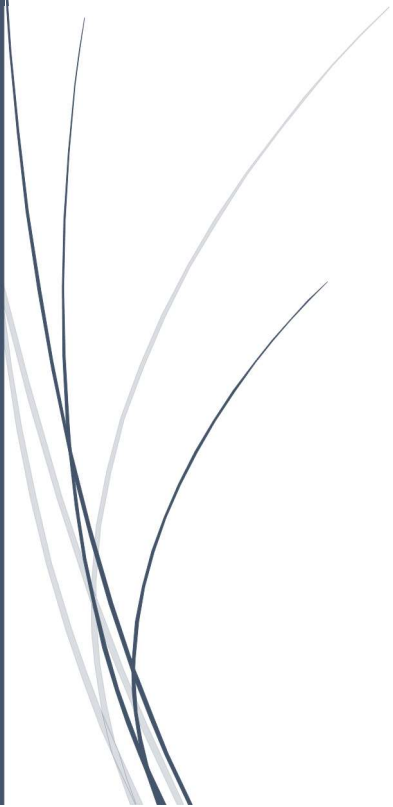


A dark blue vertical bar runs down the left side of the page. A blue arrow-shaped banner points to the right from the bar, containing the text 'Spring 2022'.

Spring 2022

# Master Thesis in Sustainable Architecture

Definition and Assessment of Advanced  
Control Strategies for Double Skin  
Façades with Building Performance  
Simulation

Several thin, curved lines in shades of blue and grey originate from the bottom left and sweep upwards and to the right, creating a sense of movement and design.

*Student:* Francesco Vasco (Student n° 567265)

*Supervisors:* Prof. Francesco Goia, *NTNU*

Dr. Fabio Favoino, *Politecnico di Torino*

*Co-Supervisor:* Elena Catto Lucchino, *NTNU*



## Table of contents of the Thesis

<i>List of Figures</i> .....	4
<i>List of Tables</i> .....	7
<i>Abstract of the Thesis work</i> .....	9
<i>List of abbreviations</i> .....	10
1. <i>Introduction of the Thesis work</i> .....	11
1.1. <i>Energy consumption and carbon emission in the building sector</i> .....	11
1.2. <i>Responsive Building Elements: a paradigm shift in the envelope design</i> .....	12
1.3. <i>Scope and research domain of the Thesis work</i> .....	13
1.4. <i>The control of responsive building elements</i> .....	14
1.5. <i>Aim and goals of the Thesis in relation to the control of the double skin façade</i> ..	17
1.5.1. <i>Simulation workflow development for responsive building elements</i> .....	17
1.5.2. <i>Performance optimization for a double skin façade</i> .....	18
1.6. <i>Objectives of the Thesis</i> .....	18
1.7. <i>Research hypothesis and methodology of the Master Thesis</i> .....	18
2. <i>The control of the double skin façade</i> .....	21
2.1. <i>Characteristics of the control for a double skin façade</i> .....	21
2.2. <i>Control logics and double skin façade performance</i> .....	22
2.2.1. <i>Definition of the performance requirements</i> .....	22
2.2.2. <i>Connection between performance goals and control strategies</i> .....	23
2.2.3. <i>Selection of the control variables</i> .....	24
2.2.4. <i>Selection of the façade actuators and their possible states</i> .....	25
2.2.5. <i>Implementation of the control strategies for the double skin façade</i> .....	27
2.3. <i>Combinations of the different control logics</i> .....	36
2.3.1. <i>Combinations for the summer season</i> .....	57
2.3.2. <i>Combinations for the winter season</i> .....	57
2.3.3. <i>Control for the week-end days</i> .....	58
3. <i>Research method definition for the performance evaluation</i> .....	60
3.1. <i>Double skin system modelling</i> .....	60
3.2. <i>Thermal zone modelling</i> .....	62
3.3. <i>Boundary conditions selection and analysis of the climate conditions</i> .....	64
3.4. <i>Multi-domain performance evaluation using IDA ICE</i> .....	70
3.5. <i>Comparison with the reference façade systems and selection of the optimal control combination</i> .....	72
4. <i>Result analysis</i> .....	75

4.1.	<i>Energy performance analysis</i> .....	75
4.1.1.	<i>Summer conditions</i> .....	76
4.1.2.	<i>Winter conditions</i> .....	82
4.2.	<i>Indoor climate analysis</i> .....	88
4.2.1.	<i>Summer conditions</i> .....	89
4.2.2.	<i>Winter conditions</i> .....	97
5.	<i>Findings and conclusions</i> .....	106
5.1.	<i>Definition of the optimal control for the summer season</i> .....	106
5.1.1.	<i>Energy Efficiency</i> .....	106
5.1.2.	<i>Indoor Environmental Quality</i> .....	107
5.2.	<i>Definition of the optimal control for the winter season</i> .....	110
5.2.1.	<i>Energy Efficiency</i> .....	110
5.2.2.	<i>Indoor Environmental Quality</i> .....	111
5.3.	<i>Critical points of the rule-based control effectiveness</i> .....	113
6.	<i>Further developments of the Thesis work</i> .....	116
6.1.	<i>Analysis of different climates and different façade orientations</i> .....	116
6.2.	<i>Application of the model-based control</i> .....	118
<i>Appendix A: The use of BPS tools for the modelling of RBEs and IDA ICE features</i> .....		122
<i>Appendix B: The DSF system</i> .....		128
<i>Appendix C: DSF modelling in IDA ICE</i> .....		136
<i>Appendix D: Control implementation in IDA ICE</i> .....		142
<i>Sources and Bibliography</i> .....		154



## List of Figures

<i>Figure 1: Global share of buildings and construction final energy and emissions (2020) [1].</i>	11
<i>Figure 2: Examples of adaptive and responsive envelope technologies: Thermo-tropic glazing (up) and movable solar shading (down) [8]. The movable solar shading is from Kieferttechnik Building, Ernst Giselbrecht + Partner, Styria, Austria, 2007.</i>	13
<i>Figure 3: Scheme of the three levels of the control [9].</i>	15
<i>Figure 4: Research methodology scheme</i>	20
<i>Figure 5: Functional scheme of the flexible double skin model to model inside IDA ICE</i>	25
<i>Figure 6: Variation of DSF configurations with the implementation of the control combination SC#3 (Summer Day). Output signal from IDA ICE.</i>	30
<i>Figure 7: Variation of DSF configurations with the implementation of the control combination SC#5 (Summer Day). Output signal from IDA ICE.</i>	31
<i>Figure 8: Variation of DSF configurations with the implementation of the control combination SC#10 (Summer Day). Output signal from IDA ICE.</i>	31
<i>Figure 9: Variation of DSF configurations with the implementation of the control combination SC#15 (Summer Day). Output signal from IDA ICE.</i>	32
<i>Figure 10: Variation of DSF configurations with the implementation of the control combination SC#18 (Summer Day). Output signal from IDA ICE.</i>	32
<i>Figure 11: Variation of DSF configurations with the implementation of the control WC#3 (Winter Day). Output signal from IDA ICE.</i>	33
<i>Figure 12: Variation of DSF configurations with the implementation of the control WC#8 (Winter Day). Output signal from IDA ICE.</i>	34
<i>Figure 13: Variation of DSF configuration with the implementation of the control combination WC#9 (Winter Day). Output signal from IDA ICE.</i>	34
<i>Figure 14: Variation of blind slat angle with the implementation of the control combination SC#3 (Summer Day). Output signal from IDA ICE.</i>	35
<i>Figure 15: Variation of blind slat angle with the implementation of the control combination SC#20 (Summer Day). Output signal from IDA ICE.</i>	35
<i>Figure 16: Variation of blind slat angle with WC#3 (Winter Day). Output signal from IDA ICE.</i>	36
<i>Figure 17: Variation of blind slat angle with WC#12 (Winter Day). Output signal from IDA ICE.</i>	36
<i>Figure 18: SAC#1 decision tree</i>	41
<i>Figure 19: SAC#2 decision tree</i>	42
<i>Figure 20: SAC#3 decision tree</i>	43
<i>Figure 21: SAC#4 decision tree</i>	44
<i>Figure 22: SAC#5 decision tree</i>	45
<i>Figure 23: SSC#1 decision tree</i>	48
<i>Figure 24: SSC#2 decision tree</i>	49
<i>Figure 25: SSC#3 decision tree</i>	49
<i>Figure 26: SSC#4 decision tree</i>	49
<i>Figure 27: WAC#1 decision tree</i>	52
<i>Figure 28: WAC#2 decision tree</i>	52
<i>Figure 29: WAC#3 decision tree</i>	53

<i>Figure 30: WSC#1 decision tree</i> .....	55
<i>Figure 31: WSC#2 decision tree</i> .....	55
<i>Figure 32: WSC#3 decision tree</i> .....	56
<i>Figure 33: WSC#4 decision tree</i> .....	56
<i>Figure 34: Scheme for the construction of the control combinations in summer and winter conditions</i> .....	58
<i>Figure 35: DSF modelling workflow</i> .....	62
<i>Figure 36: The BESTEST cell used for the thermal zone modelling, with the two identical double skin façades applied on the South wall</i> .....	63
<i>Figure 37: Location of Frankfurt with respect to the other European climates [29]</i> .....	65
<i>Figure 38: Average monthly values of outdoor air temperature for Frankfurt [30]</i> .....	66
<i>Figure 39: Average monthly values of cloudiness for Frankfurt [30]</i> .....	66
<i>Figure 40: Average monthly values of solar radiation on the horizontal surface for Frankfurt [30]</i> .....	66
<i>Figure 41: Hourly variation of outdoor temperature during the month of July</i> .....	67
<i>Figure 42: Hourly variation of cloudiness in the month of July</i> .....	67
<i>Figure 43: Hourly variation of solar radiation on the horizontal façade in the month of July</i> .....	68
<i>Figure 44: Hourly variation of outdoor temperature during the month of January</i> .....	69
<i>Figure 45: Hourly variation of solar radiation on the horizontal façade in the month of January</i> .....	70
<i>Figure 46: Hourly variation of cloudiness in the month of January</i> .....	70
<i>Figure 47: The single skin façade system used as second comparison system for the performance evaluation</i> .....	74
<i>Figure 48: Heating energy requirements for the different façade systems (July)</i> .....	78
<i>Figure 49: Cooling energy requirements for the different façade systems (July)</i> .....	80
<i>Figure 50: Artificial lighting energy requirements for the different façade systems (July)</i> ...	82
<i>Figure 51: Heating energy requirements for the different façade systems (January)</i> .....	84
<i>Figure 52: Cooling energy requirements for the different façade systems (January)</i> .....	86
<i>Figure 53: Artificial lighting energy requirements for the different façade systems (January)</i> .....	88
<i>Figure 54: Number of occupied hours above 26°C for the different façade systems (July)</i> ...	91
<i>Figure 55: Variation of the comfort indexes in the room for the different façade systems (July)</i> .....	95
<i>Figure 56: Number of occupied hours below the limit of 500 lux (July)</i> .....	97
<i>Figure 57: Number of occupied hours below 20°C for the different façade systems (January)</i> .....	99
<i>Figure 58: Variation of the comfort indexes in the room for the different façade systems (January)</i> .....	101
<i>Figure 59: Number of occupied hours below the limit of 500 lux for the different façade systems (January)</i> .....	103
<i>Figure 60: Number of occupied hours above the limit of 3000 lux for the different façade systems (January)</i> .....	104
<i>Figure 61: Location of the different climate conditions that can be analysed for the double skin performance evaluation (Frankfurt, Oslo and Madrid)</i> .....	116
<i>Figure 62: IDA API script inside VS Code</i> .....	119
<i>Figure 63: Graphic user interface of IDA ICE</i> .....	124

<i>Figure 64: Mathematical model of a window in IDA ICE: list of interfaces, variables and parameter in the Outline tab of the element.....</i>	<i>125</i>
<i>Figure 65: Control macro example from IDA ICE for the control of the shading system ...</i>	<i>126</i>
<i>Figure 66: Intersection of all the different domains for different BPS tools [9].....</i>	<i>127</i>
<i>Figure 67: Structure of a double skin façade, with the different components of the system: primary façade (outer skin), second glass layer (inner skin), cavity and integrated solar shading device [52].....</i>	<i>130</i>
<i>Figure 68: Pictures of the DSF layouts: a) box window, b) shaft-box, c) corridor façade and d) multi-storey façade [20]. .....</i>	<i>133</i>
<i>Figure 69: DSF ventilation modes classification [20].....</i>	<i>135</i>
<i>Figure 70: 3D view of the double skin façade in-built model from the IDA ICE graphic interface. ....</i>	<i>136</i>
<i>Figure 71: Detailed window form in IDA ICE. The glazing properties are referred to the inner skin of the double skin façade. In the “Ventilated construction” field the selection “Wall” enables the creation of the double skin façade model. ....</i>	<i>137</i>
<i>Figure 72: The form referred to the double glass façade component: here it is possible to define the properties of the external skin, the cavity and the integrated shading system.....</i>	<i>138</i>
<i>Figure 73: Definition of the shading system properties (in this case a venetian blind): materials, slat angle, distances. ....</i>	<i>139</i>
<i>Figure 74: Schematic view of the double skin façade created on IDA ICE. On the left, it is visible the inner skin and the opening towards the zone, while on the right it is possible to see the ventilated cavity and the outer skin.....</i>	<i>140</i>
<i>Figure 75: The modified configuration of the double skin façade system implemented inside IDA ICE .....</i>	<i>141</i>
<i>Figure 76: Example of decision tree for the cavity air flows built in IDA ICE.....</i>	<i>142</i>
<i>Figure 77: Control implementation for the cavity air flows (on the left) and the shading system (on the right) in the central Control Macro of the double skin façade.....</i>	<i>143</i>
<i>Figure 78: Example of switch modules at the end of a decision tree implemented in IDA ICE .....</i>	<i>146</i>
<i>Figure 79: Application of the Max module for the definition of the output of the Macro ....</i>	<i>147</i>
<i>Figure 80: Definition of the actuators state in function of the decision tree .....</i>	<i>147</i>
<i>Figure 81: Definition of the fan configuration (on/off) and the related air flow (min/mx) inside the cavity fan Control Macro.....</i>	<i>148</i>
<i>Figure 82: Use of the IDA ICE Control Macro for the application of the shading control. ....</i>	<i>149</i>
<i>Figure 83: The Control Macro for the supply fan of the AHU.....</i>	<i>150</i>
<i>Figure 84: Distinction between the operating strategies for the shading system during the week days .....</i>	<i>150</i>
<i>Figure 85: The Sliding Average module (left) and the definition of the interval parameter (right) .....</i>	<i>151</i>
<i>Figure 86: Definition of the control macro for the artificial lighting system of the room ...</i>	<i>152</i>

## List of Tables

<i>Table 1: List of possible air flows configurations that can be implemented inside the cavity</i>	28
<i>Table 2: Definition of the eight different groups of rule-based control types</i>	29
<i>Table 3: Control combinations for the airflows during the summer season</i>	40
<i>Table 4: Definition of the threshold value for the blind drawn mechanism during the summer season (month of July)</i>	46
<i>Table 5: comparison between the fixed slat angle values and the average illuminance levels at the working plane during the morning, the midday and the afternoon hours (for Frankfurt, in the month of July)</i>	47
<i>Table 6: Control combinations for the shading system during the summer season</i>	48
<i>Table 7: Control combinations for the airflows during the winter season</i>	51
<i>Table 8: Definition of the threshold value for the blind drawn mechanism during the winter season (month of January)</i>	53
<i>Table 9: Comparison between the fixed slat angle values and the average illuminance levels at the working plane during the morning, the midday and the afternoon hours (for Frankfurt, in the month of January)</i>	54
<i>Table 10: Control combinations for the shading during the winter season</i>	54
<i>Table 11: The 20 combinations of control for the summer season</i>	57
<i>Table 12: 12 combinations of control for the winter season</i>	58
<i>Table 13: Layers of the two skins of the double skin façade</i>	61
<i>Table 14: Optical, solar and thermal properties of the outer and the inner skins automatically calculated by IDA ICE</i>	61
<i>Table 15: Main data about the zone inserted inside IDA ICE</i>	64
<i>Table 16: Average monthly values for July in Frankfurt</i>	67
<i>Table 17: Average monthly values for July in Frankfurt</i>	68
<i>Table 18: Thermal conductivity calculations for the envelope ideal materials. The thermal transmittance value is expressed in <math>W/m^2K</math>, the thermal resistance is expressed in <math>m^2K/W</math> while the thermal conductivity is expressed in <math>W/m K</math></i>	70
<i>Table 19: The two different typologies of simulation performed on IDA ICE and the related simulation outputs</i>	72
<i>Table 20: Heating energy requirements for the different façade systems (July)</i>	77
<i>Table 21: Cooling energy requirements for the different façade systems (July)</i>	79
<i>Table 22: Artificial lighting energy requirements for the different façade systems (July)</i>	81
<i>Table 23: Heating energy requirements for the different façade systems (January)</i>	83
<i>Table 24: Cooling energy requirements for the different façade systems (January)</i>	85
<i>Table 25: Artificial lighting energy requirements for the different façade systems (January)</i>	87
<i>Table 26: Number of occupied hours above 26°C for the different façade systems (July)</i>	90
<i>Table 27: Number of occupied hours above 1100 ppm for the different façade systems (July)</i>	92
<i>Table 28: Variation of the comfort indexes in the room for the different façade systems (July)</i>	93
<i>Table 29: Number of occupied hours below the limit of 500 lux (July)</i>	96
<i>Table 30: Number of occupied hours below 20°C for the different façade systems (January)</i>	98

<i>Table 31: Variation of the comfort indexes in the room for the different façade systems (January)</i> .....	100
<i>Table 32: Number of occupied hours below the limit of 500 lux (January)</i> .....	102
<i>Table 33: Number of occupied hours above the limit of 3000 lux (January)</i> .....	103
<i>Table 34: Effectiveness of the different control combinations (Summer) in function of the variation respect to SSF</i> .....	105
<i>Table 35: Effectiveness of the different control combinations (Winter) in function of the variation respect to SSF</i> .....	105
<i>Table 36: Selection of the optimal control for the summer season in terms of energy efficiency</i> .....	107
<i>Table 37: Selection of the optimal control for the summer season in terms of indoor environmental quality</i> .....	109
<i>Table 38: Comparison between the optimal controls (for energy efficiency and IEQ) selected for the summer season</i> .....	109
<i>Table 39: Selection of the optimal control for the winter season in terms of energy efficiency</i> .....	111
<i>Table 40: Selection of the optimal control for the winter season in terms of indoor environmental quality</i> .....	112
<i>Table 41: Positive features and negative aspects of the selected optimal control logic for energy efficiency and indoor environmental quality in the winter season</i> .....	113
<i>Table 42: Overall number of boundary conditions that can be considered for the performance evaluation of the double skin façade control (climate context, façade orientation and season)</i> .....	117
<i>Table 43: Exit codes for the DSF configurations and related actuators states</i> .....	145
<i>Table 44: States of the different actuators in relation to each configuration code</i> .....	146

## ***Abstract of the Thesis work***

The increasing environmental impact of the *AEC* sector is one of the most challenging tasks that the construction industry is now facing. For this reason, the designers are now called to find new technologies and innovative processes to reach the ambitious level of the complete decarbonization of the building sector by 2050.

A possible path to follow in this field is the improvement of the existing envelope technologies. Indeed, dynamicity and responsivity to different operating and seasonal conditions are new requirements that these new innovative envelope systems must provide. This Thesis deals with a particular typology of this kind of envelopes: the *Double Skin Façades*.

Dynamic envelope systems indeed must be provided with a control logic that should be able to ensure the adaptability to the different operating and seasonal conditions, guarantying both, energy performance and occupant's comfort: the definition and the subsequent implementation of the control logic are consequently crucial steps in the design of this typology of building enclosures. Connected to these concepts, the Thesis aims to develop different control strategies for a *DSF*, trying to understand the interconnections between them and the overall performance of the building system. The final purpose is indeed to define strengths and weaknesses of the different implemented controls, selecting the optimal solution that can be applied in a certain boundary condition.

## **List of abbreviations**

- *AEC: Architecture, Engineering and Construction*
- *DSF: Double Skin Façade*
- *SSF: Single Skin Façade*
- *RBEs: Responsive Building Elements*
- *BPS: Building Performance Simulation*
- *NMF: Neutral Model Format*
- *ICE: Indoor Climate and Energy*
- *HVAC: Heating, Ventilation and Air Conditioning*
- *AHU: Air Handling Unit*
- *CAV: Constant Air Volume*
- *AS: Air Supply*
- *AE: Air Exhaust*
- *TB: Thermal Buffer*
- *OAC: Outdoor Air Curtain*
- *IAC: Indoor Air Curtain*
- *CF: Climate Façade*
- *U: Thermal Transmittance*
- $\tau_e$ : *Total Solar Transmission*
- $\tau_v$ : *Visible Transmission*
- *SHGC: Solar Heat Gain Coefficient*
- *IEA: International Energy Agency*
- *IEQ: Indoor Environmental Quality*
- *IAQ: Indoor Air Quality*
- *ASHRAE: American Society of Heating, Refrigerating and Air-Conditioning Engineers*
- *PMV: Predicted Mean Vote*
- *PPD: Predicted Percentage of Dissatisfied*

## 1. Introduction of the Thesis work

### 1.1. Energy consumption and carbon emission in the building sector

According to the 2020 data, *AEC* industry constitutes the 36% of the global final energy demand and the 37% of the energy related  $CO_2$  emissions [1]. In 2014, the final energy consumption from the building sector was the 31% of the overall global value of energy consumption, while the emission share was only 29% [2]. In 2018 energy-related  $CO_2$  emissions from the building sector reached the highest recorded percentage of 39% [3] (Figure 1).

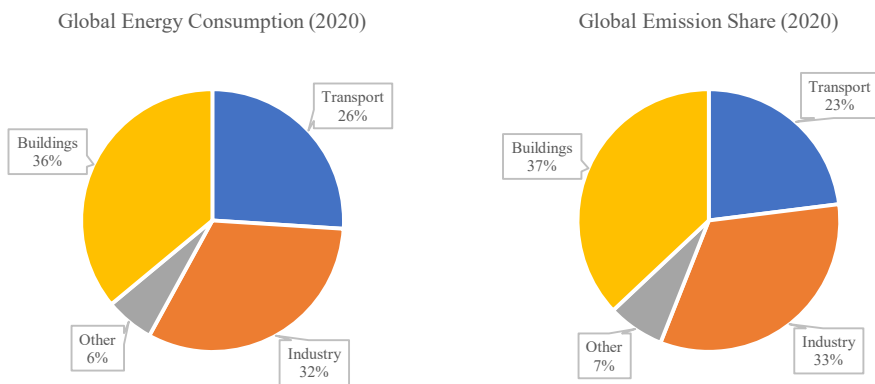


Figure 1: Global share of buildings and construction final energy and emissions (2020) [1].

In this perspective, to achieve the *Paris Agreement* goal of keeping global temperature rise below  $2^{\circ}C$ , the global construction sector must be almost completely decarbonized by 2050. Crucial strategies for the building industry in the next decades must be consequently entirely devoted to the reduction of the  $CO_2$  outputs. Indeed, important performance targets to achieve are the reduction of the overall building energy demand and the increased use of renewable energy sources. Adopting these two solutions, it could be possible to nearly eliminate the carbon emissions from the building operations by 2050 [1].

According to these ambitions, the *European Union's Energy Performance of Buildings Directive* recast of 2018 states that by the 31<sup>st</sup> December 2020 all new buildings shall be nearly zero energy buildings. This means that new constructions are required to have a very high energy performance, corresponding to a very low energy consumption for all the end uses. New technologies and innovative processes for the building sector are consequently required to reach these ambitious targets in the next years. This Thesis indeed tries to analyze possible innovative solutions that are focused on this objective.



## **1.2. Responsive Building Elements: a paradigm shift in the envelope design**

A better performance of the external enclosures of the building (both opaque and transparent) is always linked with a greater energy efficiency of the whole system [4]. Indeed, during the last 100 years, the focus in the building envelope design was the reduction of the thermal transmittance value to enhance the insulation level and reduce in this way the transmission heat losses during the heating season. Regarding in detail the transparent portion of the building envelope, significant progresses have been reached in the last decades for the reduction of the overall thermal transmittance, thanks to the adoption of multiple glazing units, high-performance coatings or transparent insulation.

The reduction of the heat losses through the envelope is of course the optimal solution for the lowering of the building space heating demand during the winter season but other important performance targets are required, as for example the energy reduction for space cooling, the optimization of the daylight accessibility and the solar energy exploitation (both passive and active). An efficient building envelope should be consequently able to perform all these different tasks, with the main aim of guarantee the optimal indoor comfort conditions with lowered energy consumption. Further and innovative research is therefore necessary to improve existing envelope technologies for a better efficiency of the buildings. The Thesis indeed tries to analyze an innovative kind of envelope technology that can be used for the achievement of these ambitious goals: the *double skin façade* system (or *DSF*).

The responsivity to different functional scenarios that can contradict each other could be indeed a possible feature of such kind of innovative envelope systems. In this field, new functions for the envelope systems can be for example the adaptability to different weather conditions and seasonal operations and the capability to counterbalance opposite performance criteria of the whole system (as, for example, energy performance and comfort for the occupants) [5]: from a static and isolated component, the façade had changed its role into an active and dynamic element, functionally integrated with the other building systems (a *paradigm shift* in the building design process).

The dynamicity of the façade stays indeed in its adaptive characteristics and functions that can be adjusted to respond to environmental variations, with the main purpose to keep comfort conditions for the occupants with the lowest possible energy demand [6]. Such kinds of innovative technologies are commonly named as *Responsive Building Elements (RBEs)* and systems. Being characterized by a variation of their features along the year, two crucial requirements for such kinds of elements are the adaptability to different boundary conditions (both internal or external) and the autonomy in the change between a configuration to another one [7] (*Figure 2*).

Indeed, dynamic systems are always managed by a control system, that can change the façade performance requirements in autonomous way if there is a variation in the system boundary conditions [7]. From these first considerations, the impact of the control strategy implementation for an adaptive façade performance is considerably relevant: a wrong control strategy implemented for the dynamic façade and its interaction with other technical systems can have indeed a negative impact on the whole building energy performance.

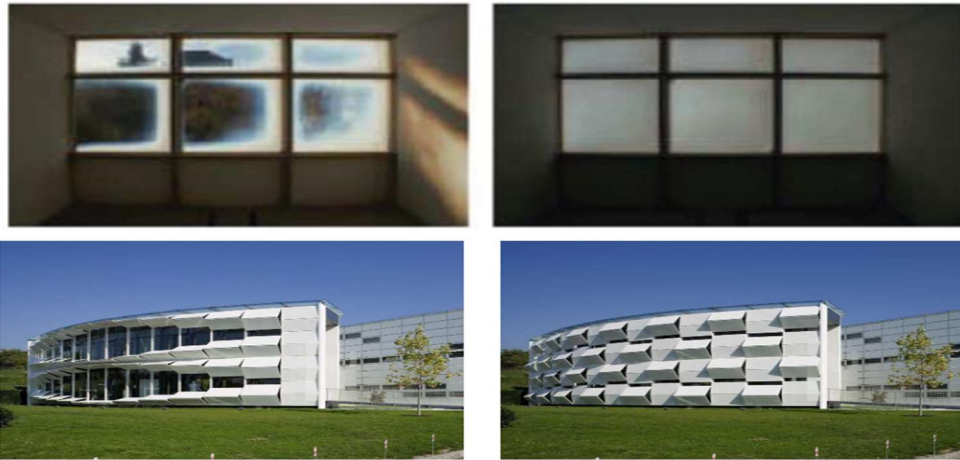


Figure 2: Examples of adaptive and responsive envelope technologies: Thermo-tropic glazing (up) and movable solar shading (down) [8]. The movable solar shading is from Kiefertech Building, Ernst Giselbrecht + Partner, Styria, Austria, 2007.

### 1.3. Scope and research domain of the Thesis work

In function of what it has been stated about the building energy performance and the control implementation of adaptive envelope systems, it is now possible to define the main purpose and the wider objective of the Thesis work.

The Thesis scope is basically the study of optimal control strategies for a responsive building element (in this specific case a *DSF*) and the subsequent evaluation of their effectiveness in the improvement of the overall building performance under a multi domain point of view (indeed, considering both the energy efficiency and indoor comfort for the occupants). For these tasks, a *Building Performance Simulation (BPS)* tool (IDA ICE) has been used.

The research domain of the Thesis can be consequently articulated in the following elements:

- The control strategies implementation for a *RBE* (a *DSF* in the specific)
- The effectiveness evaluation of the implemented control

- The performance assessment of the whole system (the responsive building element and the building itself)

At the same time, in the research domain will be not covered the topics regarding the constructional features of the *DSF* since the priority will be given to the study of the influence of the control on the façade performance.

#### **1.4. The control of responsive building elements**

At this point it is necessary to introduce some concepts and information regarding the control implementation for adaptive and dynamic envelope systems.

The control of a building system can be articulated in 3 different levels [9]:

- *Sensor level*
- *Actuator level*
- *Control logic level*

The sensor level is composed by the so-called *sensed variables* or *control variables* that are used by the control logic to monitor the state of the different façade components, the outdoor climate and/or the building. The sensed variables can be referred therefore to the external boundary conditions (outdoor air temperature, incident solar radiation, wind velocity, etc.), to the indoor environmental conditions (indoor air temperature, illuminance levels,  $CO_2$  concentrations, etc.) or to the different façade components (cavity air temperature, internal surface temperature, etc.).

The actuators level comprises all the façade and building components that can be controlled by the implemented control logic. In general, dealing with adaptive façade systems, the main actuators are the operable façade components (blinds, openings, fans, windows, etc.) or the other building technical systems (connection to the *HVAC* system, indoor artificial lighting, etc.) that can change their configurations and operational settings.

At the end, the control logic level provides the link between the sensed variables and the actuator actions, defining the way the different actuators should response to a variation in the boundary conditions. The different levels of the control are showed in a schematic view in *Figure 3*.

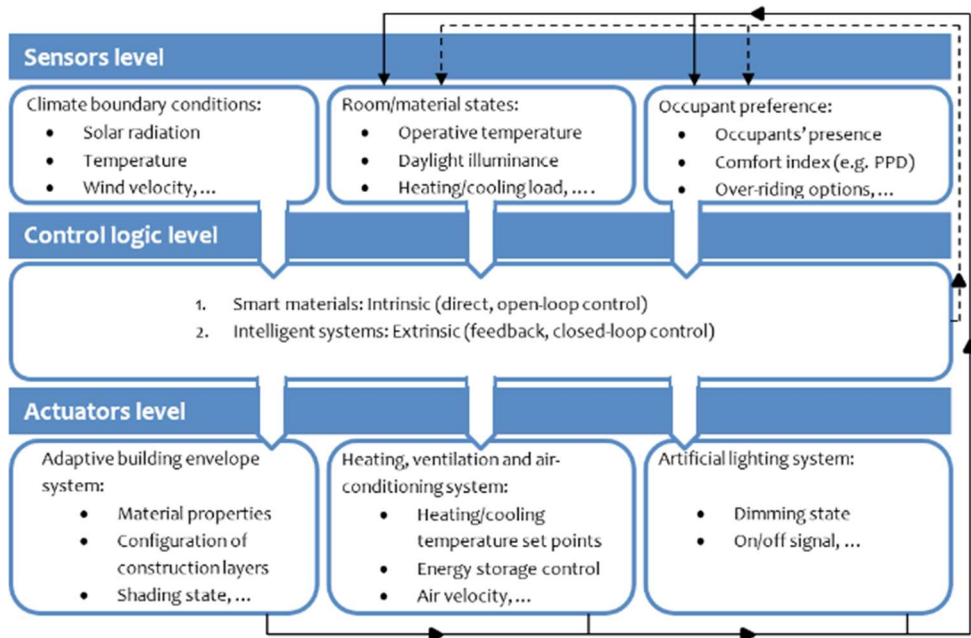


Figure 3: Scheme of the three levels of the control [9].

Another important distinction between different control implementations is the one existing between the two different approaches that can be followed during the control design:

- *Rule-based*
- *Model-based*

In the first case, the designer defines a specific set of rules focused on one or more control variables. It is usually defined with the expression *if condition, then action*: this means that if a certain threshold value for a given control variable is reached, a specific actuator state is defined. For this reason, rule-based algorithms usually take the shape of *decision trees* in which to a certain set of predefined conditions correspond the possible configurations of the system. The rule-based approach is the simplest path to follow when the designer must deal with adaptive façade systems, and it is also the most diffused way to control responsive façade elements in actual buildings.

The rule-based approach has anyway two great disadvantages [10]:

- It is entirely based on the knowledge and experience of the designer about the physical behavior of the façade and its components: he indeed must understand a priori which will be the operating conditions of the façade and in function of them define the most appropriate set of rules.

- It can offer a response just to a predefined set of boundary conditions, without considering the dynamic and transient behavior of the system (it is a sort of *discretization* of the real boundary conditions that can affect the system performance): even if the number of implemented conditions is high (corresponding to a higher number of rules), it is impossible to cover all the possible changes in the operating conditions of the system.

For these reasons, more advanced control strategies have been implemented: it is the case of the *model-based* approach, the optimal asset for the actuators is defined for each time step by means of simulations on a virtual model of the system: optimal control actions for the system are therefore defined by means of an embedded dynamic simulation, not in function of a pre-defined set of rules [11]. For the actuation of this control strategy, it is necessary to define a priori some performance indicators that will be used by the simulation environment to address the control mechanism of the façade: the performance indicators can be related for example to the indoor climate conditions or to the whole building energy performance, according to the designer decisions.

With such a kind of control, the dynamic simulation can define which one of the many possible façade configurations and actuators states produces the best results in terms of overall performance [10]. It is evident that the model-based approach can cover a wider range of configurations and boundary conditions for the dynamic façade but anyway there are two main disadvantages to consider:

- It is more complex to implement than a simpler set of rules and therefore a greater designer knowledge about mathematical modelling and control strategies implementation is required.
- It requires a greater computational effort to run all the different dynamic simulations.

The role of the designer in the control implementation phase is therefore to find the right *trade-off* between the level of performance that is required by the façade and the building as a whole and the complexity degree of the defined control mechanism.

Indeed, during this Thesis work, given the higher complexity of the model-based approach compared to the rule-based one, the latter approach will be followed for the implementation of the *DSF* control and the subsequent evaluation of its effectiveness. One of the objectives of the Thesis, anyway, is the one to show the limitations in the use of less advanced forms of control in the performance optimization of a *DSF* system.

As mentioned before, for the implementation of the control for the *DSF* and the subsequent evaluation of the performance of the system, a *BPS* tool (IDA ICE) has been used. Given the high complexity of this kind of simulation environments and the additional difficulties in the modelling of *RBEs* inside them, more details about this

topic are inserted inside *Appendix A: The use of BPS tools for the modelling of RBEs and IDA ICE features*, to offer to the reader a wider knowledge about the tools used during the Thesis work.

As written in 1.2 the analyzed *RBE* in this Master Thesis is a *DSF*. It is assumed that the reader of the Thesis already knows the main features of this kind of envelope system and its evolution across the last decades. For a better and more detailed description of the *DSF* concept, it is possible to read *Appendix B: The DSF system*.

Also, the modelling process of this kind of elements inside the IDA ICE simulation environment is illustrated in detail in *Appendix C: DSF modelling in IDA ICE*. In the appendix indeed it is described the process for the creation of a *flexible DSF* concept inside the simulation environment, following the approach and the methodology adopted by Elena Catto Lucchino in her PhD Thesis. This flexible *DSF* model has been used in this Master Thesis for the implementation of the control for this kind of *RBE*.

### **1.5. Aim and goals of the Thesis in relation to the control of the double skin façade**

In function of what has been illustrated in the previous sections of the report, the specific aim of the Master Thesis related to control strategies development for *DSF* can be defined. The aim of the Thesis is indeed the development of advanced control strategies for a *DSF* by means of the *BPS* tool IDA ICE and the subsequent evaluation of their effects on the overall performance of the system. The two goals of the Master Thesis, that are specifically interconnected between each other, together aim to reach the wider and more general scope of the work.

#### **1.5.1. Simulation workflow development for responsive building elements**

The first goal is to define a simulation workflow on the *BPS* tool IDA ICE that can be applied to *DSF* (and more in general to *RBEs*) for the study and the effectiveness evaluation of advanced control strategies on the overall energy performance of the building. This goal is specifically linked to the definition of a set of methods inside a simulation environment that must be able to assess the effectiveness of different control strategies under a multi-domain point of view. In synthesis, the result of this goal is to understand how to assess in a quantitative way the effectiveness of a certain control logic by means of a *BPS* tool.

The simulation workflow can be indeed summarized as the definition of a certain boundary condition (for example based on climate conditions, operating season and façade orientation) for which the implemented strategies will be tested and evaluated.

### **1.5.2. Performance optimization for a double skin façade**

The second goal is to understand the relation between the typology of the implemented control logic and the performance of the *DSF* (in typical summer and winter operations), in relation to the boundary condition set by means of the first goal. The second goal indeed is more related to the performance optimization of the *DSF*: using the set of methods implemented thanks to the achievement of the first goal, it can be possible to develop optimal control strategies for the performance improvement of the adaptive envelope system, considering both energy efficiency and comfort for the occupants.

### **1.6. Objectives of the Thesis**

This section is focused on the definition of the more specific objectives that are linked to the two main goals of the Master Thesis:

- About the first goal, focused on the simulation workflow development for *RBEs*, the main objectives of the Thesis are:
  - 1) Define the performance targets that the analyzed *RBE* must guarantee.
  - 2) Understand which control strategies can be specifically linked to these performance targets and how they can achieve them.
  - 3) Set a group of control variables that can be used for the addressing of the control strategies for the *RBE*.
  - 4) Define the performance metrics that can be used for a quantitative evaluation of the performance.
- About the second goal, focused on the performance optimization for a *DSF*, the main objectives of the Thesis are:
  - 1) Define which priority needs and performance targets the *DSF* must optimize.
  - 2) Understand in which way the actuators of the *DSF* can be used for its performance optimization.
  - 3) Define different combinations of rule-based control strategies (for summer and winter conditions) and evaluate their effects on the whole performance of the system.
  - 4) Define and understand strengths and limitations in the application of the different combinations of control for the *DSF*.

### **1.7. Research hypothesis and methodology of the Master Thesis**

Connecting the concepts explained in 1.5 and 1.6, it is possible to define the methodology of the Master Thesis and the related research hypothesis. The expected research outcomes regarding the control of the *DSF* are the following ones:

- The multi-domain performance of a *RBE* such as a *DSF* is better than a standard *SSF* (for example a traditional openable window) only if the correct control strategy is implemented for the different façade actuators.
- Different control strategies have different degrees of effectiveness, affecting consequently in a different way the different performance domains of the *RBE*.
- The main challenge of the control implementation for a *DSF* is the optimization of both, overall energy performance and comfort for the occupants.
- The combination of different rule-based algorithms for the control of the *DSF* can be ineffective for a *multi-domain* optimization of the system, compared to more sophisticated forms of control.

The different research hypothesis, that can be linked to specific research questions, are mainly related to two research domains, indeed:

- How to evaluate in a quantitative way the performance of a complex system like a *DSF*?
- How to assess the effects of different control strategies on the performance of the whole building?

These two questions will be discussed more in detail in 3.4 and 3.5, which are focused on the performance evaluation of the *DSF* and the selection of the optimal control strategy for a certain boundary condition. Indeed, the main research questions which have been addressed the Thesis work are listed here:

- How can the adaptive envelope system guarantee performance objectives of energy efficiency and comfort for the occupants?
- Which specific control strategies can be connected to these objectives and how they can achieve them?
- Which control variables should be selected?
- Which performance metrics must be then considered for a quantitative evaluation of the *DSF* efficiency in a *multi-domain* perspective?
- Which are the benefits and the disadvantages of the different control methods that can be implemented?
- Which is the optimal control strategy to be applied for a particular boundary condition (in particular, season, façade orientation and climate?)

Being a scientific report, this Master Thesis has followed a quantitative approach for the collection and analysis of the data generated inside the simulation environment of IDA ICE. According to the research methodology followed during the Thesis work, the testing of the different research hypothesis regarding the dynamic behavior of the *DSF* and the subsequent analysis of the results are carried on a virtual model of a *DSF* model realized on the *BPS* tool IDA ICE. The simulation environment will be



therefore used for the control strategies development and the subsequent evaluation of the system performance.

Indeed, it is possible to set inside the *BPS* tool a set of:

- Inputs, indeed the boundary conditions of the simulations performed on IDA ICE. They are in particular:
  - 1) The climate and the orientation in which the façade is located.
  - 2) The operating season of the façade system (heating or cooling period).
  - 3) The implemented control logic for the façade actuators (cavity air flows and shading system).
  
- Outputs, indeed, the simulated data, corresponding to the results of the simulations performed on the *BPS* tool):

These outputs have been used for the definition of the performance of the *DSF*. According to the outputs, it is possible to verify or modify the previously defined research hypothesis regarding the control of the *DSF* and its effectiveness.

The general scheme of the methodology applied in the Thesis work is illustrated in *Figure 4*. The research method that has been used for the performance assessment and the control effectiveness evaluation during the Thesis work will be discussed more in detail in 3, after the description of the control implementation for *DSF* systems in 2.

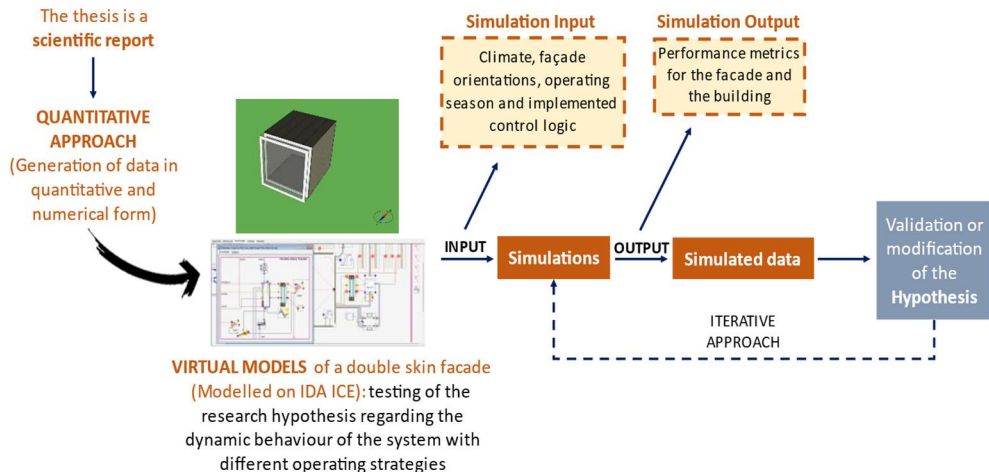


Figure 4: Research methodology scheme

## **2. The control of the double skin façade**

Being the Thesis focused on the control implementation for a *DSF* system, in this chapter are described more in detail the concepts regarding the control of this typology of *RBE*.

### **2.1. Characteristics of the control for a double skin façade**

*DSF* systems, as adaptive envelope systems, require an efficient control to manage the variations of different boundary conditions (mainly, seasonal weather variations and changes in the operations of the building).

The two main aims of the control strategies implementation for a *DSF* are therefore the following ones [12]:

- Provide an efficient use of the solar gains during the heating period
- Provide an acceptable environmental comfort during the whole year

In addition to these two major objectives of the control, other two performance targets must be followed:

- During the unoccupied periods (for example the night-time and the weekend), the focus of the control strategy must be the overall energy savings of the building.
- During the occupied periods, the focus of the control strategy must be the comfort conditions for the occupants.

All these aspects must be considered by the designer during the control implementation for the *DSF*. To sum up, the aim of the control strategy is the adaptation of the thermophysical behavior of the *DSF* according to the different boundary conditions, for a better energy and indoor climate performance. Considering typical summer and winter operations for the façade, the main aims for its configurations can be summarized as [4]:

- For summer period, the main aim is the one to reduce the passive solar gains and the related overheating risk. The most feasible ventilation modes of the façade for this aim are the *OAC* and the *AE*. In some cases, also the *AS* configuration can be adopted, to provide the indoor environment with fresh air.
- For winter period, on the contrary, the main aim of the control strategy is to maximize the passive solar gains to reduce heat losses through the envelope and energy for ventilation heating. The most feasible ventilation modes that can be associated to these aims are *AS*, *TB*, *IAC* and *CF*. Anyway, for some

warmer climates, also the use of the *OAC* can be required in winter season, to avoid possible overheating inside the cavity.

## **2.2. Control logics and double skin façade performance**

In this section, the focus of the analysis is the evaluation of the possible relations between a certain performance target of the *DSF* and the control strategies that can be used to achieve them. Indeed, this study process can be articulated through the following 5 steps:

- 1) *Definition of the performance requirements*
- 2) *Connection between performance requirements and control strategies*
- 3) *Selection of the control variables.*
- 4) *Selection of the façade actuators*
- 5) *Implementation of the control strategies for the DSF*

### **2.2.1. Definition of the performance requirements**

About the first point, there are basically four domains of the performance for a generic façade system [13]. The first three are mainly linked with the indoor environmental quality (*IEQ*) while the fourth one is focused on the energy performance of the whole building.

- Thermal comfort, linked to the indoor temperatures (both air and operative)
- Visual comfort, linked with the illuminance levels inside the indoor environment
- Indoor air quality, connected with the amount of *CO<sub>2</sub>* inside the indoor environment
- Energy need, focused on the energy requirements of the whole building for space heating and cooling, ventilation and artificial lighting

For these four different aspects of the performance, it is possible to identify standards and regulations (both national and international) that set optimal values for the related physical quantities (temperatures, illuminance levels, energy consumptions etc.), in relation to different performance targets. These values, since they are prescribed by specific requirements and authorities, can be used to address the control definition of the façade system. For the thermal comfort, optimal values of indoor operative temperatures that must be guaranteed inside different typologies of environments are provided in the standards *EN ISO 7730:2005* and *EN 16798-1:2019* [14] [15].

For the visual comfort, minimum values of indoor illuminance levels on the working plane that must be guaranteed are provided in the standard *EN 12464-1:2011* [16]. Additional requirements for daylight are also provided inside the standard *EN 17037:2018*, regarding the glare discomfort risk [17]. About the energy savings, for some countries (Norway for example) maximum values of total net energy demand

are expressed for different categories of buildings [18]. It is not anyway possible to have related standards for other countries about the maximum energy consumption for office buildings. For this reason, for the evaluation of the energy performance, a comparison with a traditional transparent façade system can be used (defining a comparative analysis with a baseline system, as done in this Thesis work). Additional requirements, not specifically linked to the performance of the system, are referred to the ventilation of the indoor environment. The standard *EN 16798-1:2019* defines in this case default predefined ventilation air flow rates for offices, that must be provided to the indoor spaces [19].

### **2.2.2. Connection between performance goals and control strategies**

For each one of the performance targets, it is then necessary to understand which general control strategy can be defined to reach the predefined goal. In particular, the designer must understand how a specific control can be used to address a specific predefined goal.

- For the thermal comfort in the indoor environment, the possible control strategies that can be defined are for example:
  - 1) Control of the solar gains in summer to avoid possible overheating conditions.
  - 2) Control of the solar gains in winter to maximize their benefits on the indoor thermal environment.
  - 3) Control of the cavity ventilation to avoid possible overheating of the cavity air.
  - 4) Control of the air flow paths from the cavity to the indoor environment to avoid possible cold drafts or vice versa hot air streams
- For the visual comfort, the possible control strategies for the *DSF* actuators are:
  - 1) Guarantee the minimum illuminance levels on the work plane using the daylight.
  - 2) Control of the glare discomfort risk.
- For the overall energy performance:
  - 1) Control and improve the insulation level of the façade system during the winter period to reduce the transmission heat losses towards the external environment and reduce in this way the energy needs for space heating.
  - 2) Control the air flows path in the cavity to guarantee a pre-heating of the ventilation air by means of the incident solar radiation (passive use of solar gains), which can be consequently introduced in the indoor environment or in the *HVAC* system, with the purpose to reduce the energy need for ventilation heating.

- 3) Control the air flows paths in the cavity to ensure the extraction of the heated air inside it, reducing the energy need for space cooling during the summer.
- 4) Control the solar radiation entering in the indoor environment, that can cause possible overheating and therefore an increased energy demand for space cooling.
- 5) Control the amount of the daylight entering inside the indoor environment, to limit the use of artificial lighting during the occupied hours and therefore the related energy consumption.

### **2.2.3. Selection of the control variables**

After the definition of the possible control strategies, the designer should set a group of control variables that can be used for the addressing of the control strategies for the adaptive façade. The control variables for the *DSF* system can be referred to three main domains:

- Indoor environment, corresponding to the thermal zone linked with the façade system
- Outdoor environment, influenced by climate and weather conditions
- Cavity of the double skin façade

For each one of these domains, it is possible to set a group of possible control variables that can be used for the addressing of the operations of the façade system.

Regarding the indoor environment, the control variables allow to evaluate the indoor climate conditions and in function of them define the proper control strategies for the façade system. These control variables are important especially for the definition and the monitoring of the indoor comfort conditions (both thermal and visual) and the indoor air quality of the zone:

- 1) *Indoor air temperature ( $\theta_{indoor}$ )*
- 2) *Indoor illuminance levels on the horizontal plane ( $E_H$ )*
- 3) *Indoor  $CO_2$  concentrations*

For the outdoor environment, the control variables can be used to monitor external environmental conditions in which the façade system is working:

- 1) *Outdoor air temperature ( $\theta_{outdoor}$ )*
- 2) *Incident solar radiation on the façade ( $I_{sol}$ )*

For the double skin façade cavity, the main one to consider is the cavity air temperature:

- 1) *Cavity air temperature ( $\theta_{cavity}$ )*

#### 2.2.4. Selection of the façade actuators and their possible states

In the next step, it is necessary to understand which actuators of the *DSF* are more suitable for the actuation of the control. The actuators that can be used for the switching of the *DSF* configurations are the following ones (*Figure 5*), illustrated in the functional scheme of the *DSF* model that has been adopted for the Thesis work.

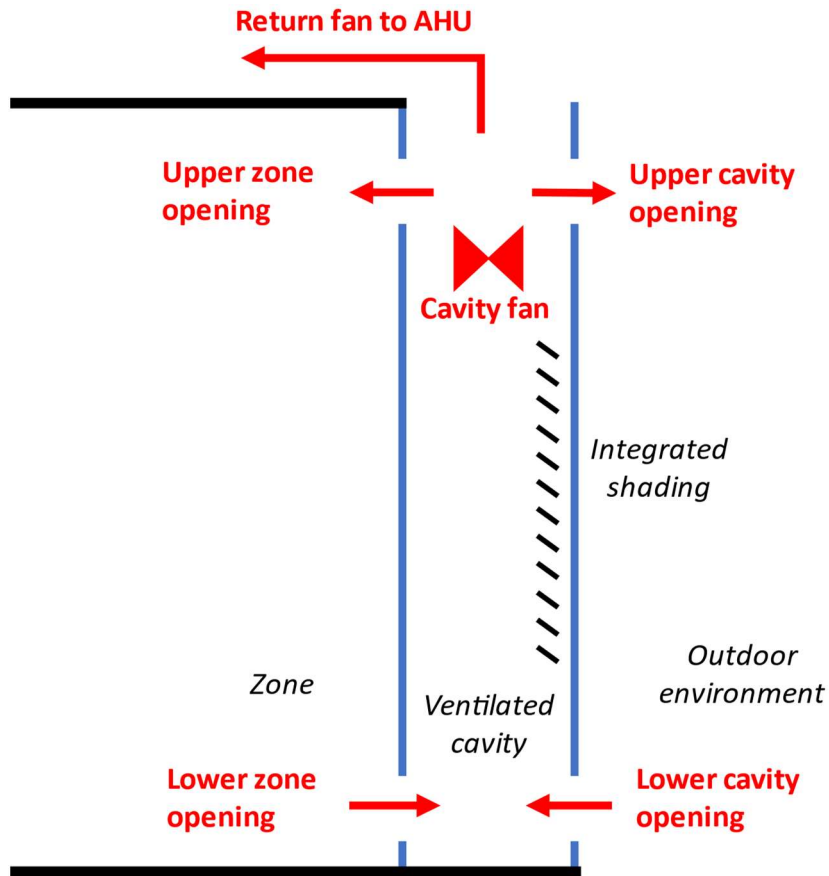


Figure 5: Functional scheme of the flexible double skin model to model inside IDA ICE

- Cavity-integrated shading devices (for the selected *DSF* system a venetian blind will be used): for them it is possible to regulate the drawn mechanism (activation of the venetian blind) and the slat angle when the blind is completely drawn.
- Zone openings (upper and lower), located in the inner skin of the *DSF*: they can be open or closed to allow or stop the air to be transferred between the cavity and the adjacent zone.
- Cavity openings (upper and lower), located at the top and at the bottom of the façade cavity: they can be basically open or closed, as seen for the zone

openings. In this case, the openings have the role to allow or stop the air to be transferred between the cavity and the outdoor environment.

- Return fan to the *AHU* (for the implementation of the *CF* configuration): it can be *Off* or *On* (with a certain implemented air flow, corresponding to the one that is provided to the zone).
- Cavity fan for the implementation of the mechanical ventilation in the cavity. It can be *On* or *Off*, with different implemented air flows, in accordance with the façade configurations.

Each one of the listed *DSF* actuators, can be suited for the application of a certain control strategy, acting on different aspects of the performance domain.

In particular:

- **Integrated shading devices:** they are the most suitable actuators that can be used for the performance control of the *DSF* [20]. The main role of the integrated shading devices is to block the direct solar radiation entering inside the indoor environment. This aspect is important both for the indoor thermal comfort conditions and the cooling energy savings during the summer season. Integrated shading devices can be also useful during the heating season: they can absorb the direct solar radiation and then release the heat to the cavity air. They are also important for the daylight availability of the indoor environment and the reduction of energy consumptions for artificial lighting.
- **Zone openings:** they are important for the *IAQ* control of the indoor environment since they can provide fresh air to the zone and reduce in this way the  $CO_2$  concentrations. The use of openings for the air circulation between the air cavity and the zone has also some important consequences on the thermal comfort of the occupants (due to the possibility of too hot or too cold air introduced inside the indoor environment by means of them). Acting on the indoor temperature of the zone, the zone openings control has also effects on the overall energy use for space cooling and heating.
- **Cavity openings:** they can be used for the definition of the façade ventilation modes, as seen for the zone openings. Consequently, the control of the cavity openings (and therefore of the air flows) has multiple effects on the thermal comfort conditions, the energy savings for space cooling, space heating and ventilation pre-heating.
- **Cavity fan:** it can basically act on the air velocity in the cavity when the mechanical ventilation is implemented inside it.
- **Return fan to the AHU:** it can be used to redirect the cavity air to the *AHU* of the thermal zone, exploiting the passive pre-heating of the ventilation air.

### **2.2.5. Implementation of the control strategies for the double skin façade**

At the end of the process, the control can be implemented for the *DSF*. As mentioned in 1.4 the focus of the control implementation will be the rule-based approach. It is a less advanced control solution compared to the model-based approach, but it is easier to define, and it also requires a lower computational effort from the control system implemented in the façade model. The typical configuration of the rule-based control logics, as mentioned, is a succession of *if-then* conditions, that assumes the shape of a control decision tree. The actuators considered for the application of the control are in this case the ones already listed in 2.2.4.

The most appropriate way to define and assess the efficacy of different rule-based control strategies is to create different combinations of control for the different façade actuators, in the way that will be illustrated in the following section.

The two main objectives of the implemented control strategies are indeed:

- The control of the configuration of the installed dynamic shading devices
- The control of the cavity air flows

These two, cavity air flows and shading system, are the so-called *control targets* of the control logic. It is also possible to make a distinction between the different validity periods of the implemented control logics:

- Cooling season (the control strategy can be applied mainly in summer)
- Heating season (the control strategy can be applied mainly in winter)

In the first case, the implemented control strategies for the air flows in the cavity are addressed to the typical summer configurations of the *DSF*:

- *OAC*, both with natural and mechanical ventilation in the cavity. The mechanical air flow in the cavity can be increased if a greater extent of heat must be removed.
- *AE*, both with natural and mechanical ventilation in the cavity. As seen for the *OAC* configuration, also in this case it is possible to increase the mechanical air flows inside the cavity if necessary.
- *AS*, with natural ventilation inside the cavity if the temperature inside it is low enough.

In the second case, on the other hand, the implemented control strategies for the air flows are referred to the typical winter configurations of the *DSF*:

- *TB*, for which no air circulation in the cavity is present



- *AS*, with natural ventilation in the cavity
- *IAC*, with natural ventilation in the cavity
- *CF*
- *OAC*, with natural ventilation in the cavity

As it is possible to see, only natural ventilation is implemented inside the cavity during the winter season, to avoid to large velocities inside the cavity that can cause an increase of the convective heat losses. Consequently, 10 different configurations are possible for the summer and winter operations of the *DSF* (Table 1). To each configuration, a number from 1 to 10 can be assigned for an easier recognition (See also, in this case, *Appendix D: Control implementation in IDA ICE*).

<b><i>Cavity air flow configurations</i></b>
#1: <i>Thermal Buffer</i>
#2: <i>Outdoor Air Curtain (with natural ventilation in the cavity)</i>
#3: <i>Outdoor Air Curtain (with mechanical ventilation in the cavity)</i>
#4: <i>Outdoor Air Curtain (with mechanical ventilation in the cavity and increased air flow)</i>
#5: <i>Air Exhaust (with natural ventilation in the cavity)</i>
#6: <i>Air Exhaust (with mechanical ventilation in the cavity)</i>
#7: <i>Air Exhaust (with mechanical ventilation in the cavity and increased air flow)</i>
#8: <i>Air Supply</i>
#9: <i>Climate Facade</i>
#10: <i>Indoor Air Curtain</i>

Table 1: List of possible air flows configurations that can be implemented inside the cavity

While for the summer just three air flows configurations are used (mainly because of the higher temperatures that can be reached inside the cavity) for the winter season there is the possibility to use the air cavity for a wider range of applications, from the envelope insulation to the air-preheating and supply, considering anyway a possible overheating risk for warmer climates in presence of high solar radiation levels (for this reason, the *OAC* configuration is proposed).

For each one of the two periods (summer and winter), specific aims are already defined a priori, as already illustrated at the end of 2.1. Inside the two selected periods, it is then possible to define control strategies for the occupied hours and control strategies for the unoccupied periods (mainly lunch hours and night periods), for which different aims must be followed by the façade behavior: comfort for the occupants in the first case and energy savings in the second one. Inside each one of

the two time periods, it is then possible to consider control strategies that are linked to the control of the configurations of the installed dynamic shading devices and on the other hand on the control of the cavity air flows.

The previously listed subdivision is consequently a 3 levels classification based on:

- *Validity period of the control* (Summer or winter season)
- *Occupancy of the zone* (Occupied or unoccupied hours)
- *Control target* (Shading system or cavity air flows)

According to these three levels it is possible to classify the different typologies of control strategies for the *DSF* in eight different groups (*Table 2*). These groups of controls can be combined in different ways, enabling the definition of different control logics.

<b>Group of controls</b>	<b>Seasonal operations</b>	<b>Occupancy condition in the zone</b>	<b>Control target</b>
Group 1	Summer	Occupied	Air flows
Group 2	Summer	Unoccupied	Air flows
Group 3	Summer	Occupied	Shading
Group 4	Summer	Unoccupied	Shading
Group 5	Winter	Occupied	Air flows
Group 6	Winter	Unoccupied	Air flows
Group 7	Winter	Occupied	Shading
Group 8	Winter	Unoccupied	Shading

*Table 2: Definition of the eight different groups of rule-based control types*

With this classification, the two *control targets* (shading systems and air flows in the cavity) are basically independent to each other and therefore different combinations of control algorithms can be applied to the façade system (as it will be shown in 2.3). Different decision blocks referred to the cavity air flows and the shading system can be merged and combined forming wider decision trees, generating in this way different combinations of control that can be implemented for the *DSF*.

According to the existing literature about the control of *DSF* and adaptive envelope systems [6] [5] [21] [22] [23] [24] [25], the possible combinations of control for the cavity air flows and the shading system during the heating and the cooling seasons are numerous. In the initial definition of the control combinations during the Master Thesis work, the total number of available combinations was 112 for the summer season and 42 for the winter season, given by 14 forms of control for the shading system and respectively 8 and 3 control logics for the cavity air flows in the two seasons.

Considering the long process necessary for the implementation of the control in IDA ICE (see *Appendix D: Control implementation in IDA ICE*) and the subsequent evaluation of the results, this number has been considerably reduced to ensure a proper

result for the Thesis work. In the next section (2.3), the analysis of the different selected combinations will be conducted, analyzing the typology of the control, the involved control variables, and the possible benefits regarding their use in the façade operations. From *Figure 6* to *Figure 10* are reported some examples of variation of the cavity ventilation modes of the *DSF* in a selected summer day in Frankfurt (11<sup>th</sup> July) with the different forms of air flows control that will be illustrated in 2.3, the section focused on the definition of the different control combinations for the façade system. The numbers of the configurations are the ones proposed in *Table 1*: in this case, the ones adopted for the summer season are 2, 3, 4, 5, 6, 7 and 8.

As it is possible to see, in function of different combinations of control, different configurations can be assumed by the *DSF* ventilation modes. Some combinations, as *SC#3* (*Figure 6*) and *SC#5* (*Figure 7*), give only 2 configurations as output for the *DSF*, in this case 5 and 7. Other combinations, as *SC#18* (*Figure 10*), on the other hand, shows more variability in the configuration change, adopting for example 2, 5 and 8 as output configurations in the selected day. The higher is the number of possible switchable configurations, the higher are of course the adaptability and the flexibility features of the façade system.

The innovative concept of this kind of *DSF* is indeed the possibility to switch between different operating strategies, in function of an implemented control logic, to ensure the best adaptability to changing boundary conditions. The implemented control logic indeed must be able to fully exploit the flexibility of the façade system.

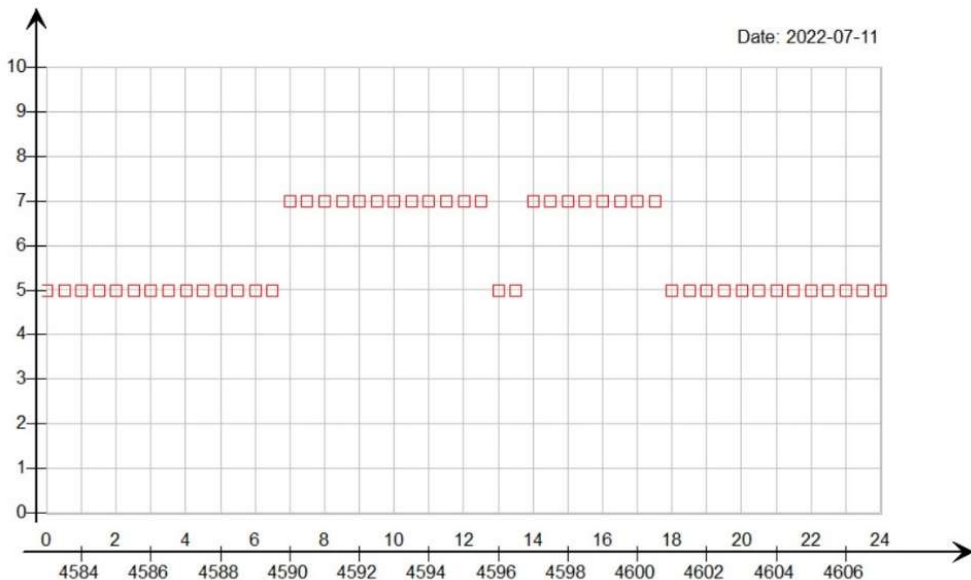


*Figure 6: Variation of DSF configurations with the implementation of the control combination SC#3 (Summer Day). Output signal from IDA ICE.*

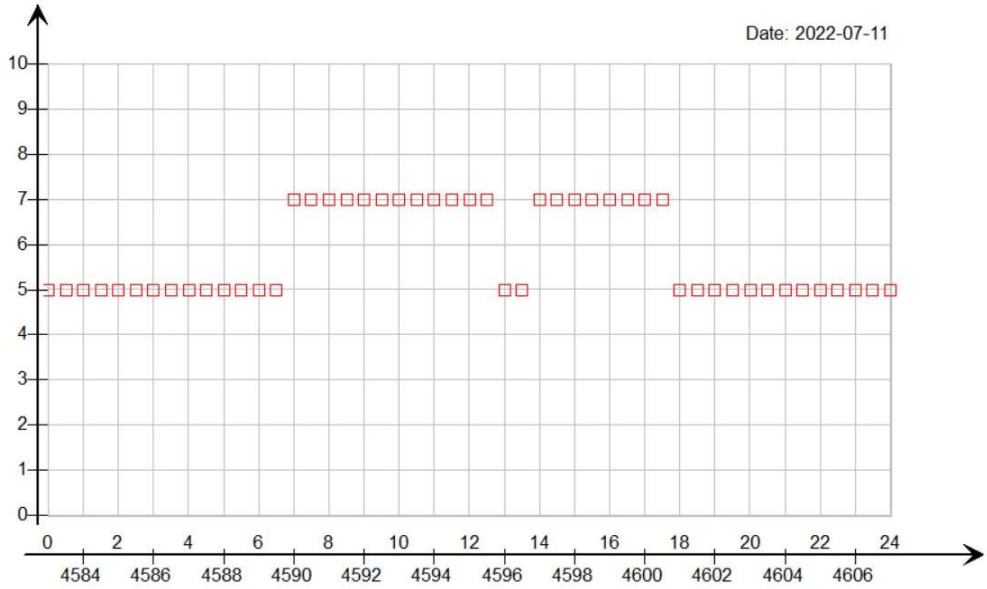


Figure 7: Variation of DSF configurations with the implementation of the control combination SC#5 (Summer Day). Output signal from IDA ICE.

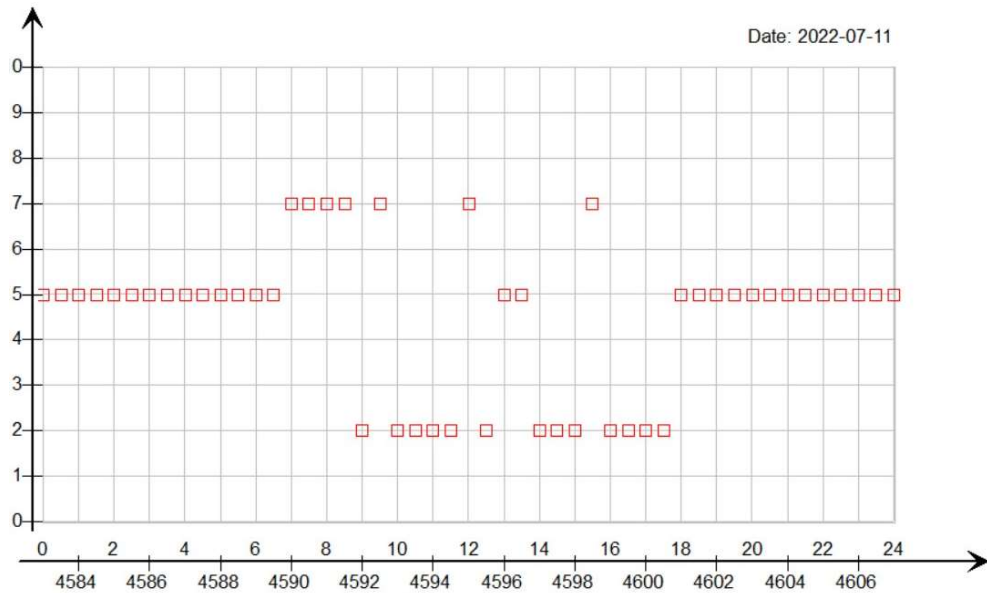


Figure 8: Variation of DSF configurations with the implementation of the control combination SC#10 (Summer Day). Output signal from IDA ICE.

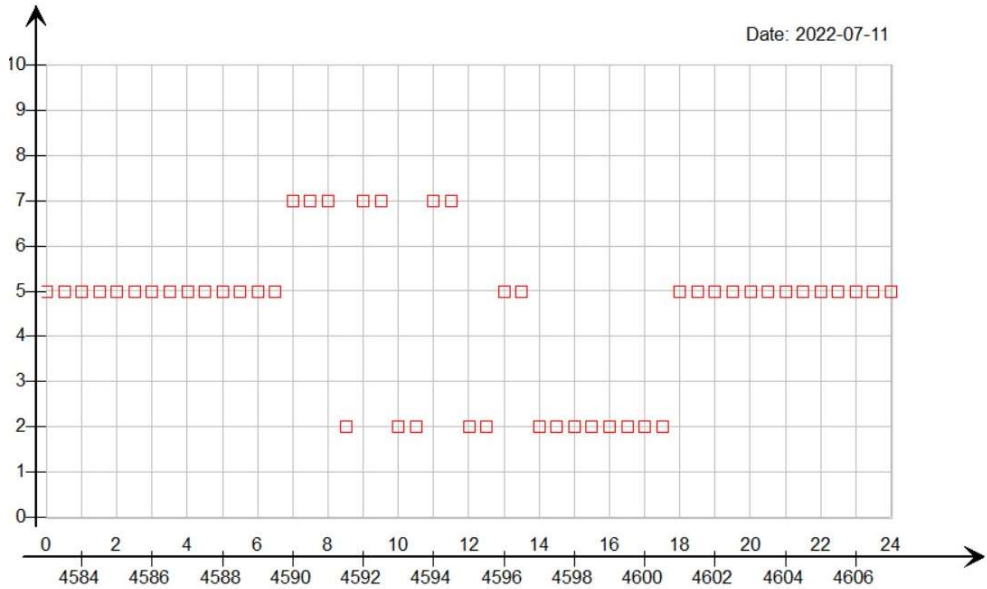


Figure 9: Variation of DSF configurations with the implementation of the control combination SC#15 (Summer Day). Output signal from IDA ICE.

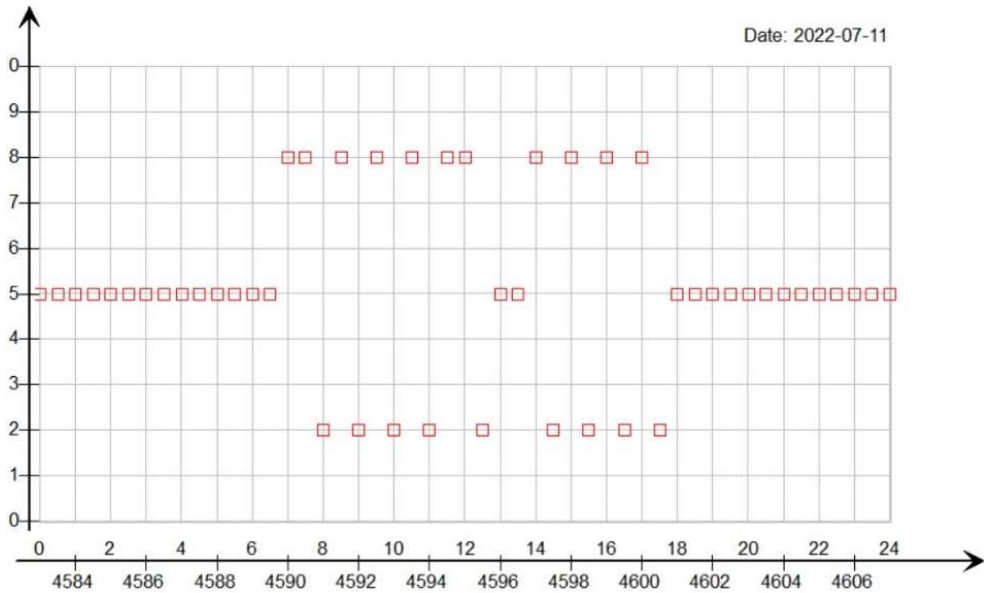
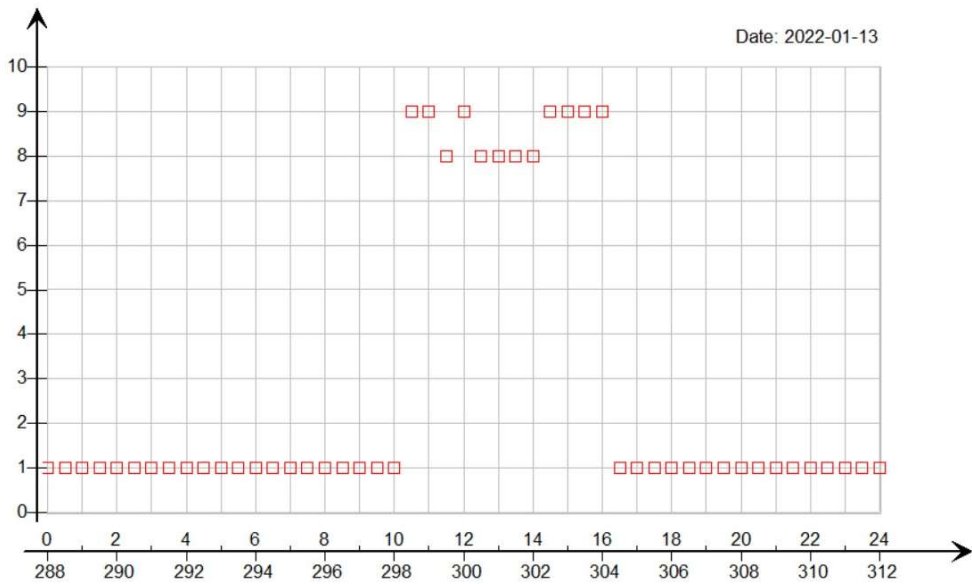


Figure 10: Variation of DSF configurations with the implementation of the control combination SC#18 (Summer Day). Output signal from IDA ICE.

The same variation can be observed in a typical winter day (13<sup>th</sup> January), but with the ventilation modes proposed for the heating season in Frankfurt (from Figure 11 to Figure 13): in this case, the possible ones proposed for the winter season are 1, 2, 8,

9 and 10. The same concepts valid for the summer season can be of course repeated for the winter: the higher is the number of switchable configurations, the higher is the adaptability capacity of the *DSF*.

As seen for the cooling season, some types of control (*Figure 11* and *Figure 12*) allow for a certain number of configurations, while other types (*Figure 13*) on the other hand generates different outputs.



*Figure 11: Variation of DSF configurations with the implementation of the control WC#3 (Winter Day). Output signal from IDA ICE.*

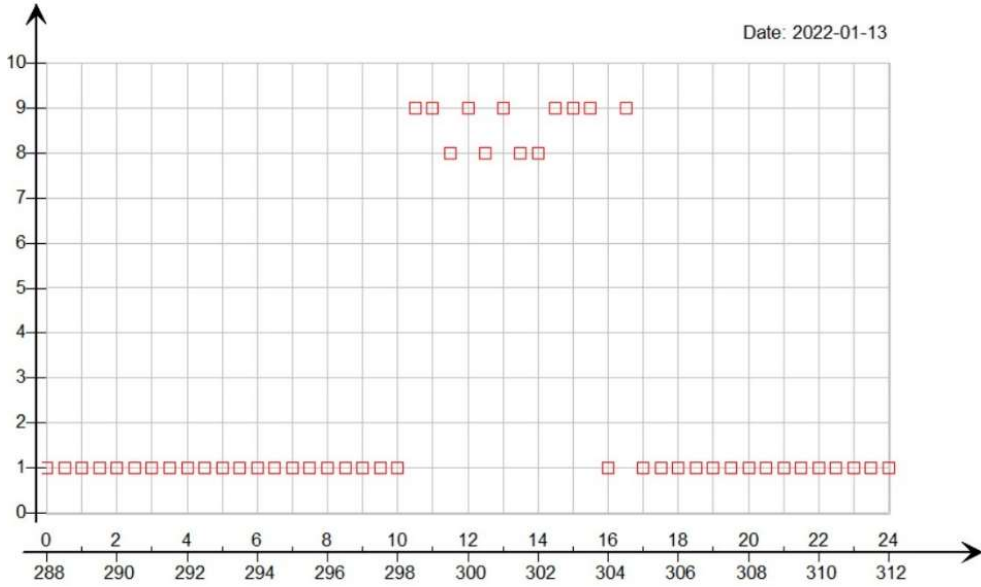


Figure 12: Variation of DSF configurations with the implementation of the control WC#8 (Winter Day). Output signal from IDA ICE.

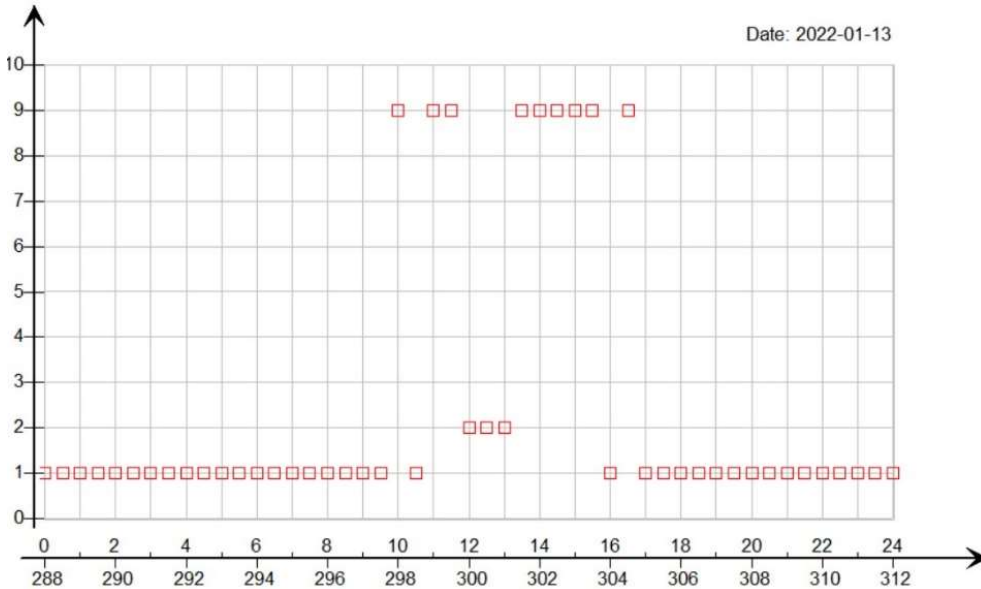


Figure 13: Variation of DSF configuration with the implementation of the control combination WC#9 (Winter Day). Output signal from IDA ICE.

In a similar way to the cavity ventilation modes, the slat angle of the blind can be regulated in a flexible way, in accordance with different forms of control. In the following pages are reported the examples of the regulation of the slat angle in

function of the *cut-off* position (Figure 14 and Figure 16) or in function of a pre-defined schedule (Figure 15 and Figure 17), in the a summer and winter day already considered in the previous examples (13<sup>th</sup> July and 11<sup>th</sup> July). Also in this case the combinations of control for the shading system of the *DSF* will be illustrated in 2.3.

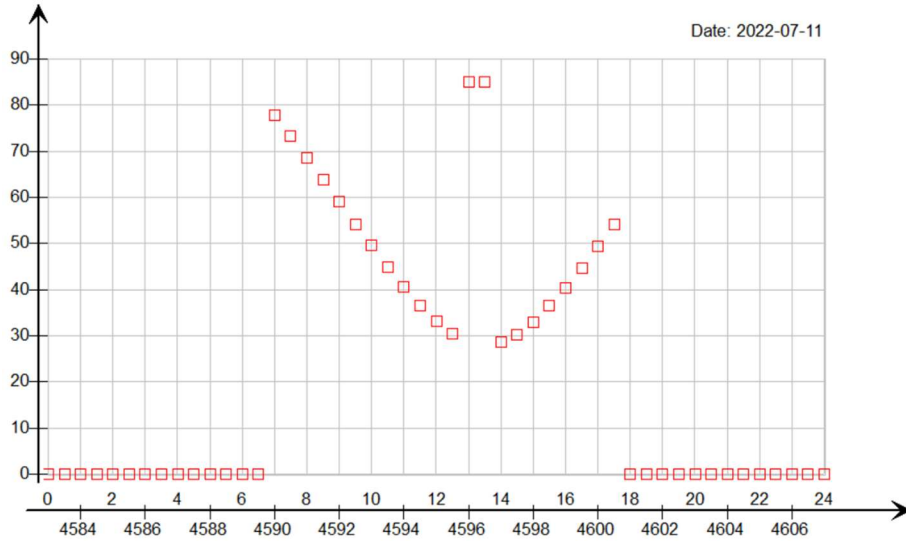


Figure 14: Variation of blind slat angle with the implementation of the control combination SC#3 (Summer Day). Output signal from IDA ICE.

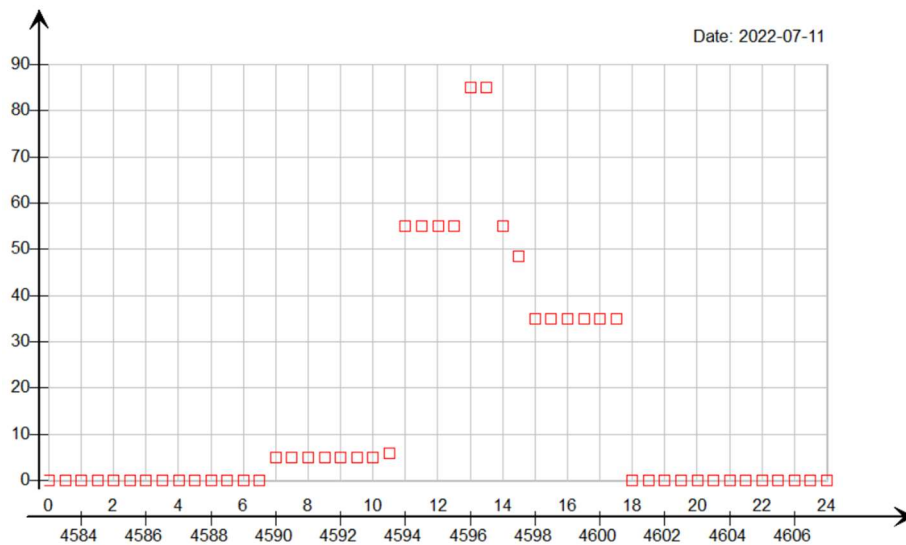


Figure 15: Variation of blind slat angle with the implementation of the control combination SC#20 (Summer Day). Output signal from IDA ICE.



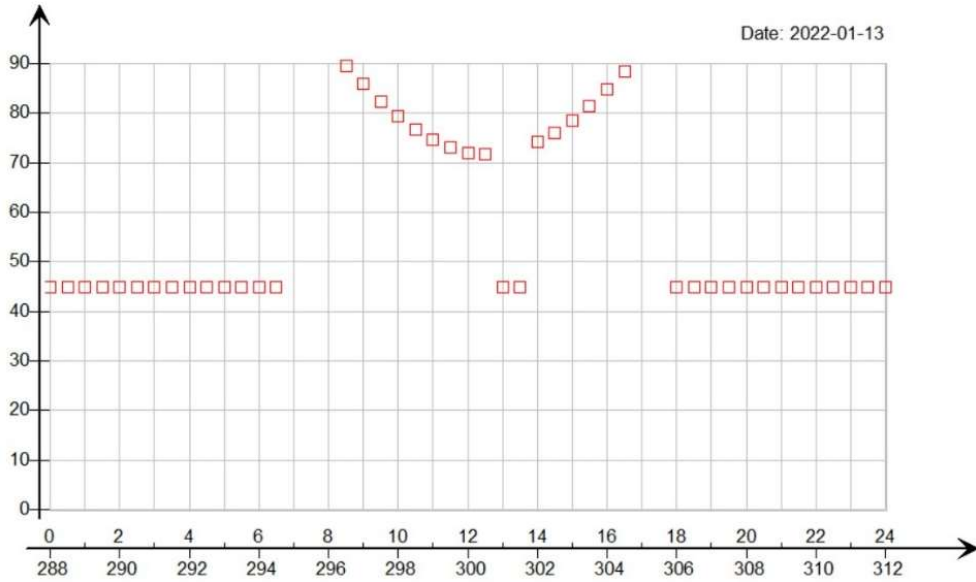


Figure 16: Variation of blind slat angle with WC#3 (Winter Day). Output signal from IDA ICE.

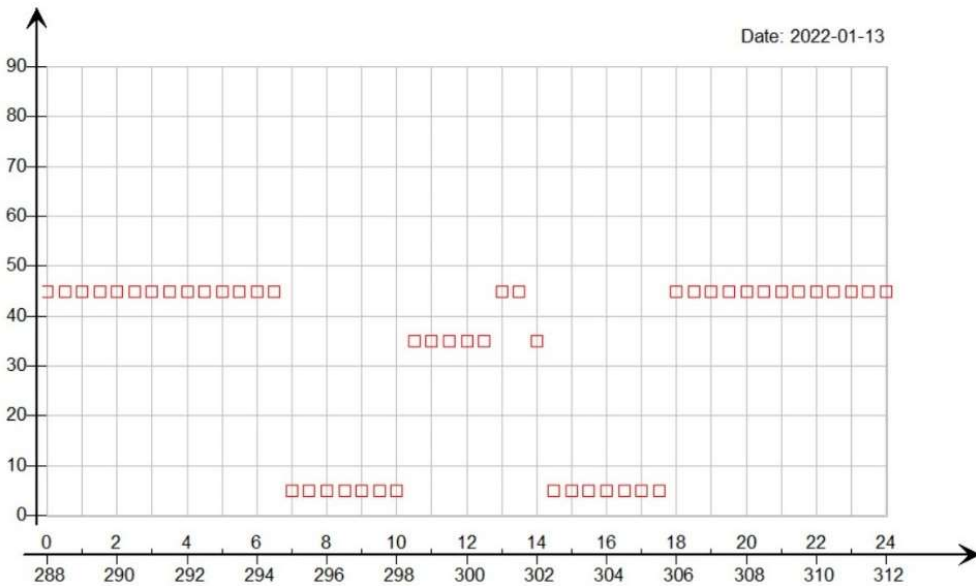


Figure 17: Variation of blind slat angle with WC#12 (Winter Day). Output signal from IDA ICE.

### 2.3. Combinations of the different control logics

As mentioned before, the different control strategies of the eight groups of control can be combined in different way, creating control decision trees for air flow control and shading control in summer and winter conditions.

The groups of control referred to the occupied and unoccupied hours in the different seasons are always coupled together, to apply different strategies during the working hours and the night (or the lunch time). In the next pages, the process used for the definition of different combinations of control strategies for the different actuators will be discussed and analyzed.

- **Control for the summer season**

*Combination of Group 1 and Group 2: Summer Airflow Control (SAC)*

Controls of the Group 1 and Group 2 can be used for the air flows control in summer, during the occupied and the unoccupied hours. The code for the identification of these controls is *SAC* (*Summer Air flow Control*). In the case of the summer control of the cavity air flows, 5 different controls will be adopted (from *SAC#1* to *SAC#5*).

In *SAC#1*, the switch between the *OAC* natural and the *AE* natural configuration is performed in function of the indoor  $CO_2$  levels inside the zone. The increasing of the required air flow when the *AE* configuration is implemented is performed in function of the indoor  $CO_2$  levels (the same has been performed also for the other 4 combinations of summer air flows control): the higher the concentration, the higher the amount of air that is extracted by the cavity of the façade. The increasing of the required air flow when the *OAC* configuration is implemented is performed on the other hand in function of the indoor air temperature of the zone: the higher the indoor temperature is, the higher is the amount of heat that is extracted from the cavity, for the over-heating prevention inside the thermal zone.

In *SAC#2*, the switch between *OAC* natural and *AE* natural is performed in the same way as *SAC#1*, but the increasing of the ventilation air flow for the *OAC* mechanical configuration is performed in function of the cavity air temperature. Also in this case the over-heating prevention is performed, using another control variable (the cavity air temperature instead of the indoor air temperature).

In *SAC#3* and *SAC#4* respectively, the increasing of the air flows for the *OAC* mechanical configuration are performed in function of the indoor air temperature and the cavity air temperature (as seen in the two previously implemented controls) but the initial switch between the *OAC* natural and the *AE* natural is performed considering the indoor air temperature and the outdoor air temperature. The *OAC* configuration is kept for the worst indoor and outdoor temperature conditions, to ensure the removal of excess heat from the cavity. The *AE* configuration on the other hand is adopted just for milder outdoor conditions (considering a maximum threshold limit of outdoor air temperature).

Finally, for the *SAC#5* control, the use of the *AS* configuration with natural ventilation inside the cavity is implemented, for the introduction of fresh air from the outdoor environment through the cavity of the double skin façade. The *AS* configuration can

be implemented if the indoor concentrations of  $CO_2$  are above a certain threshold limit. Anyway, it is necessary to check before the temperature of the cavity, to avoid the introduction of too hot air from the cavity to the room. In this case, if the cavity air temperature is too high, the *AE* configuration is preferred anyway. Consequently, the total number of ventilation modes available in *SAC#5* is 3, one more than the other 4 types of control (*SAC#1*, #2, #3 and #4): the complexity of this last control can be consequently assumed higher, given the higher number of possible configurations for the ventilation modes.

For all the control logics, the strategy for the unoccupied hours is the one to keep the *AE* natural configuration in the cavity: for the lunch break for the removal of the hot air and for the night for night cooling purposes. The initial threshold limits of the control variables for the switching between the different façade configurations have been initially set in function of the standard *EN 16798-1* regarding the indoor thermal comfort conditions and the *IAQ* [15] [26].

After the first preliminary simulations performed on IDA ICE, the values have been modified to ensure a proper flexibility of the façade system between the different configurations implemented for the summer season and at the same time avoid possible numerical instabilities of the simulation (see *Appendix D: Control implementation in IDA ICE*). In this way the control has been optimized for the simulations on the *BPS* tool and the evaluation of the flexibility effectiveness on the performance of the *DSF*.

The list with the final applied values is here reported:

For *SAC#1*:

- $CO_{2,max,1}=600\text{ ppm}$
- $CO_{2,max,2}=750\text{ ppm}$
- $CO_{2,max,3}=1100\text{ ppm}$
- $\theta_{indoor,max,1}=24.5^\circ C$
- $\theta_{indoor,max,2}=26^\circ C$

For *SAC#2*:

- Same maximum threshold limits for the  $CO_2$  concentrations applied in *SAC#1*
- $\theta_{cavity,max,1}=26^\circ C$
- $\theta_{cavity,max,2}=32^\circ C$

For *SAC#3*:

- $CO_{2,max,2}=750\text{ ppm}$
- $CO_{2,max,3}=1100\text{ ppm}$
- $\theta_{indoor,max,1}=25^\circ C$

- $\theta_{indoor,max,2}=26^{\circ}C$
- $\theta_{indoor,max,3}=27^{\circ}C$
- $\theta_{outdoor,max}=26^{\circ}C$

For SAC#4:

- Same maximum threshold limits for  $CO_2$  concentrations, outdoor air temperature and indoor air temperature applied in SAC#3
- $\theta_{cavity,max,1}=30^{\circ}C$
- $\theta_{cavity,max,2}=35^{\circ}C$

For SAC#5:

- Same maximum threshold limits for  $CO_2$  concentrations and indoor air temperature applied in SAC#1
- $\theta_{cavity,max}=27^{\circ}C$

The codes and the related strategies for the occupied and unoccupied hours are reported in *Table 3*. The decision trees of the different controls are showed from *Figure 18* to *Figure 22* (rotated in vertical orientation to allow a better visualization).

Code for the control	Occupied hours strategy	Unoccupied hours strategy (lunch time and night)
SAC#1	<ul style="list-style-type: none"> <li>• <i>OAC-AE</i> configurations switch in function of the <math>CO_2</math> level in the zone</li> <li>• Implementation of <i>OAC</i> mechanical configuration in function of indoor air temperature in the office</li> <li>• Increasing of <i>AE</i> mechanical air flows in function of the <math>CO_2</math> levels in the zone</li> </ul>	<ul style="list-style-type: none"> <li>• <i>AE</i> natural configuration during the night</li> <li>• <i>AE</i> natural configuration during the lunch hour</li> </ul>
SAC#2	<ul style="list-style-type: none"> <li>• <i>OAC-AE</i> configurations switch in function of the <math>CO_2</math> level in the zone</li> <li>• Implementation of <i>OAC</i> mechanical configuration in function of cavity air temperature</li> <li>• Increasing of <i>AE</i> mechanical air flows in function of the <math>CO_2</math> levels in the zone</li> </ul>	<ul style="list-style-type: none"> <li>• <i>AE</i> natural configuration during the night</li> <li>• <i>AE</i> configuration during the lunch hour</li> </ul>
SAC#3	<ul style="list-style-type: none"> <li>• <i>OAC-AE</i> configurations switch in function of the indoor/outdoor air temperatures</li> <li>• Implementation of <i>OAC</i> mechanical configuration in function of indoor air temperature in the office</li> <li>• Increasing of <i>AE</i> mechanical air flows in function of the <math>CO_2</math> levels in the zone</li> </ul>	<ul style="list-style-type: none"> <li>• <i>AE</i> natural configuration during the night</li> <li>• <i>AE</i> natural configuration during the lunch hour</li> </ul>
SAC#4	<ul style="list-style-type: none"> <li>• <i>OAC-AE</i> configurations switch in function of the indoor/outdoor air temperatures</li> </ul>	<ul style="list-style-type: none"> <li>• <i>AE</i> natural configuration during the night</li> </ul>

	<ul style="list-style-type: none"> <li>• Implementation of <i>OAC</i> mechanical configuration in function of cavity air temperature</li> <li>• Increasing of <i>AE</i> mechanical air flows in function of the <i>CO<sub>2</sub></i> levels in the zone</li> </ul>	<ul style="list-style-type: none"> <li>• <i>AE</i> natural configuration during the lunch hour</li> </ul>
SAC#5	<ul style="list-style-type: none"> <li>• <i>OAC-AS-AE</i> configurations switch in function of the cavity temperature and the indoor temperature</li> <li>• Increasing of the cavity air flows in function of the indoor temperature (for <i>OAC</i>) and <i>CO<sub>2</sub></i> levels in the zone (for <i>AE</i>)</li> </ul>	<ul style="list-style-type: none"> <li>• <i>AE</i> natural configuration during the night</li> <li>• <i>AE</i> natural configuration during the lunch hour</li> </ul>

*Table 3: Control combinations for the airflows during the summer season*

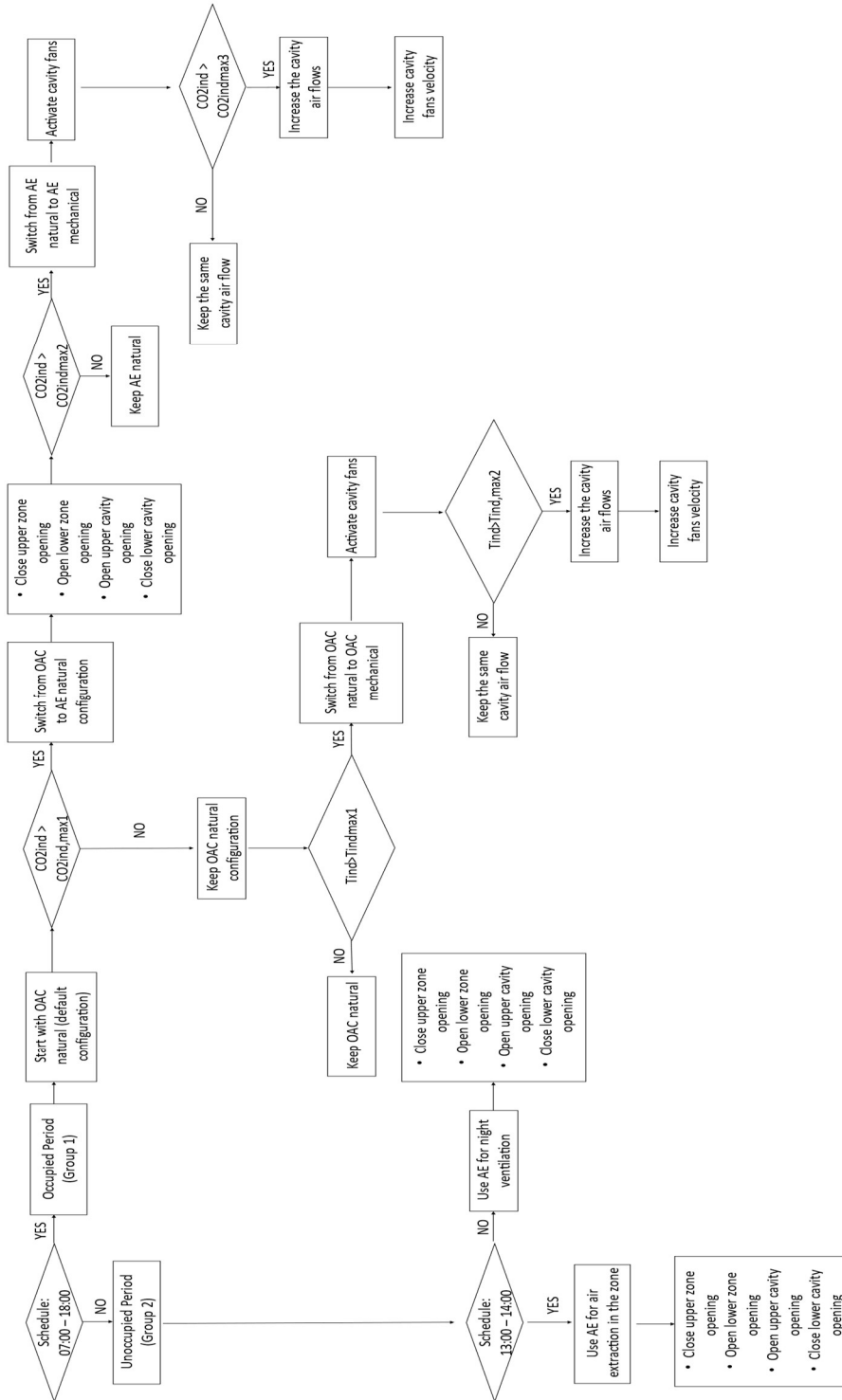


Figure 18: SAC#1 decision tree

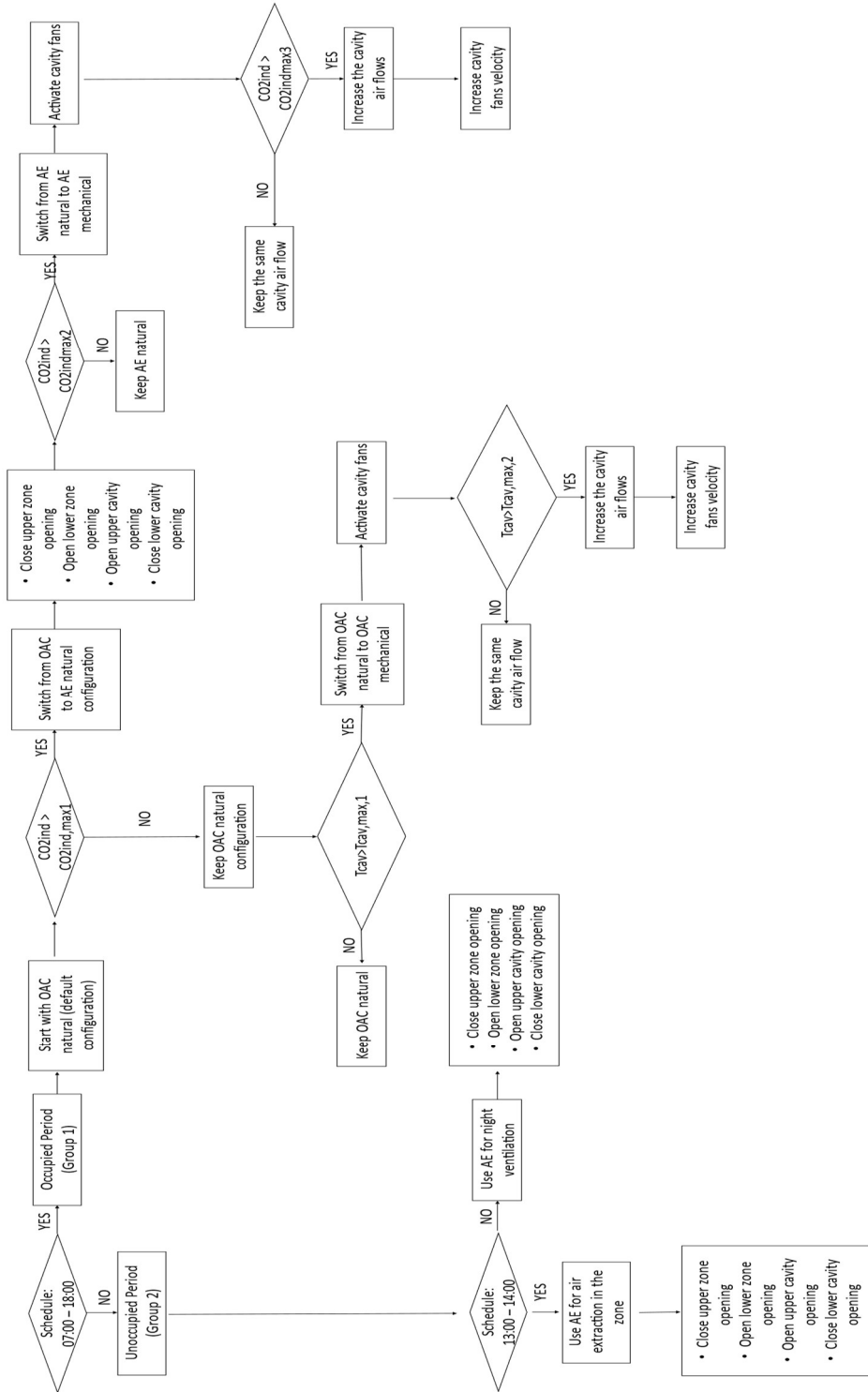


Figure 19: SAC#2 decision tree

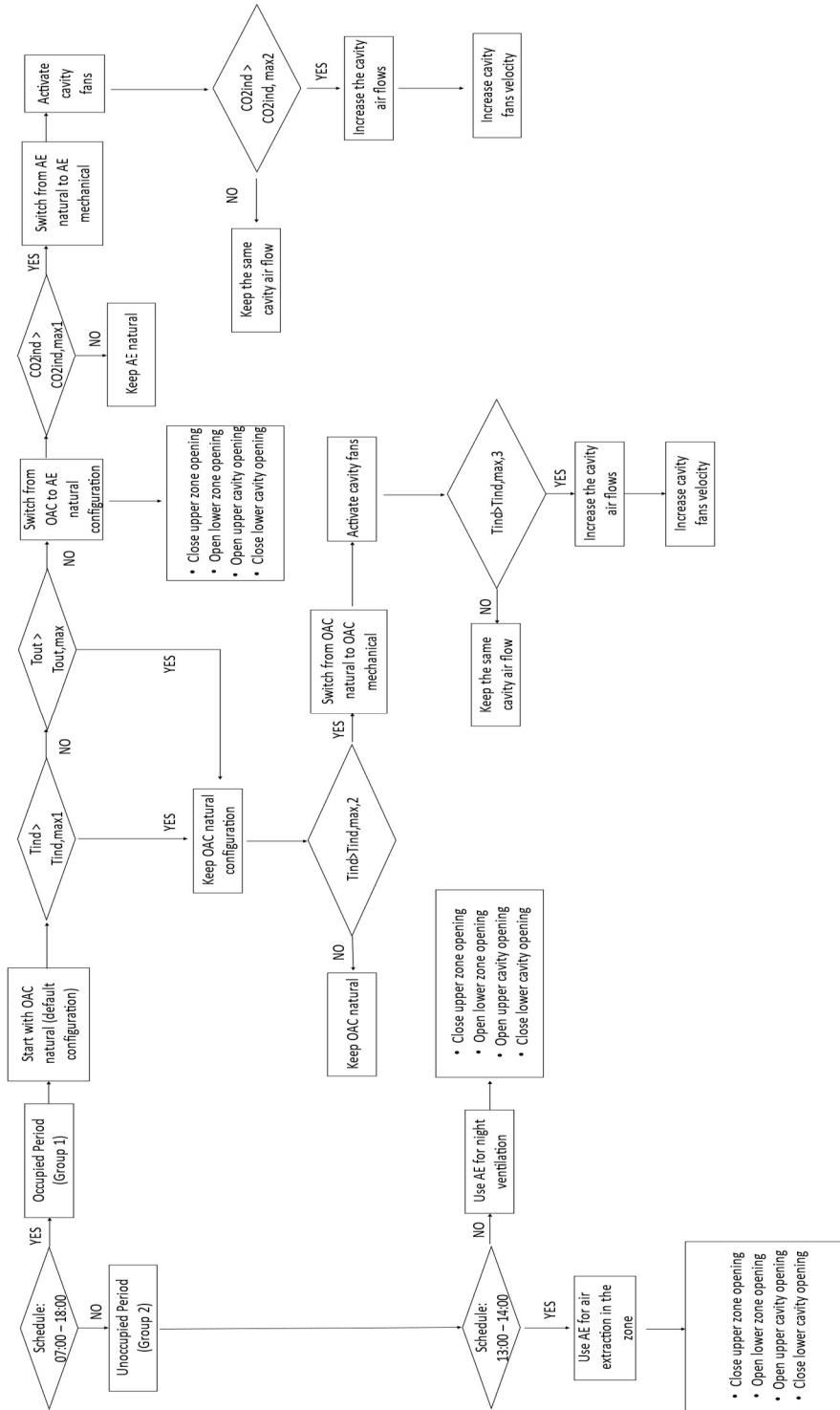


Figure 20: SAC#3 decision tree



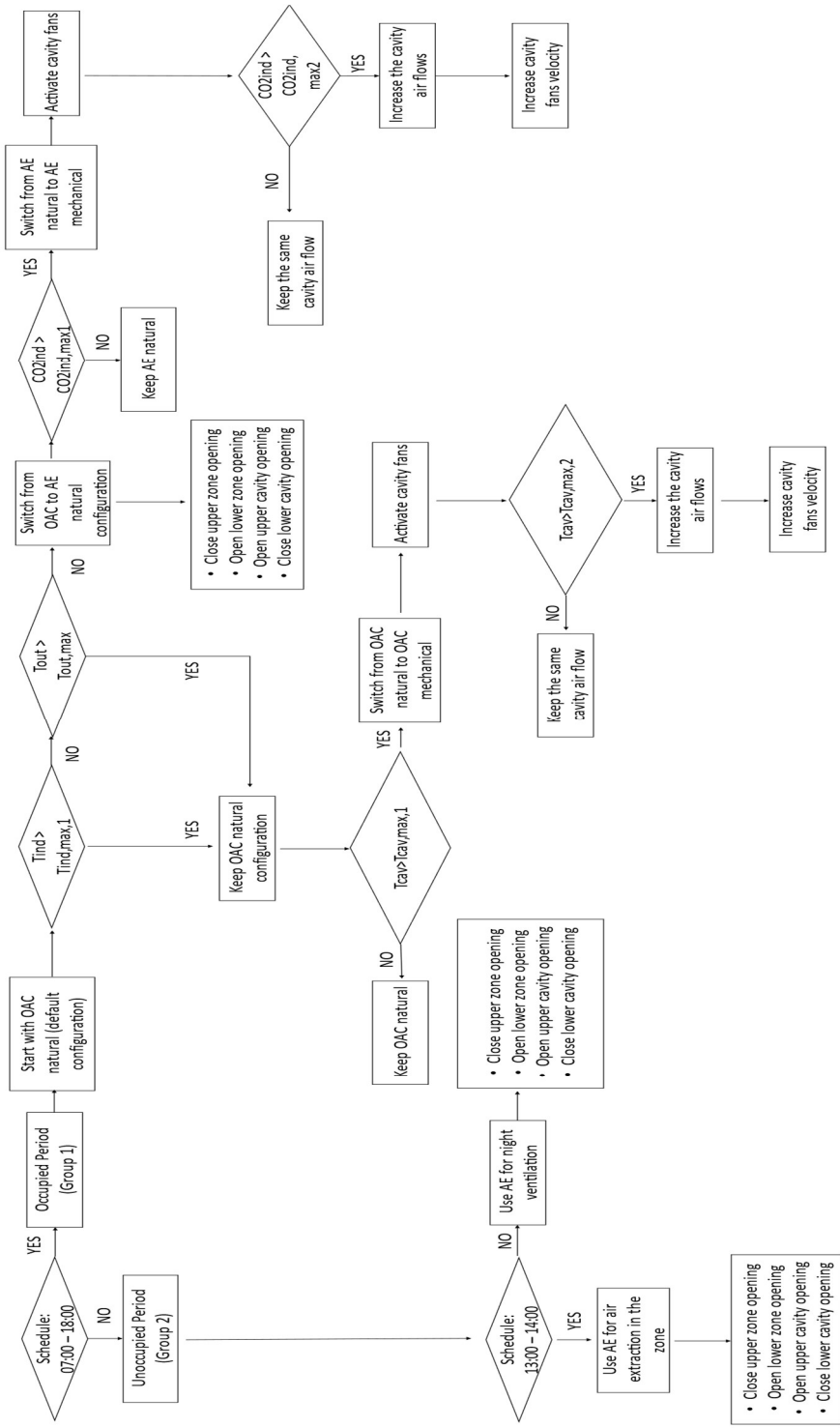


Figure 21: SAC#4 decision tree

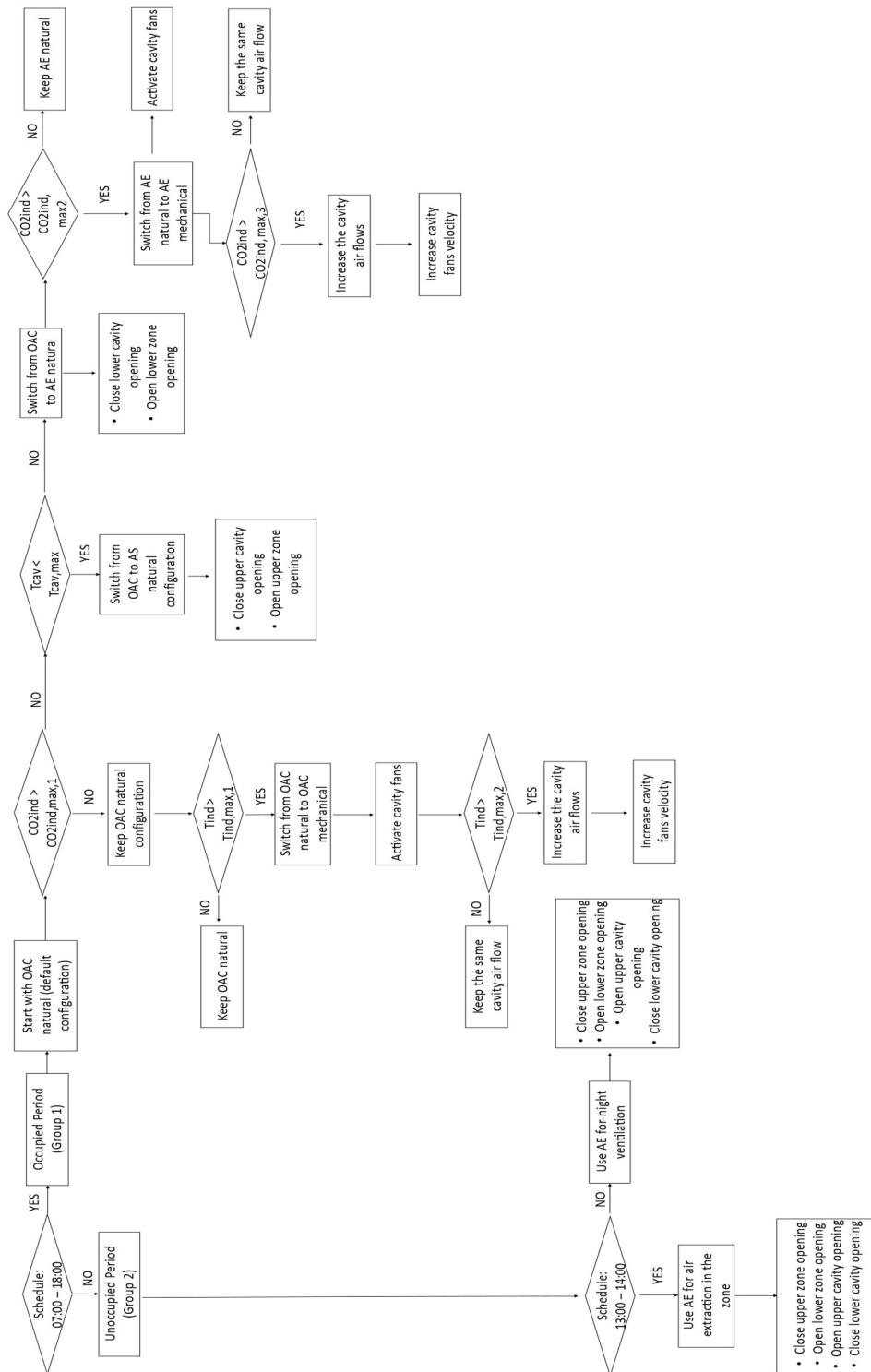


Figure 22: SAC#5 decision tree

### Combination of Group 3 and Group 4: Summer Shading Control (SSC)

Controls of the Group 3 and Group 4 can be used for the shading control in summer, during the occupied and the unoccupied hours. The code for the identification of these controls is *SSC (Summer Shading Control)*. In the case of the shading, 4 different forms of control will be adopted (from SSC#1 to SSC#4).

*SSC#1* is the simplest form of control for the venetian blinds inserted inside the cavity. In function of the incident solar radiation on the outer skin, the venetian blind is drawn: this is consequently the only control variable used for its implementation. The slat angle for the venetian blinds is assumed to be constant: The most common solution, adopted in this case in the control, is usually to fix a  $45^\circ$  slat angle. The threshold limit for the incident solar radiation on the façade is  $350 \text{ W/m}^2$ : the value is given by the average between mean and maximum incident solar radiation values on the South façade in Frankfurt (the selected location for the testing of the control), calculated by means of the preliminary simulations on IDA ICE. In *Table 4* are reported the values used for the calculations, given by the simulation performed on IDA ICE.

<b>Incident solar radiation levels (Frankfurt, Summer)</b>	
<i>Max on South</i>	<i>583.7 W/m<sup>2</sup></i>
<i>Average on South</i>	<i>122.5 W/m<sup>2</sup></i>
<i>Mean value</i>	<i>353 W/m<sup>2</sup></i>
<b><i>Control value</i></b>	<b><i>350 W/m<sup>2</sup></i></b>

*Table 4: Definition of the threshold value for the blind drawn mechanism during the summer season (month of July)*

In *SSC#2*, the activation of the blind is performed considering the indoor air temperature in the thermal zone. In general, it is better for the indoor comfort conditions compared to the simpler radiation control. Also in this case, just one control variable is assumed for the functioning of the control logic and the slat angle is kept constant ( $45^\circ$ ). The threshold value for the activation of the shading is set equal to  $24.5 \text{ }^\circ\text{C}$  during the cooling season.

In *SSC#3* and *SSC#4* the activation of the blind is performed using the indoor air temperature as control variable, as seen in *SSC#2*. Anyway, the slat angle is not constant, but variable. The complexity of the control is consequently higher, given the variability of the slat angle, compared to a fixed solution for the slat.

Indeed, in *SSC#3*, the cut-off position is implemented for the blind slat, in relation to the solar elevation angle: in this way it is possible to avoid the direct component of the solar radiation to enter inside the thermal zone, since the blind slat is always orthogonal to the incident solar radiation.

In *SSC#4*, on the other hand, the indoor illuminance conditions in the zones are considered by varying the slat angle during the day, in the way to have about *500 lux* of illuminance on the working plane [16]. The slat angle in this case is defined with a schedule: a certain slat angle is kept for the morning period (*5°*), one for the midday period (*55°*) and one for the afternoon (*35°*). The values have been defined considering the average illuminance levels in different periods of the day (morning, midday and afternoon) on the working plane for the occupants, considering different fixed slat angle values (ranging from *0°* to *85°*). In this way it is possible to define in an empirical way the relation between a certain slat angle of the blind and the related illuminance level in the room. In *Table 5*, are reported the values calculated by means of the simulations performed on IDA ICE.

Fixed slat angle of the blind[°]	5	15	25	35	45	55	65	75	85
Average illuminance in the morning (from 7:00 to 10:30) [lux]	324	318	302	280	251	206	155	92	35
Average illuminance in the midday (from 10:30 to 14:30) [lux]	884	858	807	742	662	544	406	241	93
Average illuminance in the afternoon (from 15:00 to 18:00) [lux]	606	592	559	517	462	381	285	170	65

*Table 5: comparison between the fixed slat angle values and the average illuminance levels at the working plane during the morning, the midday and the afternoon hours (for Frankfurt, in the month of July)*

The value of the angle of the slats has been defined performing a preliminary analysis on a thermal zone (with the same geometry and façade system of the one used for the simulation of the control, described in 3.2) in which the illuminance levels at the occupant desk have been calculated, for different fixed angles of the blind slats (ranging from *5°* to *85°*): for each period, the slat angle that ensured the illuminance levels closer to *500 lux* has been selected. This is a way to consider the visual comfort for the occupants inside the thermal zone.

For all the controls, during the night the blind is not drawn, to ensure a better cavity ventilation during the night with the *AE* configuration. In the lunch hours, since it is not necessary to perform working tasks in the zone, the maximum slat angle (*85°*) is applied, reducing the illuminance levels at the minimum level provided by the related standard (corresponding to *20 lux* according to [16]).

The codes and the related strategies for the occupied and unoccupied hours are reported in *Table 6*. The corresponding decision trees are reported from *Figure 23* to *Figure 26*.

Code for the control	Occupied hours strategy	Unoccupied hours strategy (lunch time and night)
SSC#1	<ul style="list-style-type: none"> <li>Radiation control with fixed slat angle (<i>45°</i>)</li> </ul>	<ul style="list-style-type: none"> <li>Blind not drawn during the night</li> </ul>

		<ul style="list-style-type: none"> <li>Slat angle is regulated to keep minimum illuminance levels in the zones during the lunch hour</li> </ul>
SSC#2	<ul style="list-style-type: none"> <li>Temperature control of the blind with fixed slat angle (45°)</li> </ul>	<ul style="list-style-type: none"> <li>Blind not drawn during the night</li> <li>Slat angle is regulated to keep minimum illuminance levels in the zones during the lunch hour</li> </ul>
SSC#3	<ul style="list-style-type: none"> <li>Temperature control of the blind drawn mechanism</li> <li>Regulation of the slat angle in function of the <i>cut-off</i> position</li> </ul>	<ul style="list-style-type: none"> <li>Blind not drawn during the night</li> <li>Slat angle is regulated to keep minimum illuminance levels in the zones during the lunch hour</li> </ul>
SSC#4	<ul style="list-style-type: none"> <li>Temperature control of the blind drawn mechanism</li> <li>Regulation of the slat angle in function of the indoor illuminance levels</li> </ul>	<ul style="list-style-type: none"> <li>Blind not drawn during the night</li> <li>Slat angle is regulated to keep minimum illuminance levels in the zones during the lunch hour</li> </ul>

Table 6: Control combinations for the shading system during the summer season

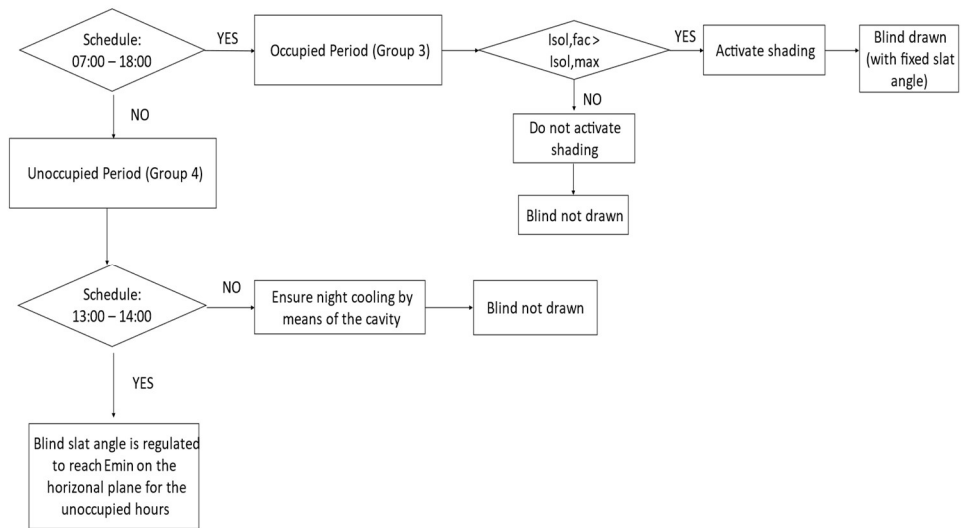


Figure 23: SSC#1 decision tree

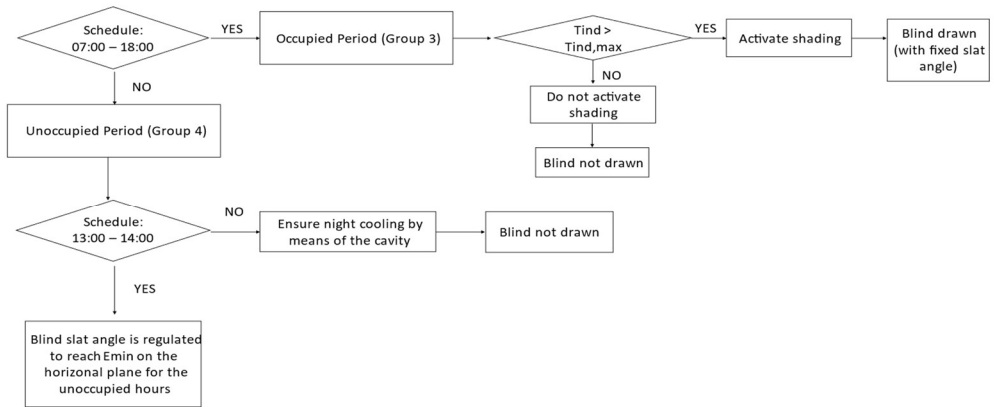


Figure 24: SSC#2 decision tree

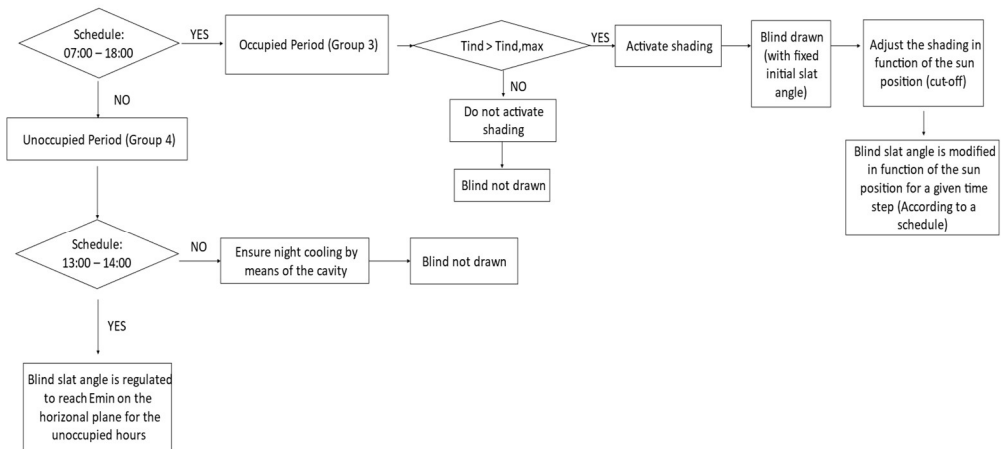


Figure 25: SSC#3 decision tree

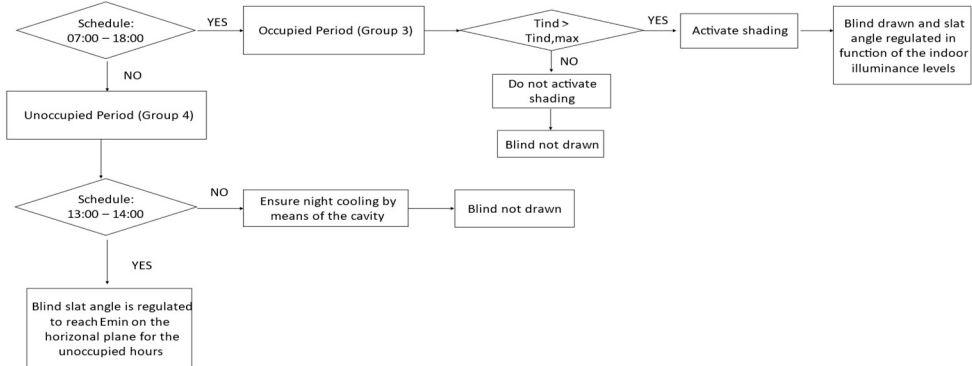


Figure 26: SSC#4 decision tree

Consequently, these two groups of control (for the airflows and the shading) are combined in summer strategies for the *DSF* control, that can be therefore applied during the summer season: they are the so-called *SC* (*Summer control*) combinations.

In this way, 20 different combinations are possible for summer control of the double skin façade (5 controls for the air flows combined with 4 controls for the shading system).

- **Control for the winter season**

*Combination of Group 5 and Group 6: Winter Airflow Control (WAC)*

Controls of the Group 5 and Group 6 can be used for the air flows control in winter. The code for the identification of these controls is *WAC* (*Winter Air flow Control*): 3 different controls have been defined in this case, from *WAC#1* to *WAC#3*.

In *WAC#1*, only the configurations *TB*, *CF*, *AS* and *IAC* are applied. The switch between *TB*, *CF* and *AS* is performed considering the cavity air temperature while for the switch to the *IAC* configuration, also the incident solar radiation on the façade is considered: only if the incident solar radiation on the façade is enough the *IAC* configuration is applied. Otherwise, it is better to keep the *TB* configuration.

In *WAC#2* and *WAC#3* also the *OAC* natural configuration is considered, for possible overheating issues inside the cavity or in the room. In the first type of control (*WAC#2*), the switch is applied considering the cavity air temperature, while in the second case (*WAC#3*) considering the temperature of the zone: in both cases, a maximum threshold value of temperature is considered.

Consequently, the total number of ventilation modes available in *WAC#2* and *#3* is 5, one more than *WAC#1*: the complexity of this last control can be consequently assumed higher, for the same criteria used in the summer season control configurations (an higher number of ventilation modes means an higher flexibility for the façade system).

For the night period, the thermal buffer configuration is applied for the heat losses reduction for all the types of control. As done for the control in the summer season, the initial threshold limits of the control variables for the switching between the different façade configurations have been initially set in function of the standard *EN 16798-1* and then modified in function of the results of the first simulation performed on IDA ICE.

For *WAC#1*:

- $\theta_{cavity,min,1}=5^{\circ}C$
- $\theta_{cavity,min,2}=16^{\circ}C$  (corresponding to the supply air temperature of the AHU of the zone)
- $\theta_{cavity,min,3}=18^{\circ}C$
- $I_{sol,min} = 75 W/m^2$

For *WAC#2*:

- Same threshold limits for the cavity temperature and the incident solar radiation on the façade adopted in *WAC#1*
- $\theta_{cavity,max}= 23.5^{\circ}C$  (for the switching to the *OAC* natural configuration)

For *WAC#3*:

- Same threshold limits for the cavity temperature and the incident solar radiation on the façade adopted in *WAC#1*
- $\theta_{indoor,max} = 20^{\circ}C$  (for the switching to the *OAC* natural configuration)

The minimum value of incident solar radiation on the façade for the adoption of *IAC* has been defined in function of the preliminary analysis carried on IDA ICE on a South exposed façade in Frankfurt during the month of January (as seen for the definition of the threshold limit for the activation of the shading system, as showed in *Table 8*): the average value is equal to  $52 W/m^2$ . Consequently, the incident solar radiation for the activation of the *IAC* configuration should be greater than this amount (as for example,  $75 W/m^2$ ).

The codes and the related strategies for the occupied and unoccupied hours are reported in *Table 7*. The decision trees are reported from *Figure 27* to *Figure 29*.

Code for the control	Occupied hours strategy	Unoccupied hours strategy (night)
WAC#1	<ul style="list-style-type: none"> <li>• <i>TB-CF-AS-IAC</i> configurations switching in function of the cavity air temperature</li> </ul>	<ul style="list-style-type: none"> <li>• Night thermal buffer</li> </ul>
WAC#2	<ul style="list-style-type: none"> <li>• <i>TB-CF-AS-IAC</i> configurations switching</li> <li>• <i>OAC</i> switching in function of the cavity air temperature</li> </ul>	<ul style="list-style-type: none"> <li>• Night thermal buffer</li> </ul>
WAC#3	<ul style="list-style-type: none"> <li>• <i>TB-CF-AS-IAC</i> configurations switching</li> <li>• <i>OAC</i> switching in function of the indoor air temperature</li> </ul>	<ul style="list-style-type: none"> <li>• Night thermal buffer</li> </ul>

*Table 7: Control combinations for the airflows during the winter season*



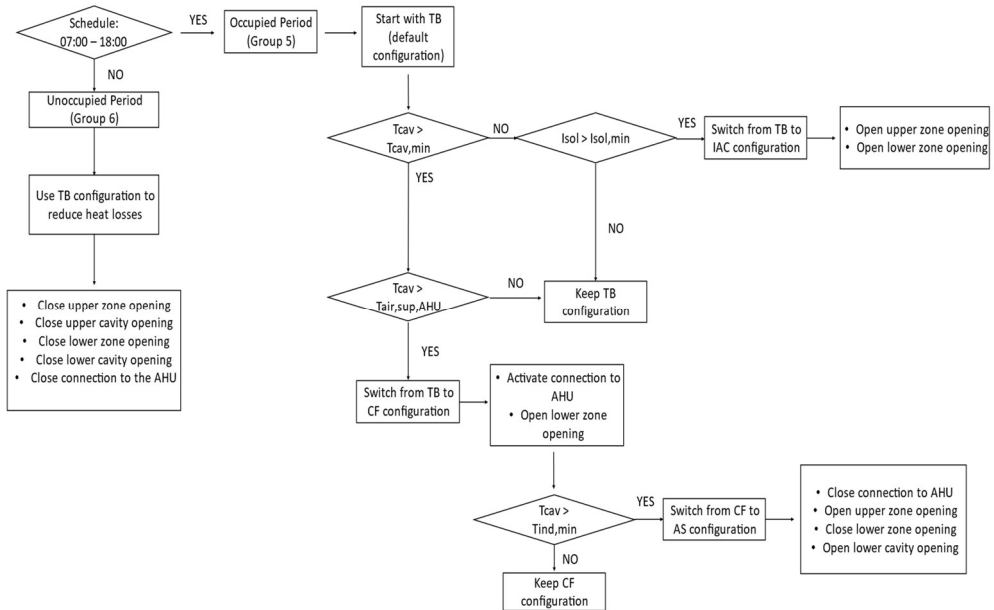


Figure 27: WAC#1 decision tree

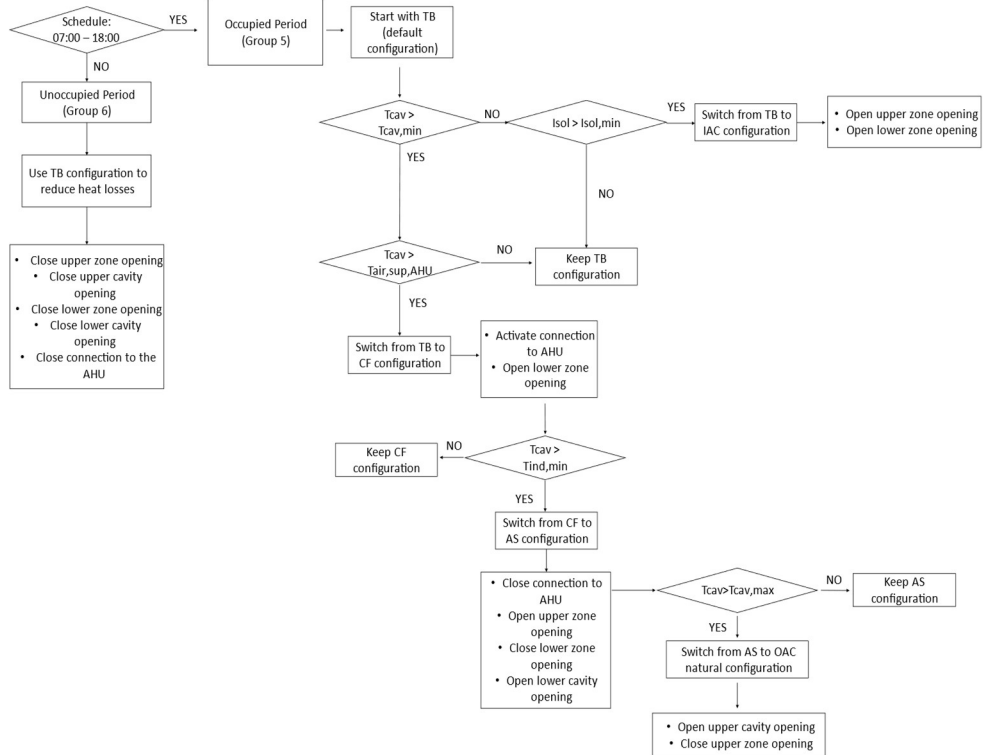


Figure 28: WAC#2 decision tree

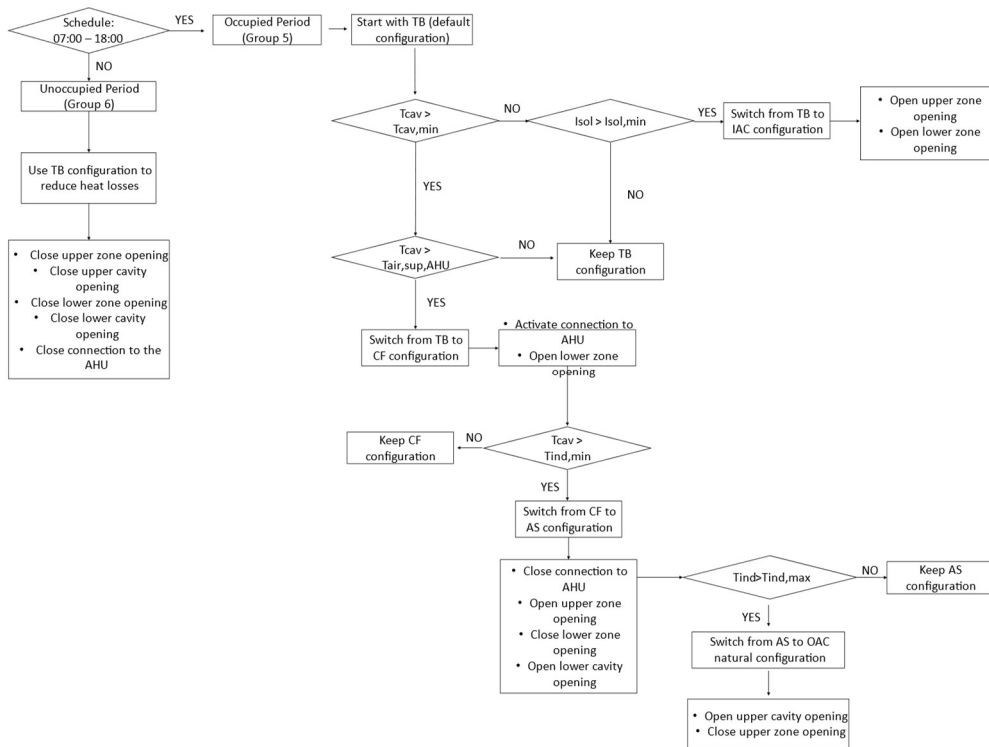


Figure 29: WAC#3 decision tree

Combination of Group 5 and Group 6: Winter Shading Control (WSC)

Controls of the Group 7 and Group 8 can be used for the shading control in winter. The code for the identification of these controls is *WSC (Winter Shading Control)*: the control for the winter season is basically the same implemented in the summer season (with 4 different forms of control from *WSC#1* to *WSC#4*). The radiation control is set at  $350 \text{ W/m}^2$  for *WSC#1* (the value has been defined in the same way as the summer season case, by means of preliminary simulations on IDA ICE) while the temperature activation in *WSC#2* is reduced to  $22^\circ\text{C}$  (instead of  $24.5^\circ\text{C}$ ) In *Table 8* are reported the values for the definition of the threshold limits of the incident solar radiation on the South façade, calculated by means of the simulations performed on IDA ICE.

Incident solar radiation levels (Frankfurt, Summer)	
Max on South	650.4 W/m <sup>2</sup>
Average on South	52.2 W/m <sup>2</sup>
Mean value	351 W/m <sup>2</sup>
<b>Control value</b>	<b>350 W/m<sup>2</sup></b>

Table 8: Definition of the threshold value for the blind drawn mechanism during the winter season (month of January)

The slat angle for the cut off implementation in *WSC#3* is different since the sun elevation angle is different as well compared to the summer. Finally, also the scheduled slat angles for *WSC#4* are not the same:  $5^\circ$  for the morning and the afternoon and  $35^\circ$  for the midday period. The values of the slat angle have been defined following the same approach used for the summer season (considering in this case the month of January). The values are reported in *Table 9*.

Fixed slat angle of the blind[°]	5	15	25	35	45	55	65	75	85
Average illuminance in the morning (from 7:00 to 10:30) [lux]	322	272	222	178	139	111	82	49	19
Average illuminance in the midday (from 10:30 to 14:30) [lux]	1066	833	644	489	366	299	222	132	51
Average illuminance in the afternoon (from 15:00 to 18:00) [lux]	255	217	180	145	114	91	67	40	15

*Table 9: Comparison between the fixed slat angle values and the average illuminance levels at the working plane during the morning, the midday and the afternoon hours (for Frankfurt, in the month of January)*

For all the combinations, during the lunch break, if the indoor air temperature is lower than  $22^\circ\text{C}$ , the blind is not drawn to ensure solar gains in the room. Otherwise, the shading is activated with fixed slat angle of  $45^\circ$ . The codes and the related strategies for the occupied and unoccupied hours are reported in *Table 10*. The decision trees are reported from *Figure 30* to *Figure 33*.

Code for the control	Occupied hours strategy	Unoccupied hours strategy (lunch time and night)
WSC#1	<ul style="list-style-type: none"> <li>Radiation control with fixed slat angle (<math>45^\circ</math>)</li> </ul>	<ul style="list-style-type: none"> <li>Blind drawn with fixed slat angle (<math>45^\circ</math>)</li> <li>Blind not drawn during the lunch time (if no overheating risk is present in the zone)</li> </ul>
WSC#2	<ul style="list-style-type: none"> <li>Temperature control of the blind with fixed slat angle (<math>45^\circ</math>)</li> </ul>	<ul style="list-style-type: none"> <li>Blind drawn with fixed slat angle (<math>45^\circ</math>)</li> <li>Blind not drawn during the lunch time (if no overheating risk is present in the zone)</li> </ul>
WSC#3	<ul style="list-style-type: none"> <li>Temperature control of the blind drawn mechanism</li> <li>Regulation of the slat angle in function of the cut-off position</li> </ul>	<ul style="list-style-type: none"> <li>Blind drawn with fixed slat angle (<math>45^\circ</math>)</li> <li>Blind not drawn during the lunch time (if no overheating risk is present in the zone)</li> </ul>
WSC#4	<ul style="list-style-type: none"> <li>Temperature control of the blind drawn mechanism</li> <li>Regulation of the slat angle in function of the indoor illuminance levels</li> </ul>	<ul style="list-style-type: none"> <li>Blind drawn with fixed slat angle (<math>45^\circ</math>)</li> <li>Blind not drawn during the lunch time (if no overheating risk is present in the zone)</li> </ul>

*Table 10: Control combinations for the shading during the winter season*

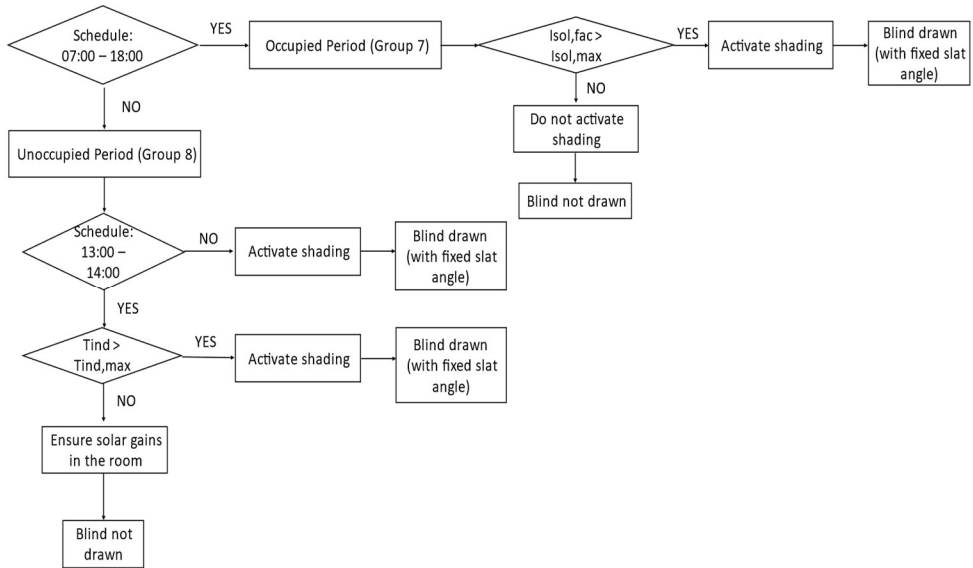


Figure 30: WSC#1 decision tree

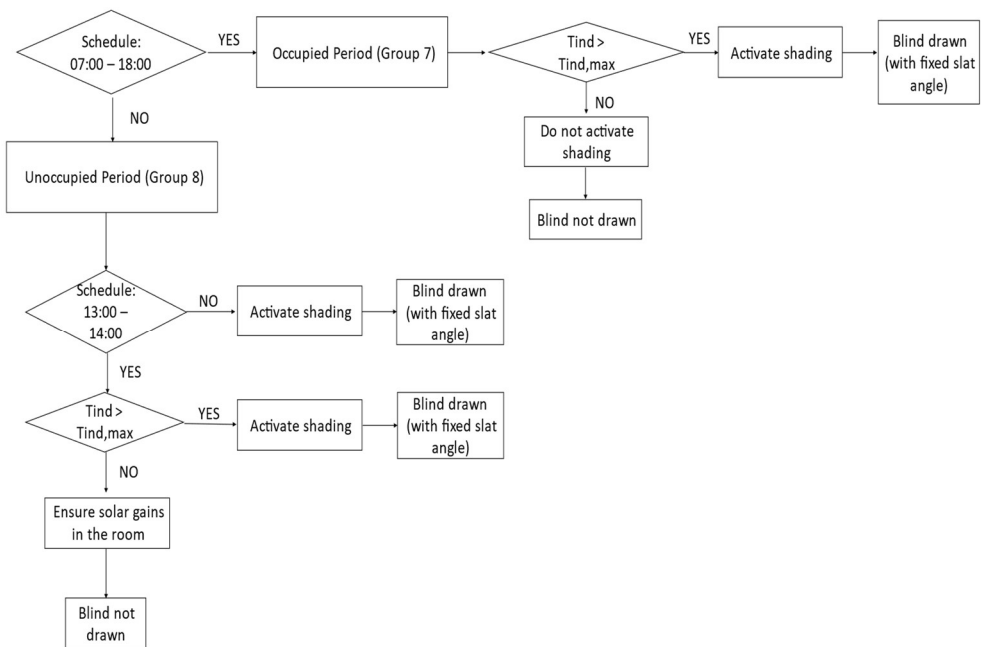


Figure 31: WSC#2 decision tree

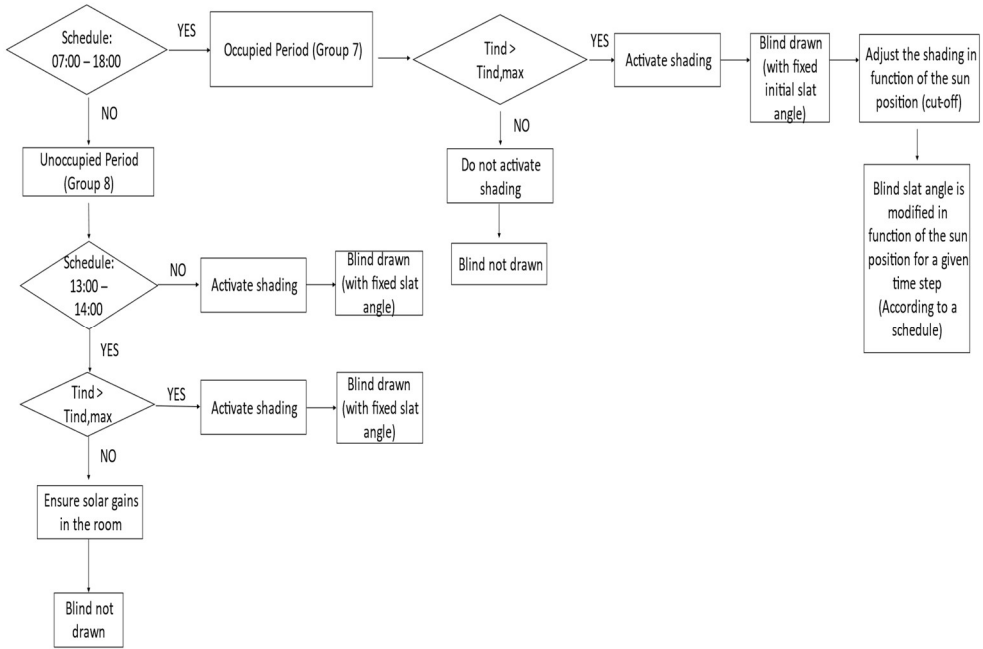


Figure 32: WSC#3 decision tree

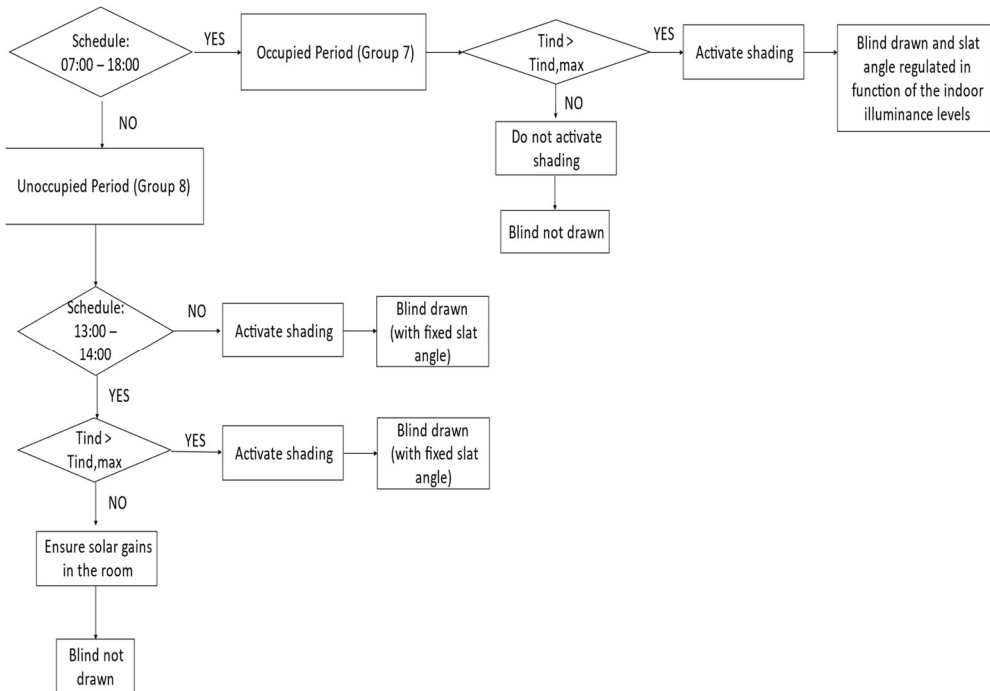


Figure 33: WSC#4 decision tree

Consequently, these two combinations for the shading and the air flows control are grouped in summer strategies for the double skin façade control, that can be therefore applied during the summer season: they are the so-called *WC* (*Winter control*) combinations. Each cavity air flow control can be indeed associated to a particular control logic of the shading system, enabling a different result (as seen for the summer season).

In this way, 12 different combinations are possible for summer control of the *DSF* (3 different controls for the air flows combined with 4 controls for the shading system).

### 2.3.1. Combinations for the summer season

Here are reported the 20 different combinations of control that can be used during the summer period (*Table 11*). The initial code (*SC*) defines the validity period, while the second (*SAC*) and the third (*SSC*) define the control adopted for the air flows in the cavity and the shading system. These control combinations will be tested in summer conditions to define their efficacy and effect on the overall system performance.

Control combinations codes
SC#1 SAC#1 SSC#1
SC#2 SAC#1 SSC#2
SC#3 SAC#1 SSC#3
SC#4 SAC#1 SSC#4
SC#5 SAC#2 SSC#1
SC#6 SAC#2 SSC#2
SC#7 SAC#2 SSC#3
SC#8 SAC#2 SSC#4
SC#9 SAC#3 SSC#1
SC#10 SAC#3 SSC#2
SC#11 SAC#3 SSC#3
SC#12 SAC#3 SSC#4
SC#13 SAC#4 SSC#1
SC#14 SAC#4 SSC#2
SC#15 SAC#4 SSC#3
SC#16 SAC#4 SSC#4
SC#17 SAC#5 SSC#1
SC#18 SAC#5 SSC#2
SC#19 SAC#5 SSC#3
SC#20 SAC#5 SSC#4

Table 11: The 20 combinations of control for the summer season

### 2.3.2. Combinations for the winter season

Here are reported the 12 different combinations of control that can be used during the winter period (*Table 12*). The initial code (*WC*) defines the validity period, while the second (*WAC*) and the third (*WSC*) define the control adopted for the air flows in the

cavity and the shading system. These control combinations will be tested in winter conditions to define their efficacy and effect on the overall system performance.

Control combinations codes		
WC#1	WAC#1	WSC#1
WC#2	WAC#1	WSC#2
WC#3	WAC#1	WSC#3
WC#4	WAC#1	WSC#4
WC#5	WAC#2	WSC#1
WC#6	WAC#2	WSC#2
WC#7	WAC#2	WSC#3
WC#8	WAC#2	WSC#4
WC#9	WAC#3	WSC#1
WC#10	WAC#3	WSC#2
WC#11	WAC#3	WSC#3
WC#12	WAC#3	WSC#4

Table 12: 12 combinations of control for the winter season

The general scheme used for the definition of the different control combinations is reported in *Figure 34*.

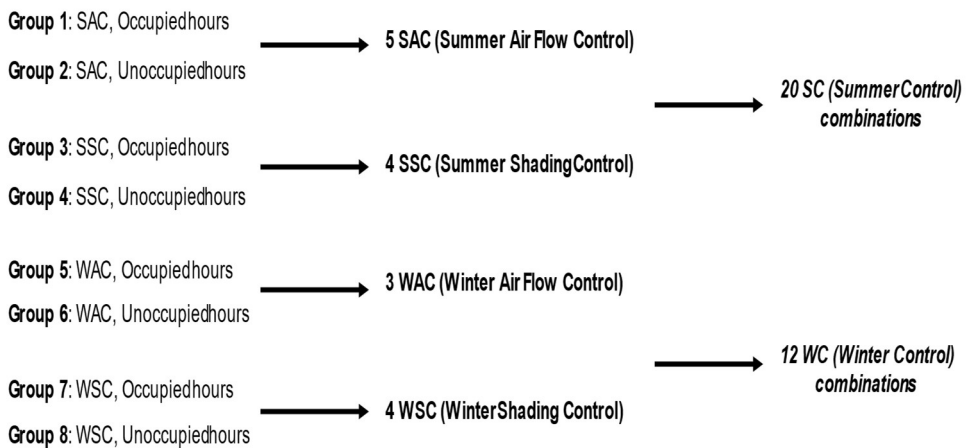


Figure 34: Scheme for the construction of the control combinations in summer and winter conditions

Given these assumptions, the total number of control combinations defined for the two seasons (summer and winter) is equal to 32 (20 for the summer and 12 for the winter).

### 2.3.3. Control for the week-end days

Other configurations should be kept in the case of the week-end days, which are unoccupied. The main distinction in this case is the one between the strategies to be applied during the night and the strategies to be applied during the day (for which

different outdoor conditions are present). All these configurations can be activated by means of a schedule, as seen for the other strategies related to the unoccupied hours during the working days.

About the shading control, for the summer season, the blind is not drawn during the night (for a better application of the night cooling by means of the façade cavity), while during the day a minimum illuminance level of is kept inside the indoor environment, by using a slat angle of  $85^\circ$ .

For the winter season, the venetian blind is kept completely drawn during the weekend period (With a fixed slat angle of  $45^\circ$ ). About the air flow control, in the summer season the *OAC* configuration (with natural ventilation inside the cavity) can be implemented, while during the night the *AE* configuration (with natural ventilation) can be used. In the winter season, it is possible to set the *TB* configuration during the whole period of the weekend.

The implementation of the control combinations inside IDA ICE by means of the *Control Macros* is illustrated in detail inside the *Appendix D: Control implementation in IDA ICE*: in the appendix it has been reported the process followed for the definition of specific decision trees, to which a specific *exit code* from 1 to 10 (as showed in *Table 1*) is associated to each configuration of the *DSF*.

In addition, the process followed for the *DSF* modelling and the creations of the different control combinations is illustrated more in detail in *3.1*.



### **3. Research method definition for the performance evaluation**

In this section, the method followed during the Thesis work will be explained and discussed in detail. Indeed, the main scope of the implemented research method is the one to create a comparative study between the controlled *DSF* (with a certain implemented control combination, among the ones defined in 2.3.1 and 2.3.2) and a baseline system to use as reference for the performance comparison.

The research method can be consequently divided into the following steps:

- 1) *Modelling of the flexible DSF in IDA ICE*
- 2) *Modelling of the adjacent thermal zone*
- 3) *Definition of the boundary conditions in which the double skin façade performance will be evaluated*
- 4) *Multi-domain performance evaluation using IDA ICE*
- 5) *Comparison with reference façade systems and selection of the optimal control combination*

The optimal control combination (in winter and summer conditions), indeed, is the one that produces the best performance improvement compared to the reference façade systems. Following these criteria, for each one of the defined boundary conditions, the optimal control combination for the *DSF* must be selected.

In this chapter all the steps of the research method have been discussed more in detail.

#### **3.1. Double skin system modelling**

A flexible *DSF* system has been defined inside the simulation environment of IDA ICE, following the process illustrated in *Appendix C*. About the driving force for the ventilation inside the cavity, the modelled double skin façade should be able to switch between the natural and the mechanical ventilation modes according to the different operating conditions. Therefore, the presence of fans inside the cavity is considered to enable the mechanical ventilation use.

About the skins, there are many different configurations that can be adopted, according to the existing literature. In general, the inner skin consists of a thermal insulating double or triple pane. The panes are usually made of toughened or unhardened float glass. On the other hand, the outer skin is usually a tempered or laminated single pane [12]. Anyway, this configuration has a particular disadvantage: in the cold winter days, when the exhaust air is introduced in the cavity from the zone, there could be condensation risk, since the exhaust air is often warm and humid while the inner surface of the outer skin surface can be very cold in these conditions.

This fact can lead to several problems related to the functioning of the façade components, due to water infiltrations [23]. Therefore, the inner surface of the outer

skin should be kept to a warmer temperature while the air from the room is introduced inside the cavity. The best solution is in this case the one to use a double glass unit (DGU) for both, inner and outer skins. The properties of the glass (both optical and thermal) and the different panes constructional characteristics are taken from the *WINDOW 7* software data base already implemented inside IDA ICE. In the following table, the characteristics of the glazing systems for the inner and outer skins are reported. The components of the two skins are showed in *Table 13*.

Outer Skin (DGU)	Inner Skin (DGU)
Clear Glass, 4 mm	Clear Glass, 5 mm
Argon filled gap, 12 mm	Argon filled gap, 12 mm
Low E Glass, 5 mm	Low E Glass, 4 mm

*Table 13: Layers of the two skins of the double skin façade.*

Visible transmission ( $\tau_v$ ), total solar transmission ( $\tau_e$ ), solar heat gain coefficient (SHGC) and thermal transmittance ( $U$ ) of the two skins are automatically calculated by the simulation environment (*Table 14*). The two skins are quite identical in terms of visible and total solar transmittance but there is a more significant difference in terms of  $g$  value and thermal transmittance  $U$ .

Outer Skin	Inner Skin
SHGC = 0.715	SHGC = 0.662
$\tau_e = 0.565$	$\tau_e = 0.565$
$\tau_v = 0.75$	$\tau_v = 0.75$
$U = 1.615 \text{ W/m}^2\text{K}$	$U = 2.141 \text{ W/m}^2\text{K}$

*Table 14: Optical, solar and thermal properties of the outer and the inner skins automatically calculated by IDA ICE.*

Cavity depth for the *DSF* is set equal to 25 cm. Both the inner and the outer skins have frame factor equal to 0.1 and the thermal transmittance of the frame equal to 2  $\text{W/m}^2\text{K}$ .

As shading system, a generic light-dark coloured slat material venetian blind has been selected (with 10 mm slat width), integrated inside the cavity. The thickness of the slats is set equal to 0.6 mm, while the thermal conductivity of the material is 160  $\text{W/m K}$ . The properties of the shading system have been defined using the related form inside the *Detailed Window* model. Transmittance and reflectance properties of the aluminium have been defined by default inside the IDA ICE database. The distance between the venetian blind and the outer skin is set equal to 0.125 cm. In this way the blind is located exactly in the middle of the façade cavity. The flexibility of the façade system is ensured by the 10 different ventilation modes configurations (5 for the heating and 6 for the cooling season) already illustrated in *Table 1*.

Indeed, for the cooling season (summer) the switchable configurations are the *OAC*, *AE* and *AS*. For these configurations, both natural and mechanical ventilation strategies can be applied inside the cavity (except for *AS*).

For the heating season (winter), on the other hand, the switchable configurations are *TB*, *CF*, *AS*, *IAC* and *OAC*. For these configurations in this season the natural ventilation is preferred to the mechanical one since the necessity for the removal of excess of heat is lower compared to the summer season. Different forms of control will be applied to the façade system in winter and summer condition to ensure the switching between the different air flow configurations.

As mentioned in *Appendix C*, the standard *DSF* already implemented in IDA ICE has been modified to enable the control from the rule-based logic: the original leaks between the zone and the façade cavity have been substituted by openings while an additional cavity fan have been added for the mechanical ventilation implementation. The cavity fan can switch between two different values of air flow: a minimum of  $41.7 \text{ l/s}$  and a maximum of  $83.3 \text{ l/s}$ . These two values correspond to  $50 \text{ m}^3/\text{h}$  and  $100 \text{ m}^3/\text{h}$  per horizontal linear meter of façade ( $3 \text{ m}$  for each window of the room).

For each combination of control, in summer and winter conditions, a different model have been defined (corresponding to a different *.idm* file), with the related *Control Macros* and decision trees (for the cavity air flows and the shading control), for a total number of 32 different flexible *DSF* models. The general workflow adopted for the *DSF* modelling phase is showed in *Figure 35*.

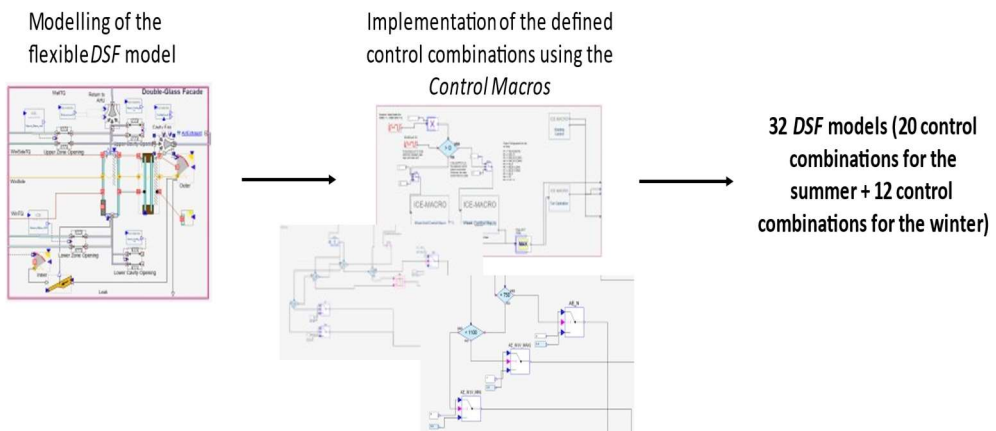


Figure 35: *DSF* modelling workflow

### 3.2. Thermal zone modelling

The next step is focused on the definition of the thermal zone to which the façade system is linked. The geometrical features of the linked thermal zone are the ones used for the *IEA Building Energy Simulation Test (BESTEST)*, as showed in *Figure*

36. The room is a rectangular thermal zone, with floor area of  $8\text{ m} \times 6\text{ m} = 48\text{ m}^2$ . The ceiling height is  $2.7\text{ m}$ . Therefore, the total heated volume of the zone is set equal to  $129.6\text{ m}^3$ .

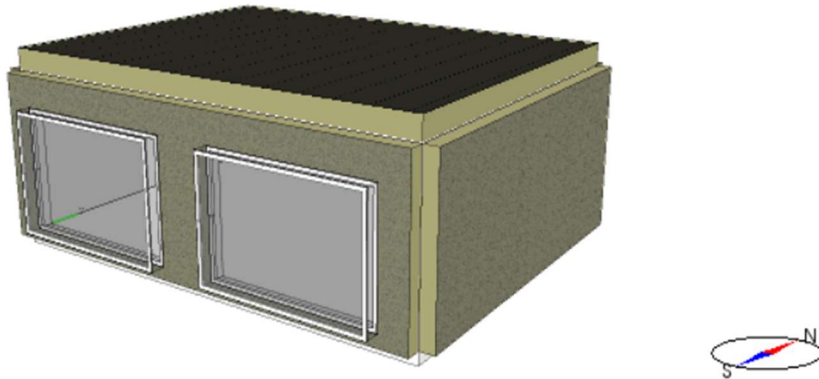


Figure 36: The BESTEST cell used for the thermal zone modelling, with the two identical double skin façades applied on the South wall.

Two different windows with identical features are present in the zone, following the procedures of the BESTEST. They have identical dimensions of  $3\text{ m} \times 2\text{ m} = 6\text{ m}^2$ . Consequently, the length of  $3\text{ m}$  of linear meter of façade has been used for the definition of the cavity air flows. Both the windows are oriented towards the South direction. This orientation is typically better from a solar gains point of view than East and West ones during the summer season but on the contrary the risk of potential overheating is greater during the winter. For this reason, this façade orientation has been preferred during the thermal zone modelling. Schedules and internal gains inside the thermal zone are defined in function of the European standard EN 16798-1:2019 [27] and the international standard ISO 23045:2008 [28]:

- Occupancy period for the zone: 07:00 – 18:00 (Lunch break is set between 13:00 – 14:00). No occupancy in the zone is therefore set during the lunch break. The total number of occupied hours is consequently 10 per day.
- Working days per week: 5 days (from Monday to Friday, no occupancy set during the weekend).
- Internal gains from appliances: a single unit with a emitted heat of  $300\text{ W}$  has been considered.
- Internal gains from lighting: 4 different lighting units have been considered inside the room. Each one of them has a rated input of  $48\text{ W}$ . The luminous efficiency is set equal to  $80\text{ lm/W}$ , the convective fraction  $0.6$ .

For the internal gains from the occupants, three people inside the room are considered, with metabolic rate equal to  $1\text{ met}$ . The clothing insulation for the occupants is  $0.85\text{ clo}$  with a possible variation of  $0.25\text{ clo}$  in function of the thermal sensation of the

occupants. The ventilation plant is a *Constant Air Volume (CAV)*, scheduled in function of the occupancy of the zone. The air flow to the zone is set equal to  $1.4 \text{ l/s m}^2$  during the occupied hours and  $0.15 \text{ l/s m}^2$  during the unoccupied hours of the office, in accordance with a *Category II* of IEQ. [19].

The *AHU* of the zone has a heat recovery efficiency of  $75\%$  and a constant air supply temperature of  $16^\circ\text{C}$  (this is the standard solution adopted in IDA ICE), both for the summer and the winter seasons. Daylight at the workplace for the electric lighting control is set as  $500 \text{ lux}$  [28]: below this level, the electric light is turned on. Infiltration through the envelope are set equal to  $0.5 \text{ ACH}$  under a pressure difference of  $50 \text{ Pa}$ , following the criteria used in the *BESTEST* procedure.

Heating and cooling set points for the indoor air temperatures are set equal to  $20^\circ\text{C}$  and  $26^\circ\text{C}$ , in accordance with a *Category II* of IEQ [15]. The indoor temperature is kept by an ideal heating and cooling system, defined in IDA ICE with the use of an ideal heater and an ideal cooler. The power for both is set equal to  $5000 \text{ W}$ , the efficiency of the heating system is set equal to 1 and the *COP* of the chiller is 2. In the following table (Table 15), it is reported a brief recap about the main data regarding the zone implemented inside IDA ICE.

Destination of Use	Office
<i>Floor Area</i>	$48 \text{ m}^2$
<i>Ceiling height</i>	$2.7 \text{ m}$
<i>Heated Volume</i>	$129.6 \text{ m}^3$
<i>Façade area</i>	$12 \text{ m}^2$ (2 windows with $6 \text{ m}^2$ of surface each)
<i>Occupancy</i>	3 person ( $M = 3 \text{ met}$ )
<i>Internal Gains from Lighting</i>	4 units, $48 \text{ W}$
<i>Internal Gains from Appliances</i>	3 units, $300 \text{ W}$ each
<i>Ventilation</i>	$1.4 \text{ l/s m}^2$ (Unoccupied periods: $0.15 \text{ l/s m}^2$ )
<i>Infiltrations</i>	$n_{50} = 0.50 \text{ ACH}$
<i>Temperature Set Points</i>	$20^\circ\text{C} - 26^\circ\text{C}$
<i>Heating System</i>	Ideal Heater (efficiency $100\%$ ), $P = 5000 \text{ W}$
<i>Cooling System</i>	Ideal Cooler ( $\text{COP} = 2$ ), $P = 5000 \text{ W}$
<i>Heat Recovery Efficiency</i>	$75\%$

Table 15: Main data about the zone inserted inside IDA ICE

### 3.3. Boundary conditions selection and analysis of the climate conditions

The next step is focused on the definition of the boundary conditions in which the *DSF* behavior will be tested and evaluated. The location and the climate for the study of the control efficacy are the ones of Frankfurt. The corresponding climate in function of the Kopper-Geiger classification is *Temperate-Oceanic Climate (Cfb)*. In the next figure, it is possible to see the location of the Frankfurt climate in relation with the other present in Europe (Figure 37). The latitude, in accordance with the climate file used inside IDA ICE, is  $50.05^\circ\text{N}$  while the altitude is  $112 \text{ m}$ .

Frankfurt is in a temperate climate condition; therefore, it is possible to evaluate in a more effective way the influence of façade system as a double skin façade to the overall energy performance of the building, compared for example to more “extreme” locations as Madrid or Oslo.

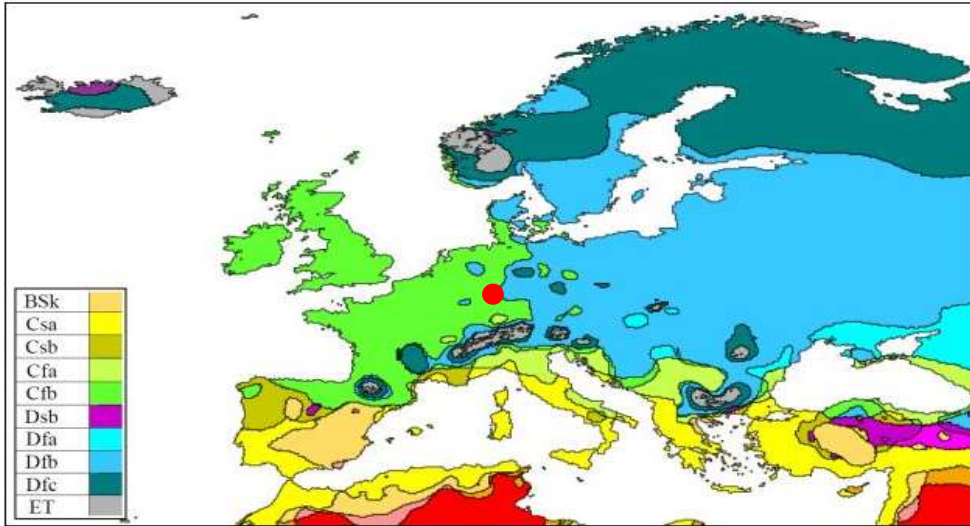


Figure 37: Location of Frankfurt with respect to the other European climates [29].

Location and climate for the building in which the double skin façade is implemented can be defined inside the *General* tab of the *.idm* file of the building. The weather data are already implemented inside the IDA ICE database. As mentioned before, the performance of the façade system will be evaluated considering two different summer and winter conditions: it is indeed more important to analyze the behavior of the façade system in this reduced period, instead of considering the whole year performance.

The duration of the selected time slices (in summer and winter seasons) is fixed to one month for all the three locations. This methodology aims to evaluate in separate way the façade control strategies during the summer season (*SC*) in separate way from the control strategies for the winter season (*WC*), in which different boundary conditions are experienced by the façade itself. At the same time, the duration of the simulation period can allow to have a consistent variation of the outdoor environmental control variables for the façade actuators (in particular, the ones concerning the outdoor air temperatures and the incident solar radiation on the façade). This fact gives more robustness to the simulation methodology and to the effectiveness evaluation of the control for the *DSF*. The selected months are July for the summer conditions and January for the winter conditions evaluation. In July, the average outdoor air temperature is the highest of the year, the same for the solar radiation. In January, on the contrary, the lowest outdoor air temperatures are experienced. This is shown in the following graphs (Figure 38, Figure 40 and Figure 39).

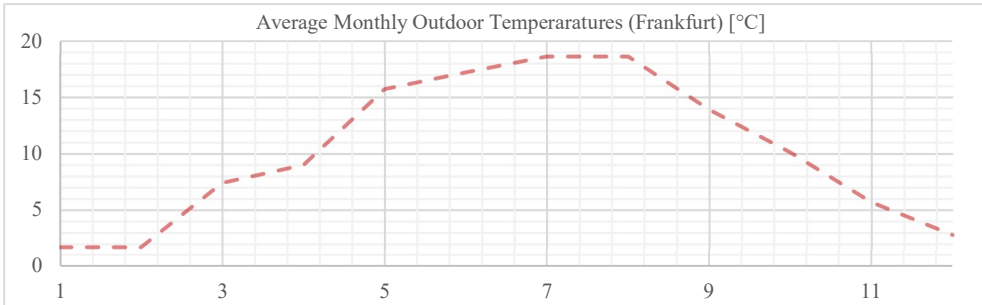


Figure 38: Average monthly values of outdoor air temperature for Frankfurt [30]

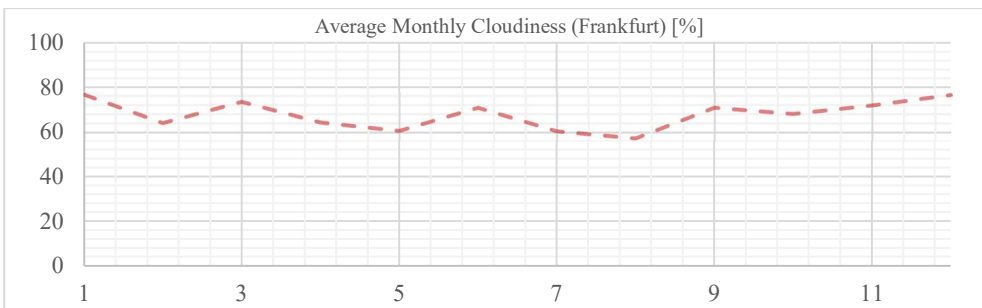


Figure 39: Average monthly values of cloudiness for Frankfurt [30]

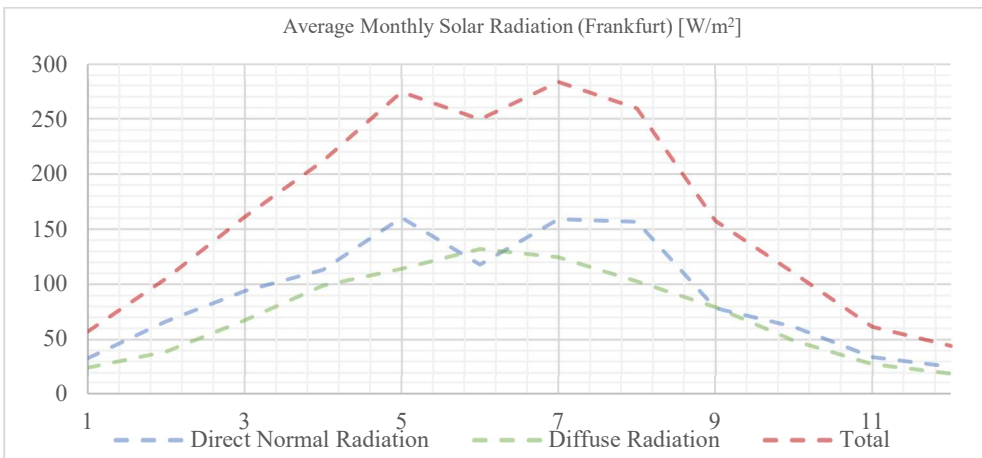


Figure 40: Average monthly values of solar radiation on the horizontal surface for Frankfurt [30]

In the next pages, the data about the climate of the location in the selected periods are reported and briefly analyzed.



## **July (Frankfurt climate)**

In the month of July, there is a consistent variation of the outdoor air temperatures, that can range from a maximum of about  $5^{\circ}\text{C}$  to a maximum of over  $30^{\circ}\text{C}$  (Figure 41). Maximum values of total radiation on the horizontal surface are in the order of  $1000\text{ W/m}^2$  in some days. The direct radiation is usually greater compared to the diffuse one (Figure 43). Also the cloudiness of the sky is highly variable, indeed there are fully overcast days, with a cloudiness of  $100\%$ , but also clear days, with a  $0\%$  of cloudiness (Figure 42). Therefore, the environmental conditions during the month of July are highly variable in Frankfurt.

The average monthly values are of course lower, as reported in Table 16.

<b>Frankfurt (July)</b>	
Average Air Temperature [ $^{\circ}\text{C}$ ]	18.6
Average Total Solar Radiation [ $\text{W/m}^2$ ]	283.1
Average Cloudiness [%]	60.4

Table 16: Average monthly values for July in Frankfurt

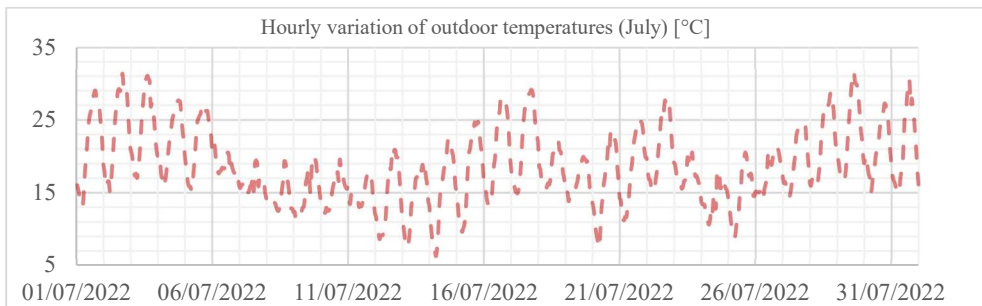


Figure 41: Hourly variation of outdoor temperature during the month of July

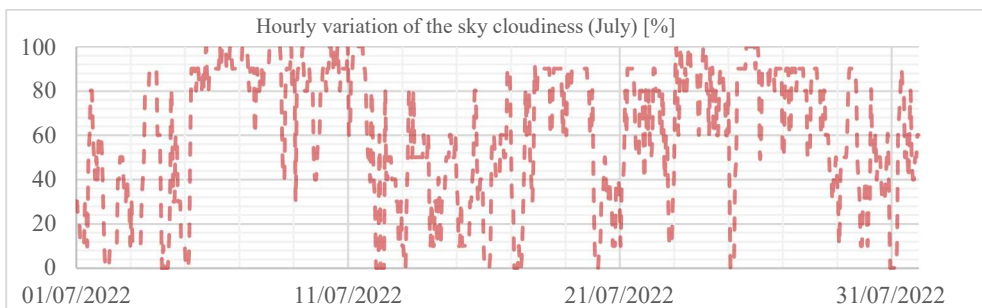


Figure 42: Hourly variation of cloudiness in the month of July



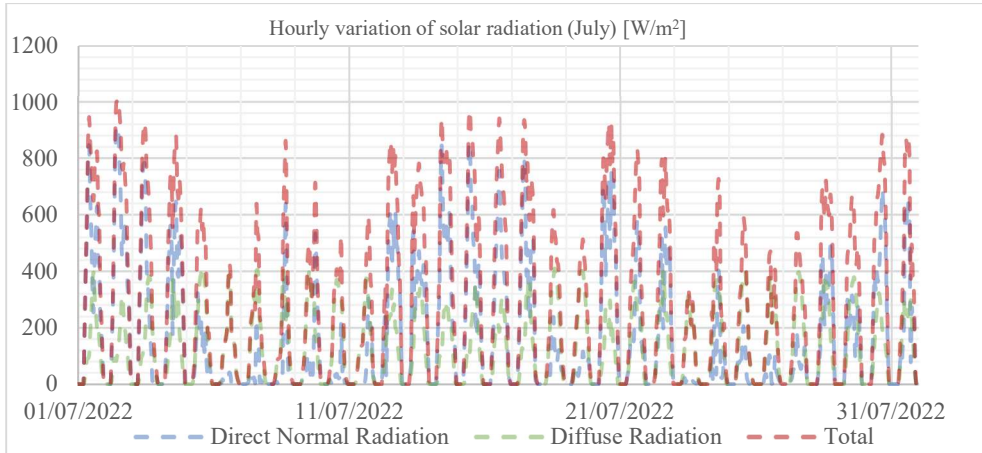


Figure 43: Hourly variation of solar radiation on the horizontal façade in the month of July

### **January (Frankfurt climate)**

In the month of January, the lowest temperatures (Figure 44) are expected at the beginning of the month (about  $-10^{\circ}\text{C}$ ) while the highest ones at the end of it (about  $15^{\circ}\text{C}$ ). As seen for the month of July, there is therefore a consistent variation of outdoor temperature conditions. The solar radiation in average is extremely lower compared to the summer, but the peaks are anyway close to  $600\text{ W/m}^2$ . In many days, more than the summer, the diffuse component is also greater than the direct normal one (Figure 45). The cloudiness in average is higher than the summer and the number of fully overcast days is larger. Anyway, some clear days are anyway present during the month (Figure 46).

Average values of the month are reported in Table 17.

<b>Frankfurt (January)</b>	
<i>Average Air Temperature [<math>^{\circ}\text{C}</math>]</i>	1.7
<i>Average Total Solar Radiation [<math>\text{W/m}^2</math>]</i>	57
<i>Average Cloudiness [%]</i>	76.5

Table 17: Average monthly values for July in Frankfurt

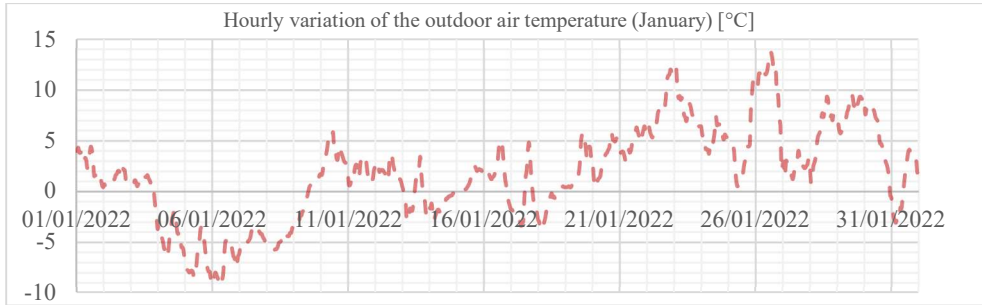


Figure 44: Hourly variation of outdoor temperature during the month of January

To make the performance evaluation of the façade system more robust and comparable to a real case study, the thermal transmittance of the external enclosures of the room (walls, floor and roof) have been defined in function of the energy requirements of the selected location (in this case the Germany). In this way the performance evaluation of the façade system is more coherent with the climate context of the simulated thermal zone. In Germany the requirements for the thermal transmittance of the building envelope components are listed inside the *Energy Savings Ordinance (EnVE) 2013* [31].

The required values are listed in *Table 18*, in the next page. Ideal materials for the external walls, the floor and the roof have been defined, to reach the minimum requirements for the thermal transmittance of the external enclosures considering an overall thickness of *25 cm* (typical for modern office buildings in Europe). The same thickness is assumed also for the other components of the envelope. The calculation for the definition of the thermal conductivity of the external enclosures of the thermal zone are showed in *Table 18*, in the next page.

The physical properties of the ideal material, for all the locations and envelope components, has been set equal to the one the *L/W concrete* (low weight concrete) material already implemented inside IDA ICE: density equal to *500 kg/m<sup>3</sup>* and specific heat equal to *1050 J/kg K*. These values allow for an external envelope that is nor too heavy nor too light, making the thermal balance of the zone less depending on the overall envelope thermal inertia.

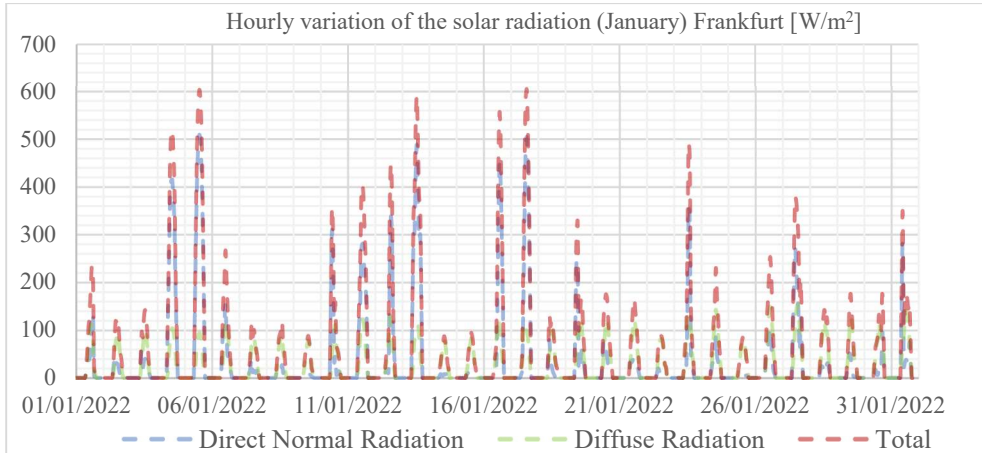


Figure 45: Hourly variation of solar radiation on the horizontal façade in the month of January

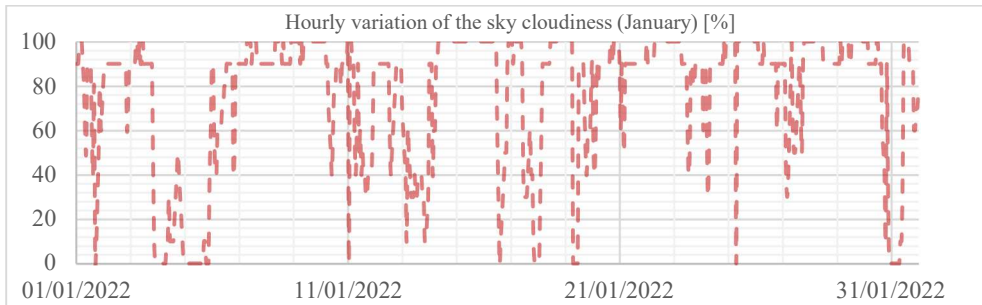


Figure 46: Hourly variation of cloudiness in the month of January

Walls		Floors		Roofs	
$U$ [ $W/m^2K$ ]	0.28	$U$ [ $W/m^2K$ ]	0.35	$U$ [ $W/m^2K$ ]	0.2
$R$ [ $m^2K/W$ ]	3.571	$R$ [ $m^2K/W$ ]	2.857	$R$ [ $m^2K/W$ ]	5
$R_{no.surf}$ [ $m^2K/W$ ]	3.401	$R_{no.surf}$ [ $m^2K/W$ ]	2.687	$R_{no.surf}$ [ $m^2K/W$ ]	4.83
$\lambda$ [ $W/mK$ ]	0.0735	$\lambda$ [ $W/mK$ ]	0.0930	$\lambda$ [ $W/mK$ ]	0.05176

Table 18: Thermal conductivity calculations for the envelope ideal materials. The thermal transmittance value is expressed in  $W/m^2K$ , the thermal resistance is expressed in  $m^2K/W$  while the thermal conductivity is expressed in  $W/m K$ .

### 3.4. Multi-domain performance evaluation using IDA ICE

In IDA ICE, different load and energy simulations can be performed according to the user preferences (in particular, heating and cooling load calculations and energy calculations). For the analysis of the results in this Master Thesis, indeed, customized energy simulations (ran for a user defined period) has been used for the testing of the research hypothesis related to the control implementation for the *DSF*.

In the *Simulation data* window, it is possible to select between a dynamic and a periodic simulation. A periodic simulation means that a certain period is simulated a certain number of times until the system has stabilized and no longer changes are recorded from a simulation to another one (stabilization process to a periodic state). A dynamic simulation means, on the other hand, that the simulation starts at a particular time and ends at another time. In this case, dynamic simulations have been performed.

The start-up period (a few days in which the system is pre-simulated before the proper simulation starts, for its stabilization) can be set equal to 14 days: the length of the start-up phase depends on the thermal mass of the building [32]. Approximately two weeks is enough for the greatest part of the modelled buildings. Tolerance for the resolution of the equations of the mathematical model is set equal to *0.02*, while the maximal time-step and the time-step for output are defined as *0.5* hours (*30 minutes*).

Two different kinds of simulations have been performed on the virtual model of the thermal zone, with different purposes and requested outputs for the performance evaluation (*Table 19*): one model with all the active systems turned on and another one with all the actives systems turned off (the so called *free running* configuration).

- Using the model with all the active systems turned on (heating, cooling, ventilation plant and artificial lighting) an energy simulation focused on the energy consumption will be performed. The requested outputs will be therefore the energy consumption for the zone (space heating and cooling, ventilation heating and cooling and artificial lighting use).
- Using the model with all the active systems turned off a simulation focused on the indoor climate conditions will be performed. The requested outputs will be consequently the main temperatures in the zones (indoor air and operative temperatures, Fanger’s comfort indices (*PMV* and *PPD*), indoor air quality and daylight on the working plane). In this way it will be possible to evaluate the indoor comfort conditions without an active system inside the zone.

Type of performed simulation	Requested outputs to IDA ICE
Energy simulation (with active systems turned on)	<ul style="list-style-type: none"> <li>• Energy for space heating [<i>kWh/m<sup>2</sup></i>]</li> <li>• Energy for space cooling [<i>kWh/m<sup>2</sup></i>]</li> <li>• Energy for ventilation heating [<i>kWh/m<sup>2</sup></i>]</li> <li>• Energy for ventilation cooling [<i>kWh/m<sup>2</sup></i>]</li> <li>• Energy for artificial lighting [<i>kWh/m<sup>2</sup></i>]</li> </ul>

Indoor climate simulation ( <i>free running</i> configuration)	<ul style="list-style-type: none"> <li>• Indoor air temperature [<math>^{\circ}\text{C}</math>]</li> <li>• Indoor operative temperature [<math>^{\circ}\text{C}</math>]</li> <li>• Indoor <math>\text{CO}_2</math> concentrations [<math>\text{ppm}</math>]</li> <li>• <math>\text{PPD}</math> and <math>\text{PMV}</math> indices [% and -]</li> <li>• Illuminance levels on the working plane [<math>\text{lux}</math>]</li> </ul>
--	--

Table 19: The two different typologies of simulation performed on IDA ICE and the related simulation outputs

The two typologies of simulation will be conducted for both, summer, and winter conditions, to evaluate the efficacy of the summer and winter control combinations under different points of view. Performing both the simulation typologies (energy and indoor climate) it is possible to make an evaluation of the efficacy of the façade system with a certain implemented control that considers on one side the comfort for the occupants and on the other side the energy consumption.

In addition, following this approach, focused on the adoption of building performance indicators (linked to both, energy efficiency and  $\text{IEQ}$ ), it is possible to analyse the effects of the adoption of an adaptive façade on the overall performance of the building (in this case, a single thermal zone).

Adopting just the performance indicators of the envelope itself, without considering its complex interconnection with the other building systems cannot be the correct approach to follow: this is caused mainly by the fact that adaptive façades are often characterised by an interconnected performance [9], that influences a wide set of physical phenomena (due to this particularity, the term *multi-domain performance* is often used regarding to advanced envelopes) [7].

The two configurations, with and without active systems, have been defined with two separate versions of the thermal zone model, with the same  $\text{DSF}$  model adopted as façade system. Consequently, given 32  $\text{DSF}$  models (as illustrated in 3.1), the total number of generate *.idm* files is 64.

### **3.5. Comparison with the reference façade systems and selection of the optimal control combination**

Analysing the results of the simulations performed in IDA ICE, it is possible to define which combination of control for the  $\text{DSF}$  (among the proposed ones) is the most appropriate for the selected boundary condition (South façade in Frankfurt), in function of the comparison of the performance with a certain reference system. This is the concept of optimal control already mentioned at the beginning of this chapter.

For the summer season, the best one among the 20 defined combinations should be selected while for the winter season the possible alternatives are 12, as illustrated before.

Of course, the effectiveness evaluation must consider both, energy savings and comfort for the occupants: it has no sense to select the control combination that produces the best results in terms of energy performance, leading to unacceptable comfort conditions for the occupants. Vice versa, it is not possible to consider in a positive way a combination that ensures optimal indoor comfort conditions but enables to very high energy consumptions compared to the other control combinations.

As reference systems for the performance comparison (both for the energy evaluation and the indoor climate one), two will be the façade solutions adopted in this case. The 2 façade systems will be applied to the same test cell and characterized with the same geometrical features of the double skin façade.

#### First reference system: static double skin façade

The first comparison system will be a “static” *DSF*, corresponding to a double skin façade for which the ventilation mode in the cavity is kept constant during the whole simulation period. Indeed, the two ventilation modes will be different for the summer and the winter performance evaluations.

A static *TB* configuration will be used for the performance comparison in the winter season while a static *OAC* configuration will be used as reference system for the summer season. For both the systems, in winter and summer conditions, the shading controls in function of the incident solar radiation on the façade (*SSC#1* and *WSC#1*) will be adopted. Also the strategies applied during the week end and the unoccupied hours for the shading system are the same implemented inside the flexible double skin façade system.

The use of a static *DSF* system aims to show how the adoption of a dynamic and flexible envelope system in a static way (with no substantial variation of the operating strategies) is basically wrong, leading to a worsening of the overall system performance.

#### Second reference system: single skin system

The second comparison system is a single skin façade system (*SSF*) (*Figure 47*), with an interior venetian blind of the same typology and material used in the double skin system (with fixed slat angle of  $45^\circ$  and drawn mechanism regulated using the incident solar radiation on the façade). Also the frame fraction and the thermal transmittance of the frame are the same inserted as parameters for the double skin façade system. The thermal transmittance of the glazing system has been defined

creating an *equivalent* single skin system, made by the two double glazing units of the inner and the outer skin, separated by an air cavity of *25 cm* (it is a sort of *quadruple* glazing unit). In this way it is possible to define a façade system that has comparable thermal properties respect to the ones of the *DSF*.

During the summer, the windows of the *SSF* can be opened by the occupants in the case of which the indoor temperature is above the set point for the cooling season (as traditionally happens with the traditional façade solutions).

As seen for the thermal zone models with the flexible *DSF* used as façade system, also in the case of the reference systems (static *DSF* and *SSF*) two different configurations (with and without active systems) have been defined. Therefore, other 4 *.idm* files have been created, for a total number of 68 of thermal zone models used for the performance analysis (64 for the flexible *DSF* configurations and 4 for the reference systems used as baseline), 34 with the active systems turned on and 34 for the *free running* configuration.

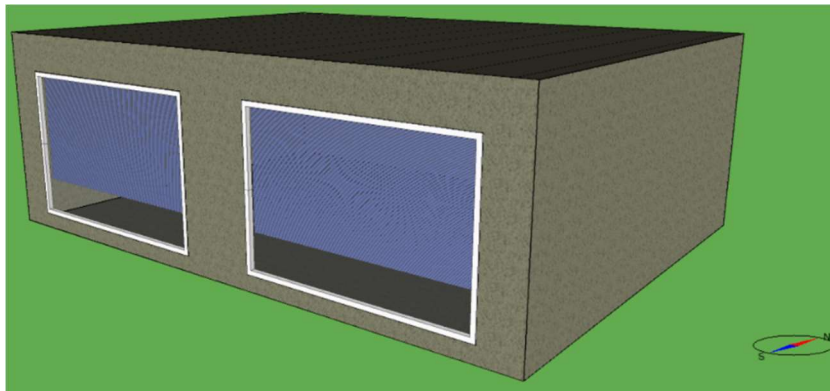


*Figure 47: The single skin façade system used as second comparison system for the performance evaluation*

## 4. Result analysis

In this section, the results of the analysis performed on IDA ICE on the test cells models (with the different façade systems: flexible *DSF*, static *DSF* and *SSF*) are reported, grouped in the different domains of the performance evaluation (energy efficiency and indoor environmental quality). The *DSF*, with different combinations of control, both in summer and winter conditions, have been compared with the selected reference systems already described in 3.5 (*SSF* and static *DSF* systems).

### 4.1. Energy performance analysis

In this section the focus of the evaluation is the energy performance of the thermal zone related to the different configurations of control of the *DSF*, performed on the model of the room with all the active systems (ventilation, cooling and heating) turned on, as in the normal operational time of the building. The values of energy consumption for the thermal zone are referred to the months of July for the summer conditions simulation and to the month of January for the winter conditions simulation, as illustrated in 3.3.

The following energy consumptions are considered for the multidomain assessment of the energy performance of the different implemented control combinations:

- Energy need for space heating: it corresponds to the overall thermal energy that is required by the ideal heater of the room to keep the indoor temperature set point values for the heating and the cooling season. It can be used to assess how much is the impact of the implemented control on the overall energy requirements for the space heating of the room.
- Energy need for space cooling: in similar way to the energy need for the space heating, it corresponds to the energy required by the ideal cooler of the room to keep the indoor temperature set point values for the heating and cooling season. It can be used to assess how much is the impact of the implemented control on the overall energy requirements for the space cooling of the room.
- Energy need for ventilation heating: it is the energy required by the heating coil of the *AHU* of the room to heat up the ventilation air to the predefined setpoint ( $16^{\circ}\text{C}$  for the whole year). It can be used to evaluate how much the passive use of solar gains inside the cavity can reduce the energy need for the pre-heating of the ventilation air (especially during the winter season).
- Energy need for the ventilation cooling: it is the energy required by the heating coil of the *AHU* of the room to cool down the ventilation air to the predefined setpoint ( $16^{\circ}\text{C}$  for the whole year).



- *Energy need for artificial lighting*: it is the energy required for the functioning of the artificial lighting inside the room. It can be used to evaluate how much the shading control can affect the energy requirements for the artificial lighting inside the considered room.

These are different kinds of energy uses for the considered room. In particular, the energy for space cooling and heating are room loads (for an ideal cooler and an ideal heater), the energy for ventilation heating and cooling is thermal energy that can be given to or extracted from the ventilation air and finally the energy need for artificial lighting is an electrical consumption.

Consequently, it is necessary to consider them in separate way. Indeed, the energy for space heating and ventilation heating are grouped together in the heating energy need for the room. In the same way, energy for space cooling and ventilation cooling are grouped together in the cooling energy need for the room. On the other hand, the energy need for artificial lighting is accounted in a separate way.

#### 4.1.1. Summer conditions

In this section are report the results regarding the energy analysis performed on the room with the different façade systems during the month of July. The variations, expressed in this case in number of times, are referred to the *SSF*.

##### 4.1.1.1. Heating energy need for summer conditions

In this section, the energy need for heating (both space and ventilation) in the different configurations of control for the *DSF* has been analyzed and compared to the ones of the static *OAC* configuration and the *SSF* system. It is not common to evaluate the energy need for heating during the summer season, but it is anyway necessary to have a wider evaluation of the façade system impact on the overall performance of the building.

The related values of energy consumption (expressed in *kWh* and *kWh/m<sup>2</sup>*) are reported in *Table 20*.

Combinations of control	TOTAL [kWh]			TOTAL [kWh/m <sup>2</sup> ]			[n°]
	Space heating	Ventilation heating	TOT	Space heating	Ventilation heating	TOT	Variation
SC#1 SAC#1 SSC#1	30.86	13.75	44.61	0.64	0.29	0.93	+8.744
SC#2 SAC#1 SSC#2	31.11	13.76	44.87	0.65	0.29	0.93	+8.801
SC#3 SAC#1 SSC#3	31.16	13.75	44.91	0.65	0.29	0.94	+8.810
SC#4 SAC#1 SSC#4	31.08	13.75	44.83	0.65	0.29	0.93	+8.792
SC#5 SAC#2 SSC#1	30.86	13.75	44.61	0.64	0.29	0.93	+8.744
SC#6 SAC#2 SSC#2	31.10	13.76	44.86	0.65	0.29	0.93	+8.799
SC#7 SAC#2 SSC#3	31.16	13.75	44.91	0.65	0.29	0.94	+8.810
SC#8 SAC#2 SSC#4	31.08	13.75	44.83	0.65	0.29	0.93	+8.792
SC#9 SAC#3 SSC#1	30.15	10.75	40.90	0.63	0.22	0.85	+7.934

<i>SC#10 SAC#3 SSC#2</i>	30.48	10.89	41.37	0.64	0.23	<b>0.86</b>	+8.037
<i>SC#11 SAC#3 SSC#3</i>	30.30	10.03	40.33	0.63	0.21	<b>0.84</b>	+7.810
<i>SC#12 SAC#3 SSC#4</i>	30.45	10.85	41.30	0.63	0.23	<b>0.86</b>	+8.021
<i>SC#13 SAC#4 SSC#1</i>	30.13	11.22	41.35	0.63	0.23	<b>0.86</b>	+8.032
<i>SC#14 SAC#4 SSC#2</i>	30.50	11.24	41.74	0.64	0.23	<b>0.87</b>	+8.118
<i>SC#15 SAC#4 SSC#3</i>	30.52	11.21	41.73	0.64	0.23	<b>0.87</b>	+8.115
<i>SC#16 SAC#4 SSC#4</i>	30.49	11.24	41.73	0.64	0.23	<b>0.87</b>	+8.115
<i>SC#17 SAC#5 SSC#1</i>	99.60	4.57	104.17	2.08	0.10	<b>2.17</b>	+21.754
<i>SC#18 SAC#5 SSC#2</i>	95.16	4.57	99.73	1.98	0.10	<b>2.08</b>	+20.784
<i>SC#19 SAC#5 SSC#3</i>	86.55	4.57	91.12	1.80	0.10	<b>1.90</b>	+18.904
<i>SC#20 SAC#5 SSC#4</i>	86.54	4.57	91.11	1.80	0.10	<b>1.90</b>	+18.902
<i>Reference Static OAC</i>	27.73	4.57	32.30	0.58	0.10	<b>0.67</b>	+6.055
<i>Reference Single Skin</i>	0.00	4.58	4.58	0.00	0.10	<b>0.10</b>	-

Table 20: Heating energy requirements for the different façade systems (July)

In the single skin system, the energy need for space heating in summer is null, while the energy need for ventilation heating is almost not relevant. The adoption of the *DSF*, both static and controlled, increases the amount of the energy that is required for both, ventilation and space heating. The configurations which cause the most relevant increase of the energy for space heating are the ones which adopt the *SAC#5* air flow control (from *SC#17* to *SC#20*), with not relevant differences in function of the shading control typology that is used for the blind in the cavity. For all the four combinations of implemented control, the increasing with respect to the *SSF* is about 20 times (about 22 in the case of *SC#17*).

The other configurations of air flow control (*SAC#1*, *SAC#2*, *SAC#3* and *SAC#4*) increase of a lower extent the energy need for heating in the room, but the impact on the overall performance of the system (compared to the single skin system) is anyway negative. For all the configurations, in this case, the increase oscillates between the 7 and 8 times compared to the *SSF*. The static *OAC* configuration increases in the same way the overall energy need for heating of the system, but in a lower extent (about 6 times). This is caused by the adoption of only the natural ventilation inside the cavity, which is less effective in the removal of excess of heat compared to the mechanical ventilation case. In addition, there is no introduction of air from the outdoor environment to the thermal zone through the façade cavity (and vice versa, no extraction of the air from the zone to the outdoor environment through the façade cavity), as visible on the other hand in the flexible *DSF*. These facts can be a possible cause of the lower increasing of the energy need for heating visible with the adoption of the static *OAC* configuration,

It is anyway possible to say that the adoption of a *DSF* in a climate as Frankfurt, in which the summer is not particularly hot compared to more southern locations, can be a cause of a consistent increase of the energy required for the heating of a building (for both space and ventilation), compared to a traditional *SSF*. A graphical comparison of the energy needs for heating is reported in *Figure 48*, in the next page.

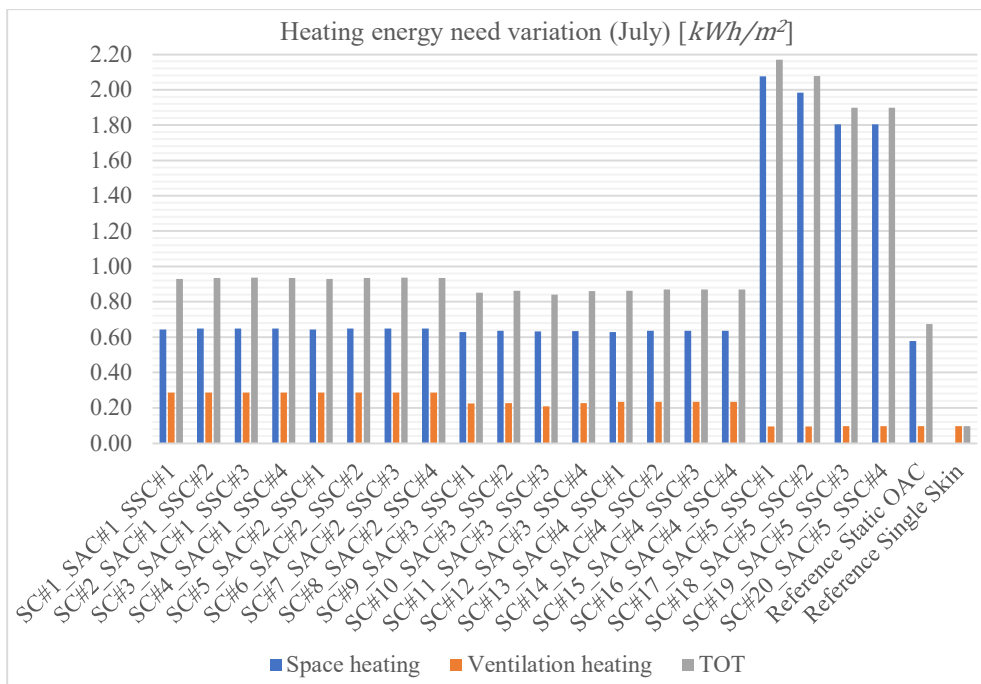


Figure 48: Heating energy requirements for the different façade systems (July)

#### 4.1.1.2. Cooling energy need for summer conditions

In this section, the energy need for cooling (both space and ventilation) in the different configurations of control for the *DSF* has been analyzed and compared to the ones of the static *OAC* configuration and the *SSF*, as done for the energy need for heating. The energy need for cooling represents the main component of the overall energy balance of a building which usually the designer wants to minimize during the summer season, for a better energy efficiency of the system. It is consequently the focus of the energy performance evaluation during the cooling season for the different façade systems.

The related values of energy consumption (expressed in *kWh* and *kWh/m²*) are reported in *Table 21*.

Combinations of control	TOTAL [kWh]			TOTAL [kWh/m²]			[n°]
	Space cooling	Ventilation cooling	TOT	Space cooling	Ventilation cooling	TOT	Variation
SC#1 SAC#1 SSC#1	697.90	115.80	813.70	14.54	2.41	<b>16.95</b>	+3.168
SC#2 SAC#1 SSC#2	683.20	115.80	799.00	14.23	2.41	<b>16.65</b>	+3.093
SC#3 SAC#1 SSC#3	682.30	115.80	798.10	14.21	2.41	<b>16.63</b>	+3.088
SC#4 SAC#1 SSC#4	686.00	115.80	801.80	14.29	2.41	<b>16.70</b>	+3.107
SC#5 SAC#2 SSC#1	697.90	115.80	813.70	14.54	2.41	<b>16.95</b>	+3.168
SC#6 SAC#2 SSC#2	683.20	115.80	799.00	14.23	2.41	<b>16.65</b>	+3.093
SC#7 SAC#2 SSC#3	682.10	115.80	797.90	14.21	2.41	<b>16.62</b>	+3.087

<i>SC#8 SAC#2 SSC#4</i>	685.90	115.80	801.70	14.29	2.41	<b>16.70</b>	+3.106
<i>SC#9 SAC#3 SSC#1</i>	84.10	112.80	196.90	1.75	2.35	<b>4.10</b>	+0.009
<i>SC#10 SAC#3 SSC#2</i>	77.42	112.80	190.22	1.61	2.35	<b>3.96</b>	-0.026
<i>SC#11 SAC#3 SSC#3</i>	83.97	95.65	179.62	1.75	1.99	<b>3.74</b>	-0.080
<i>SC#12 SAC#3 SSC#4</i>	77.09	112.80	189.89	1.61	2.35	<b>3.96</b>	-0.027
<i>SC#13 SAC#4 SSC#1</i>	106.00	112.80	218.80	2.21	2.35	<b>4.56</b>	+0.121
<i>SC#14 SAC#4 SSC#2</i>	97.95	112.80	210.75	2.04	2.35	<b>4.39</b>	+0.079
<i>SC#15 SAC#4 SSC#3</i>	97.32	112.80	210.12	2.03	2.35	<b>4.38</b>	+0.076
<i>SC#16 SAC#4 SSC#4</i>	98.35	112.40	210.75	2.05	2.34	<b>4.39</b>	+0.079
<i>SC#17 SAC#5 SSC#1</i>	21.29	58.21	79.50	0.44	1.21	<b>1.66</b>	-0.593
<i>SC#18 SAC#5 SSC#2</i>	24.66	59.63	84.29	0.51	1.24	<b>1.76</b>	-0.568
<i>SC#19 SAC#5 SSC#3</i>	25.25	45.50	70.75	0.53	0.95	<b>1.47</b>	-0.638
<i>SC#20 SAC#5 SSC#4</i>	25.31	45.45	70.76	0.53	0.95	<b>1.47</b>	-0.638
<i>Reference Static OAC</i>	59.16	113.10	172.26	1.23	2.36	<b>3.59</b>	-0.118
<i>Reference Single Skin</i>	82.43	112.80	195.23	1.72	2.35	<b>4.07</b>	-

Table 21: Cooling energy requirements for the different façade systems (July)

For what concerns the energy need for cooling, it is possible to see a consistent variation of the total amount of energy that is required in function of the combination of control that is applied to the façade system: this means that the application of different control logics for the cavity air flows in the summer is particularly effective in the influence of the energy need for cooling.

In the reference single skin system, the energy need for cooling (both space and ventilation) is relevant. With the adoption of a static *OAC* configuration, the overall energy need for cooling is reduced of about *12%*. From this point of view, it could be enough to say that a static *OAC* configuration is good for the summer period in the case of the Frankfurt climate. Anyway, it is possible to see that using the four configurations of control with *SAC#5* the reduction of the overall energy needs for cooling (both in terms of space and ventilation) is about *60%*: for *SC#19* and *SC#20* the percentage is even closer to *65%*.

The other combinations of control with the adoption *SAC#1*, *SAC#2*, *SAC#3* and *SAC#4* are considerably less effective in the reduction of the energy need for cooling. Only *SC#10*, *SC#11* and *SC#12* (that use the *SAC#3* control for the air flows) produce a reduction of the energy need for cooling (anyway lower than the one observed with the adoption of the static *OAC* configuration).

On the contrary, the overall energy need for cooling is about three times higher of the one of *SSF* in the case of the control with *SAC#1* and *SAC#2*. With the use of the control combinations with *SAC#4*, on the other hand, the increase of the overall energy need for cooling is between the *7%* and *12%*, in function of the shading control implemented for the cavity blinds: the radiation control of the blind indeed is associated to a higher increase of the energy requirements for cooling (but the difference is not particularly relevant). The same is visible in the other configurations

of control which cause an increase of the energy need for cooling (*SAC#1*, *SAC#2* and *SAC#3*).

It is consequently possible to say that the adoption of a ventilated façade system, if the proper control of the cavity air flow is implemented (as for example #*SAC5*), can be a good solution for the reduction of the overall energy need for cooling also in a temperate climate as Frankfurt.

A graphical comparison of the energy needs for cooling is reported in *Figure 49*.

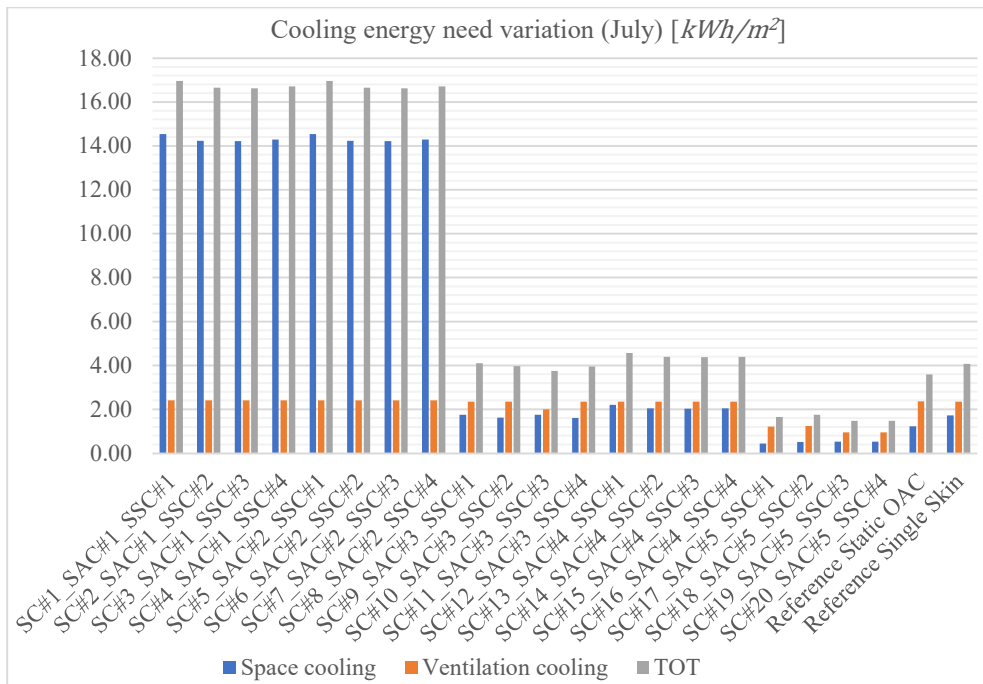


Figure 49: Cooling energy requirements for the different façade systems (July)

#### 4.1.1.3. Artificial lighting energy need for summer conditions

In this section, the energy need for the artificial lighting in the different configurations of control for the *DSF* has been analyzed and compared to the ones of the static *OAC* configuration and the *SSF*, as done for the other energy needs of the room (heating and cooling). While for the energy need for cooling and heating the overall performance of the system is mainly influenced by the control of the cavity air flows, for the artificial lighting the focus is of course on the different shading control that is implemented for the venetian blind. It is observed, indeed, that the trend in the variation of the energy need for the artificial lighting is almost (but not always) the same if a certain control of the shading system is coupled with different forms of control for the cavity air flows.

The related values of energy consumption (expressed in  $kWh$  and  $kWh/m^2$ ) are reported in *Table 22*.

<i>Combinations of control</i>	<b>TOTAL [kWh]</b> Artificial lighting	<b>TOTAL [kWh/m<sup>2</sup>]</b> Artificial lighting	<b>Variation [n°]</b>
<i>SC#1 SAC#1 SSC#1</i>	17.69	<b>0.37</b>	+1.914
<i>SC#2 SAC#1 SSC#2</i>	32.15	<b>0.67</b>	+4.296
<i>SC#3 SAC#1 SSC#3</i>	29.33	<b>0.61</b>	+3.831
<i>SC#4 SAC#1 SSC#4</i>	34.17	<b>0.71</b>	+4.628
<i>SC#5 SAC#2 SSC#1</i>	17.69	<b>0.37</b>	+1.914
<i>SC#6 SAC#2 SSC#2</i>	32.15	<b>0.67</b>	+4.296
<i>SC#7 SAC#2 SSC#3</i>	29.33	<b>0.61</b>	+3.831
<i>SC#8 SAC#2 SSC#4</i>	34.16	<b>0.71</b>	+4.627
<i>SC#9 SAC#3 SSC#1</i>	18.49	<b>0.39</b>	2.046
<i>SC#10 SAC#3 SSC#2</i>	32.78	<b>0.68</b>	+4.399
<i>SC#11 SAC#3 SSC#3</i>	29.94	<b>0.62</b>	+3.932
<i>SC#12 SAC#3 SSC#4</i>	34.11	<b>0.71</b>	+4.619
<i>SC#13 SAC#4 SSC#1</i>	18.49	<b>0.39</b>	+2.046
<i>SC#14 SAC#4 SSC#2</i>	32.73	<b>0.68</b>	+4.391
<i>SC#15 SAC#4 SSC#3</i>	29.93	<b>0.62</b>	+3.930
<i>SC#16 SAC#4 SSC#4</i>	34.55	<b>0.72</b>	+4.691
<i>SC#17 SAC#5 SSC#1</i>	18.48	<b>0.39</b>	+2.044
<i>SC#18 SAC#5 SSC#2</i>	15.22	<b>0.32</b>	+1.507
<i>SC#19 SAC#5 SSC#3</i>	16.17	<b>0.34</b>	+1.663
<i>SC#20 SAC#5 SSC#4</i>	15.80	<b>0.33</b>	+1.603
<i>Reference Static OAC</i>	17.73	<b>0.37</b>	+1.920
<i>Reference Single Skin</i>	6.07	<b>0.13</b>	-

*Table 22: Artificial lighting energy requirements for the different façade systems (July)*

The *SSF* has by default an energy need for artificial lighting that is considerably lower compared to the ones of the double skin system. This is mainly caused by the adoption of two skins of glass instead of one, that can reduce of a certain extent the amount of daylight entering inside the indoor environment.

Anyway, the implementation of a certain control has the highest impact on the overall energy need for artificial lighting. The more the control is focused on keeping the comfort for the occupants (both thermal and visual), the higher can be the amount of energy required for artificial lighting. This is because the limitation of the amount of daylight to limit unwanted solar gains or glare discomfort can increase the need of artificial lighting (when the limit of *500 lux* on the working plane is not reached).

In the configurations of control that use *SAC#1*, *SAC#2*, *SAC#3* and *SAC#4* as control for the cavity air flows, the increase of the energy requirements for artificial lighting in case of the temperature control and variable slat angle of the blind (*SSC#3* and *SSC#4*) is considerably higher compared to the case of a simple radiation control with fixed slat angle (*SSC#1*): the application of *SSC#1* increases about 2 times the energy required for artificial lighting, while with other forms of control the increase is about

4 times, compared to the single skin system (which has a simple radiation control of the blind with fixed slat angle). Consequently, the amount of daylight entering inside the indoor environment during the occupied hours is greater compared to the other three forms of control (*SSC#2*, *SSC#3* and *SSC#4*), with a subsequent reduction of the energy need for artificial lighting compared to the other configurations of controlled *DSF*.

The exception is observed in the case of the combinations that use *SAC#5* as control for the cavity air flows (from *SC#17* to *SC#20*): lower energy consumptions for artificial lighting are expected in this case if *SSC#2*, *SSC#3* and *SSC#4* are used. Indeed, in only these three cases (*SC#18*, *SC#19* and *SC#20*) the increasing in the energy for artificial lighting is lower than in the case of the static *OAC* configuration, with the *SSC#1* implementation for the shading control: in these three cases the increase is only about 1.5 compared to *SSF*. This is a consequence of a more efficient regulation of the indoor temperature produced by the adoption of the *SAC#5* control, which limits the number of times in which the blind is drawn (with a subsequent greater amount of light entering inside the indoor environment).

A graphical comparison of the energy needs for artificial lighting is reported in *Figure 50*.

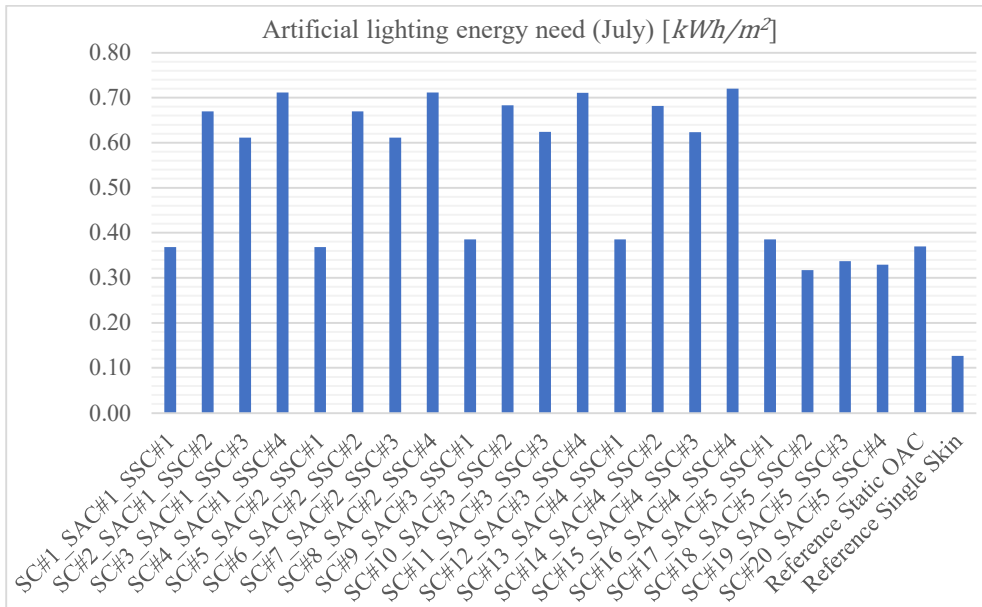


Figure 50: Artificial lighting energy requirements for the different façade systems (July)

#### 4.1.2. Winter conditions

In this section are report the results regarding the energy analysis performed on the room with the different façade systems during the month of January. The data are



reported both, in tabular and graphical way as done for the summer season. The variations, expressed in this case in number of times, are referred to the *SSF*, as done for the summer season.

#### 4.1.2.1. Heating energy need for winter conditions

In this section, the energy need for heating (both space and ventilation) in the different configurations of control for the *DSF* has been analyzed and compared to the ones of the static *TB* configuration and the *SSF*, as done during the summer season. In similar way to the cooling for the summer season, the energy need for heating represents the main component of the overall energy balance of a building which usually the designer wants to minimize during the heating season, reducing the heat losses through the envelope and exploiting the passive solar gains for the ventilation heating.

The related values of energy consumption (expressed in *kWh* and *kWh/m<sup>2</sup>*) are reported in *Table 23*.

Combinations of control	TOTAL [kWh]			TOTAL [kWh/m <sup>2</sup> ]			[n°]
	Space heating	Ventilation heating	TOT	Space heating	Ventilation heating	TOT	Variation
WC#1 WAC#1 WSC#1	473.10	89.10	562.20	9.86	1.86	11.71	+0.120
WC#2 WAC#1 WSC#2	464.50	88.87	553.37	9.68	1.85	11.53	+0.103
WC#3 WAC#1 WSC#2	465.70	88.97	554.67	9.70	1.85	11.56	+0.105
WC#4 WAC#1 WSC#3	463.50	88.71	552.21	9.66	1.85	11.50	+0.100
WC#5 WAC#2 WSC#1	469.60	89.14	558.74	9.78	1.86	11.64	+0.113
WC#6 WAC#2 WSC#2	464.50	88.75	553.25	9.68	1.85	11.53	+0.102
WC#7 WAC#2 WSC#3	458.50	84.41	542.91	9.55	1.76	11.31	+0.082
WC#8 WAC#2 WSC#4	463.90	88.50	552.40	9.66	1.84	11.51	+0.101
WC#9 WAC#3 WSC#1	466.70	90.50	557.20	9.72	1.89	11.61	+0.110
WC#10 WAC#3 WSC#2	463.50	90.95	554.45	9.66	1.89	11.55	+0.105
WC#11 WAC#3 WSC#3	464.80	91.68	556.48	9.68	1.91	11.59	+0.109
WC#12 WAC#3 WSC#4	455.40	84.68	540.08	9.49	1.76	11.25	+0.076
Reference Static TB	473.30	80.53	553.83	9.86	1.68	11.54	+0.104
Reference Single Skin	422.70	79.16	501.86	8.81	1.65	10.46	-

Table 23: Heating energy requirements for the different façade systems (January)

Compared to the summer case and the energy need for cooling, in the winter season there is a more constant trend in the values of energy required for space heating and ventilation heating with the different implemented forms of control for the *DSF*: it is not visible the high variability of performance in the cooling energy need observed for the summer season. In addition, the energy required for the heating of the room and the ventilation air with the adoption of the *SSF* is in the same order of magnitude of the one present with the adoption of the *DSF* (both static and flexible).

The energy need for space heating is slightly lower in the *SSF* than in the *DSF* (also in the case of the static *TB* configuration). The reasons for this can be different: in



particular, the presence of an additional air cavity, if not properly airtight, can increase the heat losses through the façade, respect to a single skin system (in which no air cavities are present). Moreover, if an air movement is present in the cavity, as in the case of the other configurations adopted during the winter (*AS*, *IAC*, *CF* or *OAC*) the convective heat losses through the façade can be greater, increasing in this way the overall space heating demand. For what concerns the energy need for the ventilation heating, the impact of the adoption of the cavity for the passive pre-heating of the air is not so relevant: as it is possible to see, the energy consumption required for the ventilation heating is almost the same in all the façade systems, ranging from  $1.65 \text{ kWh/m}^2$  of the *SSF* to  $1.91 \text{ kWh/m}^2$  of the *WC#11* combination, which is the less effective under this point of view.

Looking at the overall energy need for heating, the largest increase (12%) is associated to *WC#1* while the lowest one (7.62%) is linked to the adoption of *WC#12*. In the case of the static *TB* configuration, the increase is about 10.3%. Consequently, in this case it is difficult to establish which could be the optimal control configuration to apply for the double skin façade during the winter for the minimization of the overall energy need for heating.

A graphical comparison of the energy needs for heating is reported in *Figure 51*.

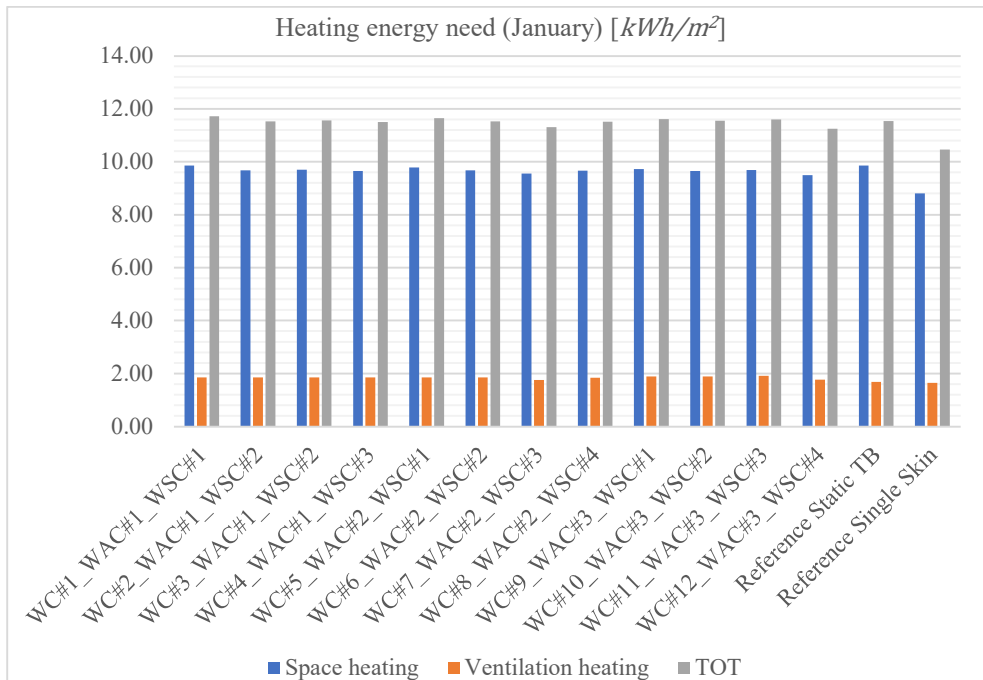


Figure 51: Heating energy requirements for the different façade systems (January)

#### 4.1.2.2. Cooling energy need for winter conditions

In this section, the energy need for cooling (both space and ventilation) in the different configurations of control for the *DSF* has been analyzed and compared to the ones of the static *TB* configuration and the *SSF*, as done for the energy need for heating.

The related values of energy consumption (expressed in *kWh* and *kWh/m<sup>2</sup>*) are reported in *Table 24*.

Combinations of control	TOTAL [kWh]			TOTAL [kWh/m <sup>2</sup> ]		
	Space cooling	Ventilation cooling	TOT	Space cooling	Ventilation cooling	TOT
<i>WC#1 WAC#1 WSC#1</i>	6.30	0.00	6.30	0.13	0.00	+0.131
<i>WC#2 WAC#1 WSC#2</i>	8.87	0.00	8.87	0.18	0.00	+0.185
<i>WC#3 WAC#1 WSC#2</i>	8.33	0.00	8.33	0.17	0.00	+0.174
<i>WC#4 WAC#1 WSC#3</i>	11.35	0.00	11.35	0.24	0.00	+0.236
<i>WC#5 WAC#2 WSC#1</i>	6.32	0.00	6.32	0.13	0.00	+0.132
<i>WC#6 WAC#2 WSC#2</i>	9.30	0.00	9.30	0.19	0.00	+0.194
<i>WC#7 WAC#2 WSC#3</i>	6.41	0.00	6.41	0.13	0.00	+0.133
<i>WC#8 WAC#2 WSC#4</i>	10.97	0.00	10.97	0.23	0.00	+0.229
<i>WC#9 WAC#3 WSC#1</i>	17.10	0.00	17.10	0.36	0.00	+0.356
<i>WC#10 WAC#3 WSC#2</i>	18.98	0.00	18.98	0.40	0.00	+0.395
<i>WC#11 WAC#3 WSC#3</i>	15.35	0.00	15.35	0.32	0.00	+0.320
<i>WC#12 WAC#3 WSC#4</i>	18.55	0.00	18.55	0.39	0.00	+0.386
<i>Reference Static TB</i>	0.00	0.00	0.00	0.00	0.00	0.00
<i>Reference Single Skin</i>	0.00	0.00	0.00	0.00	0.00	0.00

*Table 24: Cooling energy requirements for the different façade systems (January)*

The variation of the energy need for cooling during the winter season is critical as the variation of the energy need for heating during the summer season, as showed in the related table. As it is possible to see, all the configurations of flexible *DSF* produce an increase of the energy need for space cooling, that is absent in the static *TB* configuration and in the reference *SSF*. This is mainly caused by the introduction of warm air from the cavity to the indoor space (as in the case of the *AS* configuration) that can increase in some cases the energy need for space cooling.

The highest energy needs are present if the *WAC#3* control is implemented for the cavity air flows, while lower values are present in the case of the implementation of *WAC#2* and *WAC#1*. *WAC#3* control is consequently the worst in terms of increasing of the required energy for space cooling during the winter season.

A graphical comparison of the energy needs for cooling is reported in *Figure 52*, in the next page.

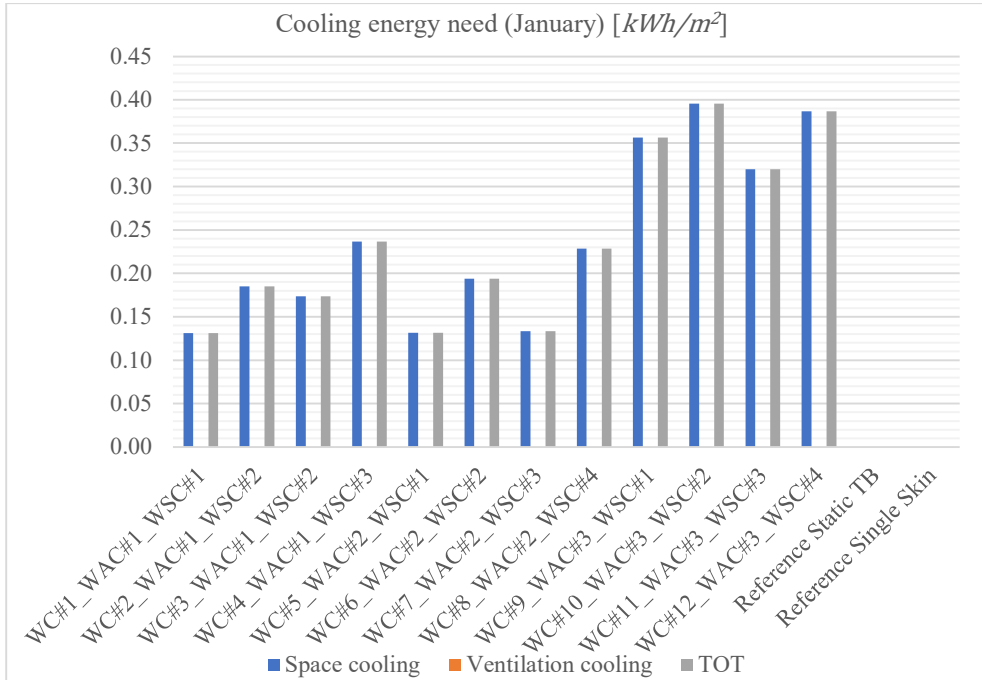


Figure 52: Cooling energy requirements for the different façade systems (January)

#### 4.1.2.3. Artificial lighting energy need for winter conditions

In this section, the energy need for the artificial lighting in the different configurations of control for the double skin façade has been analyzed and compared to the ones of the static *TB* configuration and the *SSF*.

The related values of energy consumption (expressed in *kWh* and *kWh/m²*) are reported in *Table 25*.

The same considerations illustrated in the summer season are of course valid for the winter period. The energy consumption for the artificial lighting is mainly dependent on the typology of shading control, with no significant dependence with the implemented control for the cavity air flows.

Compared to the summer season, anyway, the increase with respect to the *SSF* is considerably lower (only in three cases, the ones with the adoption of *WSC#3*, above the 50%). In the *SSF* and in the static *TB* configuration, the energy need for artificial lighting is greater than the one present during the summer season, due to the lower amount of available daylight inside the thermal zone (the same situation observed in the case of the summer season). Also for the *WSC#1* control (function of the incident solar radiation on the façade) the required energy consumption is higher in winter than in summer (this is visible in *WC#1*, *WC#2* and *WC#3*).

	<i>TOTAL [kWh]</i>	<i>TOTAL [kWh/m<sup>2</sup>]</i>	<i>[n°]</i>
<i>Combinations of control</i>	<i>Artificial lighting</i>	<i>Artificial lighting</i>	<i>Variation</i>
<i>WC#1 WAC#1 WSC#1</i>	26.56	0.55	+0.445
<i>WC#2 WAC#1 WSC#2</i>	26.07	0.54	+0.418
<i>WC#3 WAC#1 WSC#3</i>	28.72	0.60	+0.563
<i>WC#4 WAC#1 WSC#4</i>	24.85	0.52	+0.352
<i>WC#5 WAC#2 WSC#1</i>	26.56	0.55	+0.445
<i>WC#6 WAC#2 WSC#2</i>	26.05	0.54	+0.417
<i>WC#7 WAC#2 WSC#3</i>	28.67	0.60	+0.560
<i>WC#8 WAC#2 WSC#4</i>	24.86	0.52	+0.353
<i>WC#9 WAC#3 WSC#1</i>	26.56	0.55	+0.445
<i>WC#10 WAC#3 WSC#2</i>	25.98	0.54	+0.413
<i>WC#11 WAC#3 WSC#3</i>	29.75	0.62	+0.619
<i>WC#12 WAC#3 WSC#4</i>	24.89	0.52	+0.354
<i>Reference Static TB with WSC#1</i>	26.50	0.55	+0.442
<i>Reference Single Skin</i>	18.38	0.38	-

Table 25: Artificial lighting energy requirements for the different façade systems (January)

On the other hand, for the other forms of control (*WSC#2*, *WSC#3* and *WSC#4*), which are activated by the indoor temperature in the zone, the required energy need for artificial lighting is higher in summer than in winter. This is mainly caused by the fact that the overheating risk is greater in summer than in winter: consequently, the temperature activation of the blind is more frequent in summer than in winter.

This is a consistent limitation of the application of the temperature control of the blind during the summer season, which should improve the indoor thermal comfort conditions but causes at the same time a significant increase of the energy need for artificial lighting.

A graphical comparison of the energy needs for artificial lighting is reported in *Figure 53*, in the next page.

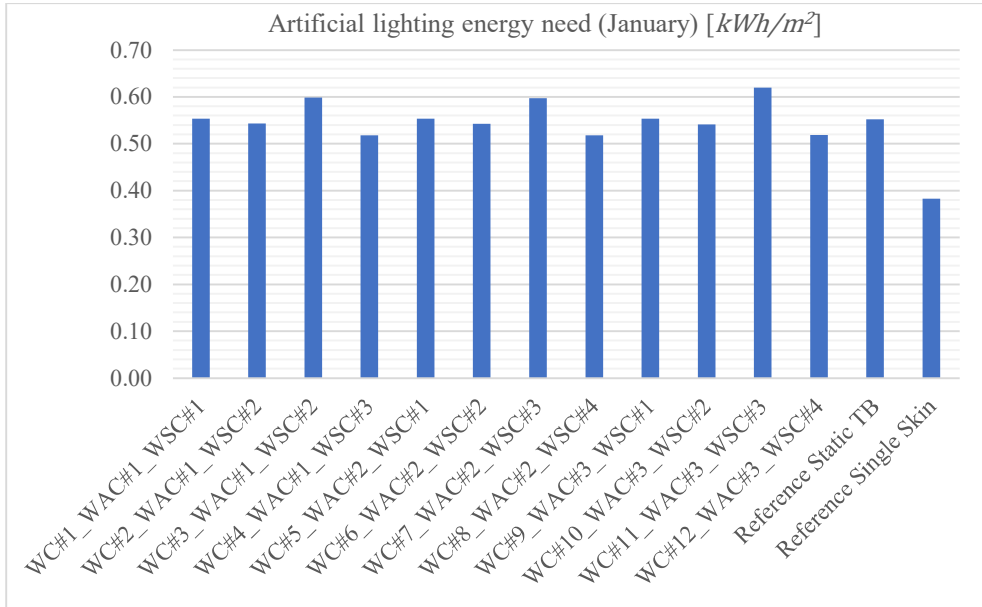


Figure 53: Artificial lighting energy requirements for the different façade systems (January)

## 4.2. Indoor climate analysis

Using the IDA ICE model with all the active systems turned off (*free running* configuration) a simulation focused on the indoor climate conditions will be performed, to evaluate the indoor comfort conditions without the presence of active systems for heating, ventilation, and cooling. The requested outputs will be consequently the main temperatures in the zones (indoor air and operative temperatures), Fanger's comfort indices, indoor air quality and daylight on the working plane.

It is quite impossible that the façade could operate in such kind of conditions. Anyway, using a *free running* configuration of the thermal zone it is possible to investigate and understand in a wider extent the relation between the façade and the indoor environmental conditions, since the comfort only depends on the façade itself, without the involvement of any active system. It is anyway necessary to implement before the simulation a *warmup* period, for the stabilization of the indoor conditions both in summer and winter season. It corresponds to a customized start up, with the duration of two weeks, defined in the *Simulation* tab in which the indoor air temperature conditions are kept constant ( $20^{\circ}\text{C}$  in winter and  $26^{\circ}\text{C}$  in summer) inside the thermal zone. The occupancy in the room is also set equal to zero (as a week-end day), to preserve a good indoor air quality condition. After this warmup period, the simulation with the free run configuration of the thermal zone can be performed.

The values of the physical quantities for the thermal zone are referred to the months of July for the summer conditions simulation and to the month of January for the

winter conditions simulation, as seen for the energy simulations. To have a more synthetic and quantitative representation of the results and a more direct comparison of the performances of the different implemented controls, the number of occupied hours (210 in total for both January and July) in which the indoor optimal comfort conditions are not met will be used.

Indeed, for the summer season, for each configuration of control the following quantities will be reported:

- Number of occupied hours above  $26^{\circ}\text{C}$ .
- Number of occupied hours above  $1000\text{ ppm}$  of  $\text{CO}_2$  concentrations.
- Number of occupied hours outside the ranges for the Fanger's comfort indices ( $PPD$  and  $PMV$ ).
- Number of occupied hours below the minimum limit of  $500\text{ lux}$  at the working plane.
- Number of occupied hours above the threshold limit for glare discomfort of  $3000\text{ lux}$  on the working plane.

On the other hand, for the winter season, in similar way, for each configuration of control the following quantities will be reported:

- Number of occupied hours below  $20^{\circ}\text{C}$ .
- Number of occupied hours above  $1000\text{ ppm}$  of  $\text{CO}_2$  concentrations.
- Number of occupied hours outside the ranges for the Fanger's comfort indices ( $PPD$  and  $PMV$ ).
- Number of occupied hours below the minimum limit of  $500\text{ lux}$  at the working plane.
- Number of occupied hours above the threshold limit for glare discomfort of  $3000\text{ lux}$  on the working plane.

In this way, it will be possible to evaluate in a quantitative way which is the impact of each control combination on the indoor climate conditions (considering of course an extreme case of *free running* configuration of the room).

#### **4.2.1. Summer conditions**

In this section are reported the results of the analysis for July, in which the summer combinations have been tested. As seen for the energy analysis, the reference systems for the performance comparison will be the static *OAC* configuration and the *SSF*. The variations, expressed in this case in number of times, are referred to the single skin façade system, as done for the energy analysis.

#### 4.2.1.1. Indoor temperatures and thermal comfort in summer conditions

The temperature trends (air and operative ones) in the month of July for all the 20 configurations have been analyzed using the simulation outputs from IDA ICE, to understand how much the implemented control can affect the indoor thermal comfort conditions inside the zone. Indoor temperatures indeed are the main physical quantities that can affect the thermal sensation of the occupants. As mentioned before, the number of occupied hours in which the threshold limit of  $26^{\circ}\text{C}$  is overcome is considered to evaluate how much the implemented control can be effective in the prevention of the overheating risk inside the room [14].

The number of occupied hours above the limit for each configuration of control are reported in *Table 26*.

<i>Combinations of control</i>	<i>n° hours <math>T_{operative} &gt; 26^{\circ}\text{C}</math></i>	<i>Variation [n°]</i>
<i>SC#1 SAC#1 SSC#1</i>	76.6	-0.433
<i>SC#2 SAC#1 SSC#2</i>	81.8	-0.394
<i>SC#3 SAC#1 SSC#3</i>	83.1	-0.384
<i>SC#4 SAC#1 SSC#4</i>	82	-0.393
<i>SC#5 SAC#2 SSC#1</i>	76.6	-0.433
<i>SC#6 SAC#2 SSC#2</i>	81.8	-0.394
<i>SC#7 SAC#2 SSC#3</i>	83.1	-0.384
<i>SC#8 SAC#2 SSC#4</i>	81.9	-0.393
<i>SC#9 SAC#3 SSC#1</i>	82.5	-0.389
<i>SC#10 SAC#3 SSC#2</i>	91	-0.326
<i>SC#11 SAC#3 SSC#3</i>	91.8	-0.320
<i>SC#12 SAC#3 SSC#4</i>	90.4	-0.330
<i>SC#13 SAC#4 SSC#1</i>	83.9	-0.379
<i>SC#14 SAC#4 SSC#2</i>	91.9	-0.319
<i>SC#15 SAC#4 SSC#3</i>	92.3	-0.316
<i>SC#16 SAC#4 SSC#4</i>	91.8	-0.320
<i>SC#17 SAC#5 SSC#1</i>	74.3	-0.450
<i>SC#18 SAC#5 SSC#2</i>	81.1	-0.399
<i>SC#19 SAC#5 SSC#3</i>	81.9	-0.393
<i>SC#20 SAC#5 SSC#4</i>	80.4	-0.404
<i>Reference Static OAC</i>	129	-0.044
<i>Reference Single Skin</i>	135	-

*Table 26: Number of occupied hours above  $26^{\circ}\text{C}$  for the different façade systems (July)*

From the point of view of the number of hours in which the indoor operative temperatures are above the overheating limit of  $26^{\circ}\text{C}$ , all the configurations produce a reduction of this number compared to the *SSF* and the static *OAC* configuration. This is mainly caused by the positive effect of the extraction of the air from the zone to the outdoor environment by means of the façade cavity (when the façade is operating in *AE* configuration), compared for example to a static *OAC* configuration in which there is not an air exchange between the indoor and the outdoor environment.

Also the adoption of the *AS* configuration in *SAC#5* produces positive effect in the reduction of the overheating risk in the room (and it is also more effective under this point of view compared to the other types of air flow control).

Among the different combinations, the one that reduces of the greatest extent the overheating risk (about 45%) is *SC#17* (which adopts *SAC#5* as control for the cavity air flows), while the lowest reduction (about 32%) is visible in *SC#14*, #15 and #16. The lowest numbers of hours above the overheating risk limit (about 75 hours) are associated to a radiation control of the blind (*SC#1*, *SC#5* and *SC#17*) and not to a temperature activation of the drawn mechanism (used in *SSC#2*, *SSC#3* and *SSC#4*). This can be caused by the fact that the drawn blind can retain a greater extent of heat, releasing it to the cavity and then to indoor environment (with a subsequent greater overheating risk): consequently, the more the blind is in drawn position, the greater is the possibility to overheat the indoor environment.

A graphical comparison of the number of hours above the overheating risk limit is reported in *Figure 54*.

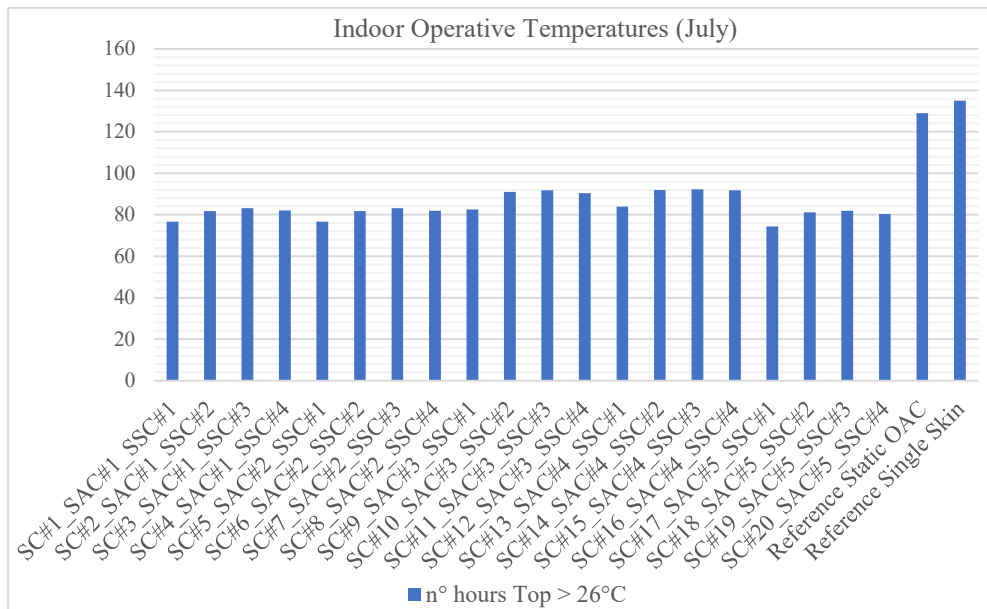


Figure 54: Number of occupied hours above 26°C for the different façade systems (July)

#### 4.2.1.2. Indoor air quality in summer conditions

As done for the indoor temperatures, also the concentrations of  $CO_2$  in the zone with the different forms of control applied to the *DSF* have been analysed, to evaluate how much the implemented control can affect the indoor air quality of the room. As done for the indoor temperatures in the zone, to have a quantitative evaluation of the impact of each control combination on the performance of the system, here it is reported, for



each configuration of control, the number of occupied hours above the limit of *1000 ppm*. This is assumed as maximum threshold limit for indoor *CO<sub>2</sub>* concentrations to provide good health conditions for the occupants, in accordance with the *ASHRAE* standards [33]. The number of hours above the limit for each configuration of control are reported in *Table 27*.

Combinations of control	n° hours CO <sub>2</sub> > 1000 ppm
<i>SC#1 SAC#1 SSC#1</i>	201
<i>SC#2 SAC#1 SSC#2</i>	201
<i>SC#3 SAC#1 SSC#3</i>	201
<i>SC#4 SAC#1 SSC#4</i>	201
<i>SC#5 SAC#2 SSC#1</i>	201
<i>SC#6 SAC#2 SSC#2</i>	201
<i>SC#7 SAC#2 SSC#3</i>	201
<i>SC#8 SAC#2 SSC#4</i>	201
<i>SC#9 SAC#3 SSC#1</i>	202
<i>SC#10 SAC#3 SSC#2</i>	202
<i>SC#11 SAC#3 SSC#3</i>	202
<i>SC#12 SAC#3 SSC#4</i>	202
<i>SC#13 SAC#4 SSC#1</i>	202
<i>SC#14 SAC#4 SSC#2</i>	202
<i>SC#15 SAC#4 SSC#3</i>	202
<i>SC#16 SAC#4 SSC#4</i>	202
<i>SC#17 SAC#5 SSC#1</i>	201
<i>SC#18 SAC#5 SSC#2</i>	201
<i>SC#19 SAC#5 SSC#3</i>	201
<i>SC#20 SAC#5 SSC#4</i>	201
<i>Reference Static OAC</i>	209
<i>Reference Single Skin</i>	36.6

*Table 27: Number of occupied hours above 1100 ppm for the different façade systems (July)*

As it is possible to see, all the configurations of control cause the same number of hours above the limit of *1000 ppm* (201 or 202). Without the presence of an active ventilation system, indeed, the façade alone is not able to limit the concentrations inside the room (even if the mechanical extraction is performed inside the cavity). Considering a total number of occupied hours equal to 210 during the month of July, basically all the time the *CO<sub>2</sub>* concentration are above the limit.

Anyway, the number of hours above the limit is lower than the one with the adoption of the static *OAC* configuration (for which an air flow between the indoor environment and the cavity is not present). Compared to a *SSF* (number of hours above the limit equal to 36.6), in which the window can be opened by the occupants, the number of hours above the limit is anyway considerably higher (about 4.5 times in the case of the controlled façade, about 4.7 times in the case of the static *OAC* configuration): the indoor air quality of the room is consequently a critical aspect of the performance of the *DSF* since it can limit its applicability for natural ventilation purposes.

#### 4.2.1.3. Fanger's comfort indices in summer conditions

For a wider evaluation of the comfort conditions in relation to temperature, radiative discomfort, moisture and draught, the Fanger's comfort indices can be used. It is therefore a better form of evaluation of the indoor environmental quality conditions compared for example to the simpler study of the indoor operative temperatures inside the room. Indeed, according to the *Comfort Category B* defined in the standard *EN ISO 7730*, *PPD* percentage should be kept below *10%*, while the *PMV* index should be always inside the range  $[-0.5; 0.5]$ , to keep acceptable indoor environmental conditions.

For this reason, for each configuration of control it is reported:

- The number of occupied hours above  $PPD = 10\%$
- The number of occupied hours above  $PMV = 0.5$
- The number of occupied hours below  $PMV = -0.5$

The number of hours above and below the limits for each configuration of control are reported in *Table 28*.

<i>Combinations of control</i>	<i>n° hours PPD &gt; 10%</i>	<i>Variation [n°]</i>	<i>n° hours PMV &gt; 0.5</i>	<i>Variation [n°]</i>	<i>n° hours PMV &lt; -0.5</i>
<i>SC#1 SAC#1 SSC#1</i>	135	+4.075	57.3	+1.187	+75
<i>SC#2 SAC#1 SSC#2</i>	131	+3.925	56.9	+1.172	+71
<i>SC#3 SAC#1 SSC#3</i>	134	+4.038	59.1	+1.256	+71.6
<i>SC#4 SAC#1 SSC#4</i>	132	+3.962	57.1	+1.179	+71.9
<i>SC#5 SAC#2 SSC#1</i>	135	+4.075	57.3	+1.187	+75
<i>SC#6 SAC#2 SSC#2</i>	131	+3.925	56.9	+1.172	+71
<i>SC#7 SAC#2 SSC#3</i>	134	+4.038	59.2	+1.260	+71.1
<i>SC#8 SAC#2 SSC#4</i>	132	+3.962	57.1	+1.179	+71.4
<i>SC#9 SAC#3 SSC#1</i>	143	+4.376	69.7	+1.660	+70.2
<i>SC#10 SAC#3 SSC#2</i>	145	+4.451	75	+1.863	+66.6
<i>SC#11 SAC#3 SSC#3</i>	146	+4.489	76.2	+1.908	+66.5
<i>SC#12 SAC#3 SSC#4</i>	144	+4.414	74.3	+1.836	+66.6
<i>SC#13 SAC#4 SSC#1</i>	144	+4.414	70.9	+1.706	+70.2
<i>SC#14 SAC#4 SSC#2</i>	147	+4.526	76.4	+1.916	+67.1
<i>SC#15 SAC#4 SSC#3</i>	147	+4.526	77.3	+1.950	+66.7
<i>SC#16 SAC#4 SSC#4</i>	146	+4.489	76	+1.901	+66.8
<i>SC#17 SAC#5 SSC#1</i>	133	+4.00	54	+1.061	+75.6
<i>SC#18 SAC#5 SSC#2</i>	129	+3.850	52.9	+1.019	+73.3
<i>SC#19 SAC#5 SSC#3</i>	130	+3.887	54.2	+1.069	+72.9
<i>SC#20 SAC#5 SSC#4</i>	128	+3.812	52.2	+0.992	+73
<i>Reference Static OAC</i>	152	+4.714	133	+4.076	+16.5
<i>Reference Single Skin</i>	26.6	-	26.2	-	0

*Table 28: Variation of the comfort indexes in the room for the different façade systems (July)*

As it is possible to see, the number of hours in which the *PPD* index is above 10% is quite different in function of the implemented air flow control inside the cavity. Anyway, the increase of all the considered quantities (*PPD* and *PMV* limits), in relation to the *SSF* is evident: the *SSF* with a traditional openable window is absolutely the best solution if the Fanger's comfort indices are considered. Indeed, with the adoption of the *SSF*, the number of hours below the limit of  $PMV = -0.5$  is zero, while with all the configurations of controlled *DSF* this number is in the order of magnitude of 70 hours.

Indeed, the lowest values among the ones of the flexible *DSF* are for the control combinations which adopt *SAC#5* as control logic for the cavity air flows (it is visible in the control combinations from *SC#17* to *SC#20*). In this case, the number is in the order of 130 hours (as for example in the case of *SC#19*). The other combinations of control (with *SAC#1*, *SAC#2*, *SAC#3* and *SAC#4*) show higher numbers of hours above the limit (in particular, the combinations with *SAC#3* and *SAC#4* are all above the 140 hours).

Looking at the *PMV* indices, the number of hours above the limit of 0.5 is of the same order of magnitude of the number of hours below -0.5, for all the 20 combinations of control that are applied to the *DSF*. This means that the occupants can experience both conditions of thermal discomfort due to too cold or too hot thermal sensations. *SAC#5* is the control which generates the lowest number of hours above the limit of  $PMV = 0.5$  but at the same time the highest number of hours below the limit of  $PMV = -0.5$ .

The same trend is visible in the combinations with *SAC#1* and *SAC#2*. On the other hand, *SAC#3* and *SAC#4* combinations show high number of hours above and below the two threshold limits of *PMV* (and for this reason they are the combinations with the most critical number of hours above the limit of  $PPD = 10\%$ ). Compared to the static *OAC* configuration, all the combinations of control show a lower number of hours above the limit for *PPD*. For the static *OAC* configuration the increasing is about 4.7 time the *SSF*, while for all the other combinations of controlled *DSF* the increase is always below 4.5 times.

In addition, the static *OAC* configuration produces a considerably higher number of hours above the limit of 0.5 for *PPM*, in comparison to the other combinations of controlled façade systems: for the static *OAC* configuration the number of hours above the limit is 133 hours, while the controlled configurations never overreach the value of 80 hours. On the other hand, the number of hours below the limit of  $PMV = -0.5$  is significantly lower in comparison with the controlled *DSF* configurations. The static *OAC* configuration is anyway in the complex largely worse in terms of overheating risk compared to the flexible *DSF* configurations.

A graphical comparison of the variation of the comfort indexes is reported in *Figure 55*, in the next page.

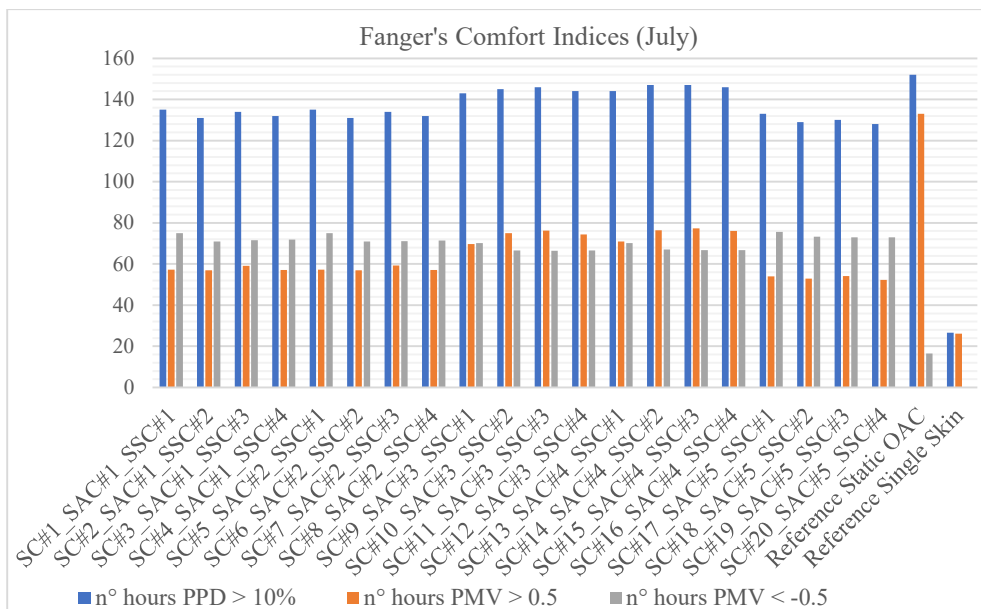


Figure 55: Variation of the comfort indexes in the room for the different façade systems (July)

#### 4.2.1.4. Daylight in summer conditions

In comparison to the indoor temperatures, the indoor  $CO_2$  concentrations and the comfort indices, the indoor illuminance levels on the working plane shows a greater variability of the results, due to the different control logics used for the definition of the slats angle of the blinds (fixed or in function of the cut-off position or of the indoor illuminance levels in the room).

In this case it is possible to analyze the duration curves of the illuminance levels inside the zone for the definition of the number of working hours in which the limit of  $500\text{ lux}$  is not reached, to define which control logic better fits with the minimum requirements established by the regulations.

The number of hours below the limit for each configuration of control are reported in Table 29.

Combinations of control	n° hours $E < 500\text{ lux}$	Variation [n°]
SC#1 SAC#1 SSC#1	95.8	+1.843
SC#2 SAC#1 SSC#2	120	+2.561
SC#3 SAC#1 SSC#3	112	+2.323
SC#4 SAC#1 SSC#4	123	+2.650
SC#5 SAC#2 SSC#1	95.8	+1.843
SC#6 SAC#2 SSC#2	120	+2.561
SC#7 SAC#2 SSC#3	112	+2.323
SC#8 SAC#2 SSC#4	123	+2.650
SC#9 SAC#3 SSC#1	95.5	+1.834

<i>SC#10 SAC#3 SSC#2</i>	123	+2.650
<i>SC#11 SAC#3 SSC#3</i>	113	+2.353
<i>SC#12 SAC#3 SSC#4</i>	124	+2.680
<i>SC#13 SAC#4 SSC#1</i>	95.7	+1.840
<i>SC#14 SAC#4 SSC#2</i>	122	+2.620
<i>SC#15 SAC#4 SSC#3</i>	114	+2.383
<i>SC#16 SAC#4 SSC#4</i>	125	+2.709
<i>SC#17 SAC#5 SSC#1</i>	95.1	+1.822
<i>SC#18 SAC#5 SSC#2</i>	119	+2.531
<i>SC#19 SAC#5 SSC#3</i>	110	+2.264
<i>SC#20 SAC#5 SSC#4</i>	122	+2.620
<i>Reference Static OAC</i>	94.5	+1.804
<i>Reference Single Skin</i>	33.7	-

Table 29: Number of occupied hours below the limit of 500 lux (July)

As it is possible to see, the number of hours below the limit of *500 lux* is independent from the typology of air flow control implemented in the combination: for this reason, the four typologies of shading control are effective in the same way if coupled with different control strategies of the cavity air flows, considering of course a *free running* configuration of the model. In particular, the best performance in terms of indoor illuminance levels is reached with the use of *SSC#1*, the only form of control for which the number of hours in which the minimum requirements are not met is below 100 hours (it is also applied in the reference *OAC* configuration). On the contrary, all the other forms of control show higher numbers, comprised between 110 hours and 120 hours. The highest numbers are associated to the controls *SSC#2* and *SSC#4* (with an increase of about 2.5 times compared to the single skin system).

As explained in the energy analysis section (see in particular *4.1.1.3*), this is mainly caused by the temperature activation of the blind in *SSC#2*, *SSC#3* and *SSC#4*, for which the shading is activated with more frequency compared to the radiation control during the summer season, also in the case of a *free running* configuration of the model, in which the cooling system is not activated and consequently the temperature increase is much more significant. Anyway, the number of hours below the limit, compared to the *SSF* with an interior venetian blind is considerably lower than the ones reached in the *DSF* (both static and flexible).

A graphical comparison of the variation of the number of hours below the minimum levels of illuminance is reported in *Figure 56*, in the next pages.

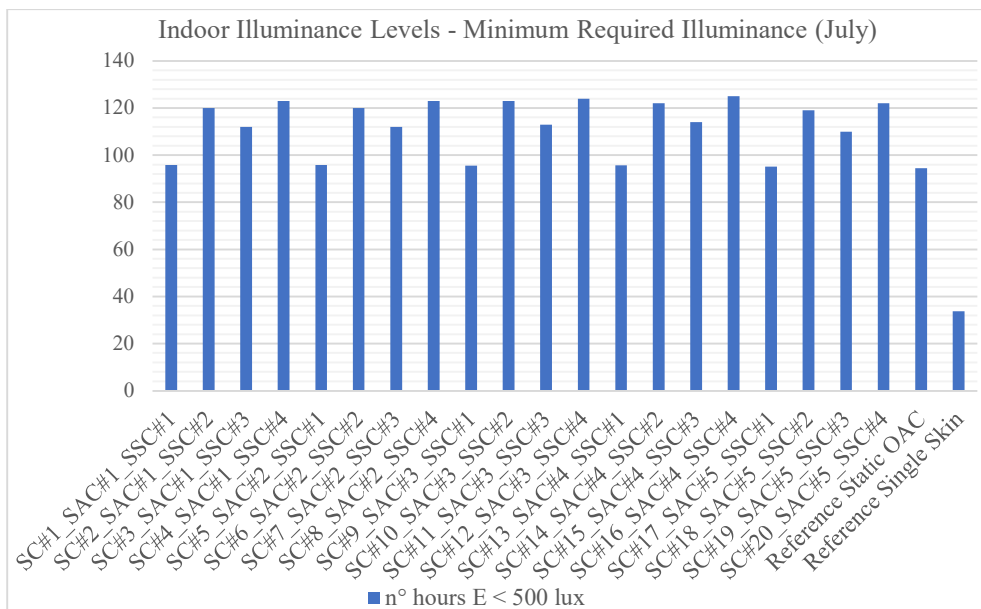


Figure 56: Number of occupied hours below the limit of 500 lux (July)

Considering the opposite case, for the evaluation of the glare risk a maximum threshold limit of horizontal illuminance equal to  $3000 \text{ lux}$  can be assumed. The glare risk should be evaluated considering vertical illuminance levels at the occupant's eye height (between  $1.2 \text{ m}$  and  $1.7 \text{ m}$ ), in accordance with the standard *EN 17037:2018* [17]. It is anyway impossible to evaluate the variation of the vertical illuminance during the selected simulation periods inside IDA ICE: for this reason, a maximum threshold limit of horizontal illuminance equal to  $3000 \text{ lux}$  can be used as reference for the evaluation of the glare risk.

Anyway, no one of the selected forms of control reaches a so high value on the working plane considering the occupied hours of the office (maximum values are around  $1400 \text{ lux}$  for all the typologies of implemented control for the shading, also in the *SSF*). The glare risk during the occupied hours in the office can be therefore assumed as null during the summer season with all the four shading control logics proposed.

#### 4.2.2. Winter conditions

In this section are reported the results of the analysis for the month of January, used for the evaluation of the winter operating conditions for the *DSF*. The results are presented in the same way used for the analysis of the results during the summer season. As seen for the energy analysis, the reference systems for the performance comparison will be the static *TB* configuration and the *SSF*.

#### 4.2.2.1. Indoor temperatures and thermal comfort in winter conditions

As done in the case of the summer season, the indoor temperatures trends have been analyzed for the different configurations of control for the air flows and the shading system. As mentioned before, the number of occupied hours in which the threshold limit of  $20^{\circ}\text{C}$  is not kept is considered to evaluate how much the implemented control can be effective in the prevention of too low operative temperatures inside the room [14].

The number of hours below the limit for each configuration of control are reported in Table 30.

<i>Combinations of control</i>	<i>n° hours <math>T_{\text{operative}} &lt; 20^{\circ}\text{C}</math></i>	<i>Variation [n°]</i>
<i>WC#1 WAC#1 WSC#1</i>	203	+0.080
<i>WC#2 WAC#1 WSC#2</i>	181	-0.037
<i>WC#3 WAC#1 WSC#3</i>	181	-0.037
<i>WC#4 WAC#1 WSC#4</i>	181	-0.037
<i>WC#5 WAC#2 WSC#1</i>	203	+0.080
<i>WC#6 WAC#2 WSC#2</i>	181	-0.037
<i>WC#7 WAC#2 WSC#3</i>	181	-0.037
<i>WC#8 WAC#2 WSC#4</i>	181	-0.037
<i>WC#9 WAC#3 WSC#1</i>	203	+0.080
<i>WC#10 WAC#3 WSC#2</i>	181	-0.037
<i>WC#11 WAC#3 WSC#3</i>	181	-0.037
<i>WC#12 WAC#3 WSC#4</i>	181	-0.037
<i>Reference Static TB</i>	190	+0.011
<i>Reference Single Skin</i>	188	-

Table 30: Number of occupied hours below  $20^{\circ}\text{C}$  for the different façade systems (January)

In the winter season (more than in the summer), the number of hours in which the indoor temperature is below the limit of  $20^{\circ}\text{C}$  is strongly dependent with the typology of shading control that is implemented, since this can affect the amount of solar gains entering inside the room, which can be significant also in a temperate climate as Frankfurt. Indeed, in a free running configuration of the room, they are the only form of thermal energy that is able to increase the indoor temperature.

Analysing the values, the radiation control of the blind produces a higher number of hours below the limit, since the shading is activated with higher frequency compared to the temperature-controlled blind: this is caused by the fact that in the *free running* system, with no space heating activated, it is less frequent to overcome the threshold limit for the indoor temperature. Anyway, the difference is in the order of only 20 hours compared to the other forms of temperature activation (*WSC#2*, *WSC#3* and *WSC#4*). The static *TB* configuration and the *SSF*, with a radiation control of the blind, cause several more hours below the limit in comparison with the *DSF* configurations. In the cases in which the temperature control of the blind is activated, in particular,

the number of hours below the limit is lower compared to the cases of the two reference systems. For the winter season the indoor thermal comfort conditions are therefore less critical in comparison with the summer season, in relation to the *SSF* system.

A graphical representation of the number of hours below the limit of 20°C for the different façade systems is reported in *Figure 57*.

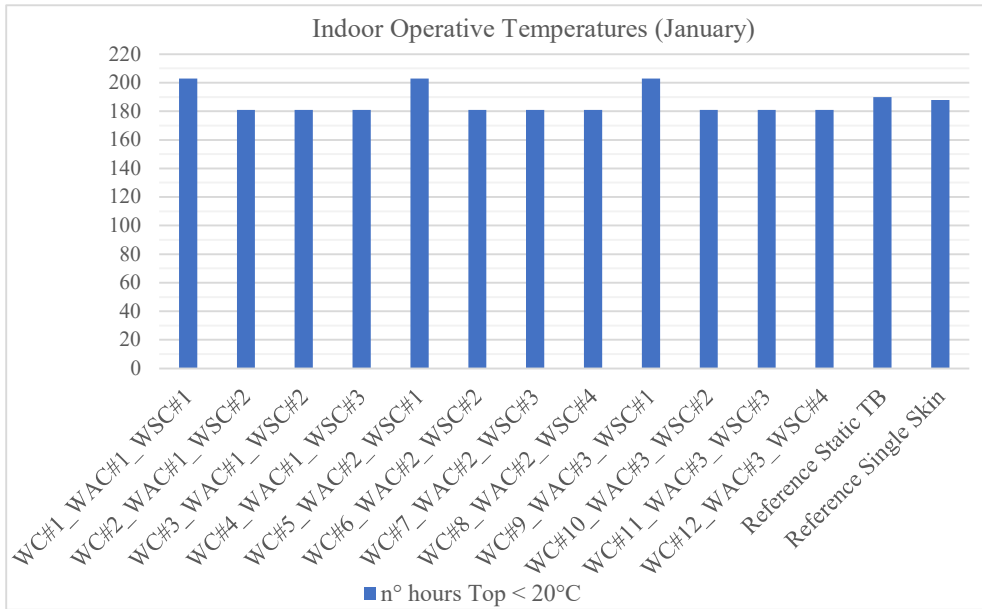


Figure 57: Number of occupied hours below 20°C for the different façade systems (January)

#### 4.2.2.2. Indoor air quality in winter conditions

The analysis of the indoor concentrations of  $CO_2$  in the zone has been performed in the same way as the summer case, analyzing the concentrations trend during the month of January. As done for the summer season, to have a quantitative evaluation of the impact of each control combination on the performance of the system, here it is reported, for each configuration of control, the number of occupied hours above the limit of 1000 ppm.

The  $CO_2$  concentrations inside the zones are higher compared to the summer case (about 10 times), because of the adoption of the *IAQ* and *TB* configurations that do not allow the air exchange between the indoor and the outdoor environment. For this reason, the number of hours above the limit is basically the same (209 hours) for all the façade system (also the *SSF*, in which the opening of the window is controlled in function of the indoor temperature in the room and for this reason the window is quite always kept closed).



#### 4.2.2.3. Fanger's comfort indices in winter conditions

For a wider evaluation of the comfort conditions in relation to temperature, radiative discomfort, moisture and draught, the Fanger's comfort indices can be used, as done for the summer season.

The number of hours above and below the limits for each configuration of control are reported in *Table 31*.

<i>Combinations of control</i>	<i>n° hours PPD &gt; 10%</i>	<i>Variation [n°]</i>	<i>n° hours PMV &gt; 0.5</i>	<i>n° hours PMV &lt; -0.5</i>	<i>Variation [n°]</i>
<i>WC#1 WAC#1 WSC#1</i>	202	+0.074	2.68	197	+0.059
<i>WC#2 WAC#1 WSC#2</i>	181	-0.037	3.37	175	-0.059
<i>WC#3 WAC#1 WSC#3</i>	181	-0.037	3.05	176	-0.054
<i>WC#4 WAC#1 WSC#4</i>	181	-0.037	3.48	175	-0.059
<i>WC#5 WAC#2 WSC#1</i>	202	+0.074	2.65	197	+0.059
<i>WC#6 WAC#2 WSC#2</i>	181	-0.037	3.37	175	-0.059
<i>WC#7 WAC#2 WSC#3</i>	181	-0.037	3.04	176	-0.059
<i>WC#8 WAC#2 WSC#4</i>	181	-0.037	3.48	175	-0.054
<i>WC#9 WAC#3 WSC#1</i>	202	+0.074	2.65	197	+0.059
<i>WC#10 WAC#3 WSC#2</i>	181	-0.037	3.43	175	-0.059
<i>WC#11 WAC#3 WSC#3</i>	181	-0.037	3.02	176	-0.054
<i>WC#12 WAC#3 WSC#4</i>	181	-0.037	3.4	175	-0.059
<i>Reference Static TB</i>	186	-0.011	0	184	-0.011
<i>Reference Single Skin</i>	188	-	0	186	-

*Table 31: Variation of the comfort indexes in the room for the different façade systems (January)*

In the case of the *PPD* index, the trend is the same already observed in the number of hours below the threshold limit of  $20^{\circ}\text{C}$  for the indoor operative temperatures. Highest *PPD* index, corresponding to lower indoor operative temperatures, are associated to the radiation control of the blind (202 hours for all the combinations). For these reasons, the combinations of control with *WSC#2*, *WSC#4* and *WSC#4* as shading control show a lower number of hours above the limit of 10% (181 hours for all the combinations): the temperature control of the blind is consequently more effective during the winter season compared to the summer case considering the thermal comfort parameters.

Another substantial difference from the cooling season is that the number hours in which the limit of 0.5 for the *PMV* index is overcome is considerably lower compared to the opposite case (*PMV* lower than -0.5). This means that the main cause of thermal discomfort during the winter season will be caused by cold sensations for the occupants. Also analysing the *PMV* values, the temperature control of the blind is more effective in the limitation of the number of hours in which the occupants can experience a too cold thermal sensation (with a reduction of the number of hours below -0.5 compared to reference *SSF*). On the contrary, the radiation control is more effective in the limitation of the number of hours in which the value of  $PMV = 0.5$  is

overreached. Anyway, the overall number of occupied hours above this limit is basically insignificant compared to the total number of occupied hours in the month: the maximum reached number above 0.5 is 3.48 hours (with *WC#8*), less than 1.7% of the total number of occupied hours during the month.

In the complex, the impact of the controlled façade configurations on the overall thermal comfort conditions for the occupants is considerably better in winter than the summer operational conditions, in which a worsening of both, *PPD* and *PMV*, was observed.

A graphical comparison of the number of hours above and below the threshold limits is reported in *Figure 58*.

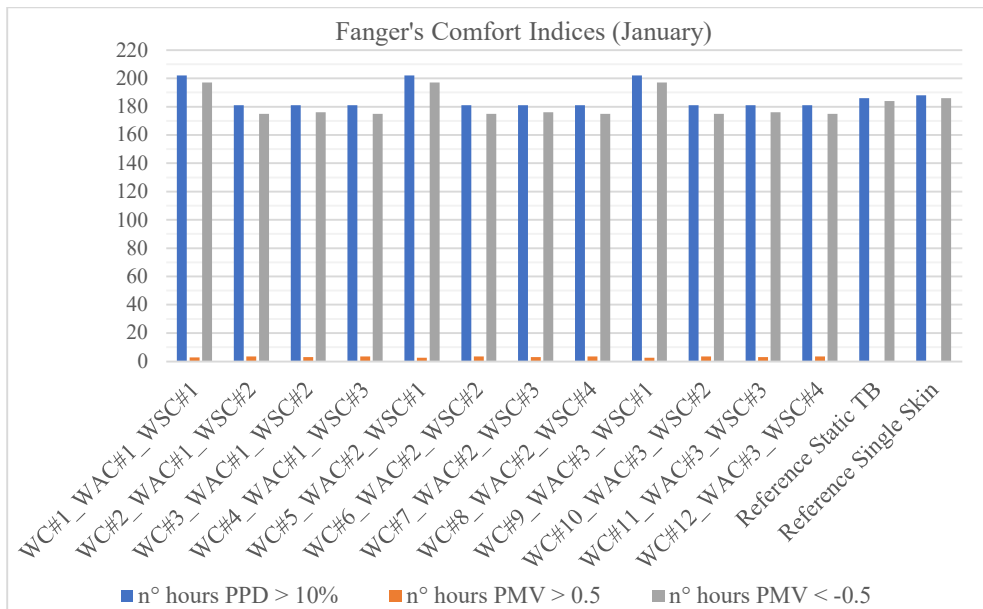


*Figure 58: Variation of the comfort indexes in the room for the different façade systems (January)*

#### 4.2.2.4. Daylight in winter conditions

As done for the summer season, it is possible to analyze the duration curves of the illuminance levels inside the zone for the definition of the number of working hours in which the limit of 500 lux is not reached, to define which control logic better fits with the minimum requirements established by the regulations, as done for the summer season. The number of hours below the limit for each configuration of control are reported in *Table 32*.

Combinations of control	n° hours E < 500 lux	Variation [n°]
<i>WC#1 WAC#1 WSC#1</i>	136	+0.295
<i>WC#2 WAC#1 WSC#2</i>	124	+0.181
<i>WC#3 WAC#1 WSC#2</i>	127	+0.210

<i>WC#4 WAC#1 WSC#3</i>	122	+0.162
<i>WC#5 WAC#2 WSC#1</i>	136	+0.295
<i>WC#6 WAC#2 WSC#2</i>	124	+0.181
<i>WC#7 WAC#2 WSC#3</i>	127	+0.210
<i>WC#8 WAC#2 WSC#4</i>	122	+0.162
<i>WC#9 WAC#3 WSC#1</i>	136	+0.295
<i>WC#10 WAC#3 WSC#2</i>	124	+0.181
<i>WC#11 WAC#3 WSC#3</i>	127	+0.210
<i>WC#12 WAC#3 WSC#4</i>	122	+0.162
<i>Reference Static TB with WSC#1</i>	136	+0.295
<i>Reference Single Skin</i>	105	-

Table 32: Number of occupied hours below the limit of 500 lux (January)

The number of hours below the limit of *500 lux*, as seen for the summer case, is influenced by the typology of control implemented for the shading. In this case, anyway, the observed trend is opposite compared to the cooling season: in winter, indeed, the number of hours below the limit of indoor illuminance is greater for radiation control of the blind, compared to the temperature control.

This is caused by the fact that in winter the activation of the blind caused by the temperature is less frequent compared to the one with incident solar radiation on the façade, as said in the previous sections of the analysis. All the combinations with *WSC#1* show the same number of hours below the limit (136 hours) while for the combinations with *WSC#2*, *WSC#3* and *WSC#4* the numbers vary from 122 to 127 hours. The static *OAC* configuration, with the implementation of *WSC#1* shows of course the same numbers of hours below the limit of the other configurations of flexible double skin façade. Anyway, the single skin system, with the adoption of the same typology of radiation control of the blind shows lower numbers of hours below the limit of *500 lux*, as observed in the summer season.

A graphical representation of the variation of the number of hours below the limit of 500 lux is showed in *Figure 59*, next page.

For the evaluation of the glare risk a maximum threshold limit of horizontal illuminance equal to *3000 lux* can be assumed, as seen for the summer season. Differently from the summer season, anyway, peak values of horizontal illuminance levels during the occupied hours are considerably higher and consequently this threshold limit can be overreached in some cases.

The number of hours above the limit for each configuration of control are reported in *Table 33*, next page.

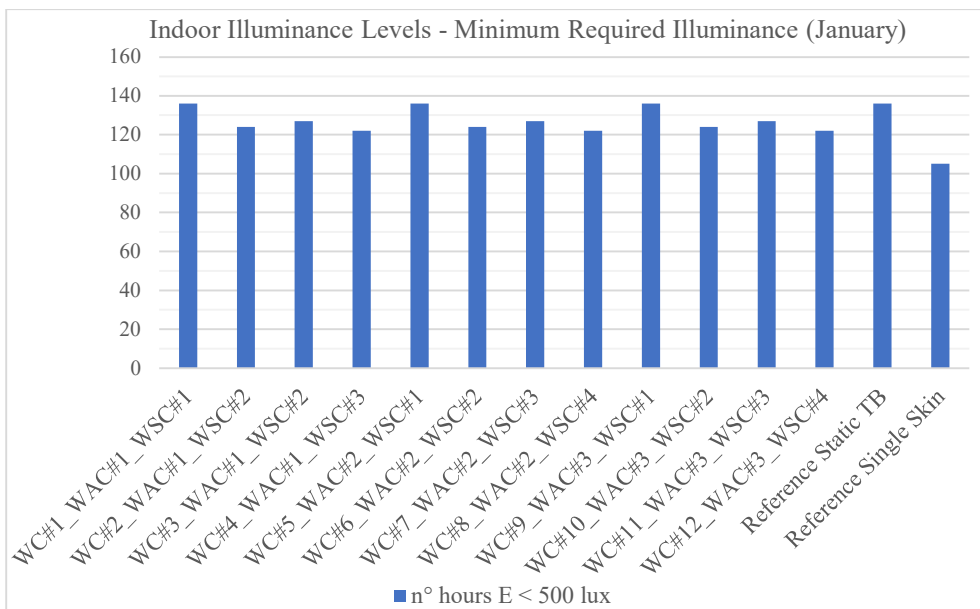


Figure 59: Number of occupied hours below the limit of 500 lux for the different façade systems (January)

Combinations of control	n° hours E > 3000 lux	Variation [n°]
WC#1 WAC#1 WSC#1	0.555	-0.938
WC#2 WAC#1 WSC#2	19.4	+1.182
WC#3 WAC#1 WSC#2	19.4	+1.182
WC#4 WAC#1 WSC#3	20	+1.250
WC#5 WAC#2 WSC#1	0.555	-0.938
WC#6 WAC#2 WSC#2	19.4	+1.182
WC#7 WAC#2 WSC#3	19.4	+1.182
WC#8 WAC#2 WSC#4	20	+1.250
WC#9 WAC#3 WSC#1	0.555	-0.938
WC#10 WAC#3 WSC#2	19.4	+1.182
WC#11 WAC#3 WSC#3	19.4	+1.182
WC#12 WAC#3 WSC#4	20	+1.250
Reference Static TB	0.564	-0.937
Reference Single Skin	8.89	-

Table 33: Number of occupied hours above the limit of 3000 lux (January)

In all the façade systems (also in the *SSF*), it is possible to observe a certain number of occupied hours in which the limit of *3000 lux* is reached. Indeed, only the control configuration in function of the incident solar radiation on the façade shows a number of hours above the limit that is approximately zero (0.555 hours in all the month, with a reduction of *94%* compared to the *SSF*). The other forms of control cause several hours above the limit, in the order of 20 hours. Consequently, the only configurations of control for which the glare risk can be assumed null (and lower than in the case of the single skin system) are the ones with the radiation control implemented in *WSC#1*.

A visual comparison between the number of hours above the glare risk limit for the different façade configurations is reported in *Figure 60*.

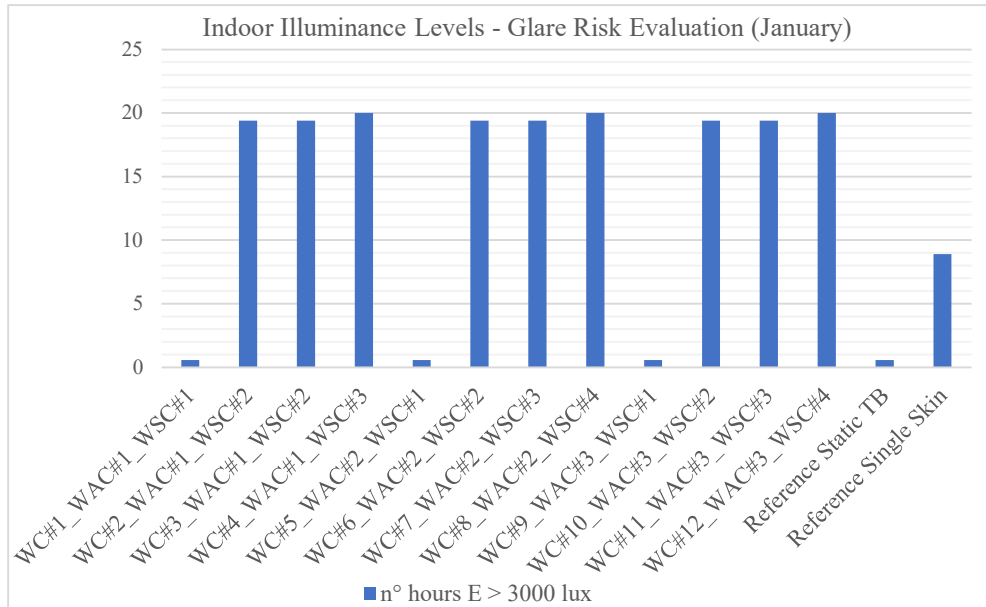


Figure 60: Number of occupied hours above the limit of 3000 lux for the different façade systems (January)

A recap regarding the effectiveness of the implemented control combinations for the summer season in the performance optimization of the system (under the point of view of the different performance domains) is reported in *Table 34*: H, C and L are in this case the energy needs for heating, cooling and artificial lighting. The variations are showed in number of times with respect to the *SSF*, expect for the number of hours above 3000 lux and the number of hours below  $PMV = -0.5$  (for which the corresponding number is zero in *SSF* and therefore the variation is showed in absolute numbers). Also the performance of the static *OAC* configuration is reported.

Variation with respect to the <i>SSF</i> [n° of times]										
Code	Energy efficiency			Indoor Environmental Quality						
	H	C	L	PPD	PVM >0.5	PMV < -0.5	$T_{op}$	IAQ	500 lux	Glare
SC#1	8.74	3.17	1.91	4.08	1.19	+75 h	-0.43	4.49	1.84	+0 h
SC#2	8.80	3.09	4.30	3.92	1.17	+71 h	-0.39	4.49	2.56	+0 h
SC#3	8.81	3.09	3.83	4.04	1.26	+71.6 h	-0.38	4.49	2.32	+0 h
SC#4	8.79	3.11	4.63	3.96	1.18	+71.9 h	-0.39	4.49	2.65	+0 h
SC#5	8.74	3.17	1.91	4.08	1.19	+75 h	-0.43	4.49	1.84	+0 h
SC#6	8.80	3.09	4.30	3.92	1.17	+71 h	-0.39	4.49	2.56	+0 h
SC#7	8.81	3.09	3.83	4.04	1.26	+71.1 h	-0.38	4.49	2.32	+0 h
SC#8	8.79	3.11	4.63	3.96	1.18	+71.4 h	-0.39	4.49	2.65	+0 h
SC#9	7.93	0.01	2.05	4.38	1.66	+70.2 h	-0.39	4.52	1.83	+0 h
SC#10	8.04	-0.03	4.40	4.45	1.86	+66.6 h	-0.33	4.52	2.65	+0 h
SC#11	7.81	-0.08	3.93	4.49	1.91	+66.5 h	-0.32	4.52	2.35	+0 h

<b>SC#12</b>	8.02	-0.03	4.62	4.41	1.84	+66.6 h	-0.33	4.52	2.68	+0 h
<b>SC#13</b>	8.03	0.12	2.05	4.41	1.71	+70.2 h	-0.38	4.52	1.84	+0 h
<b>SC#14</b>	8.12	0.08	4.39	4.53	1.92	+67.1 h	-0.32	4.52	2.62	+0 h
<b>SC#15</b>	8.12	0.08	3.93	4.53	1.95	+66.7 h	-0.32	4.52	2.38	+0 h
<b>SC#16</b>	8.12	0.08	4.69	4.49	1.90	+66.8 h	-0.32	4.52	2.71	+0 h
<b>SC#17</b>	21.75	-0.59	2.04	4.00	1.06	+75.6 h	-0.45	4.49	1.82	+0 h
<b>SC#18</b>	20.78	-0.57	1.51	3.85	1.02	+73.3 h	-0.40	4.49	2.53	+0 h
<b>SC#19</b>	18.90	-0.64	1.66	3.89	1.07	+72.9 h	-0.39	4.49	2.26	+0 h
<b>SC#20</b>	18.90	-0.64	1.60	3.81	0.99	+73 h	-0.40	4.49	2.62	+0 h
<b>OAC</b>	6.06	-0.12	1.92	4.71	4.08	+16.5 h	-0.04	4.71	1.80	+0 h

Table 34: Effectiveness of the different control combinations (Summer) in function of the variation respect to SSF

The same recap is proposed also for the winter season combinations (Table 35): also in this case the variations are expressed in number of times with respect to the SSF. The exception is for the cooling energy need, the number of hours above  $PMV > 0.5$  and the number of hours above 1000 ppm of  $CO_2$  concentrations (in these cases the increase is showed in absolute numbers). The reference TB configuration performance is also reported in the table, as done for the summer season.

Variation with respect to the SSF [n° of times]										
Code	Energy efficiency			Indoor Environmental Quality						
	H	C	L	PPD	PVM >0.5	PMV < -0.5	$T_{op}$	IAQ	500 lux	Glare
<b>WC#1</b>	0.12	0.13 kWh/m <sup>2</sup>	0.45	0.07	+2.68 h	0.06	0.08	+0 h	0.30	-0.94
<b>WC#2</b>	0.10	0.18 kWh/m <sup>2</sup>	0.42	-0.04	+3.37 h	-0.06	-0.04	+0 h	0.18	1.18
<b>WC#3</b>	0.11	0.17 kWh/m <sup>2</sup>	0.56	-0.04	+3.05 h	-0.05	-0.04	+0 h	0.21	1.18
<b>WC#4</b>	0.10	0.24 kWh/m <sup>2</sup>	0.35	-0.04	+3.48 h	-0.06	-0.04	+0 h	0.16	1.25
<b>WC#5</b>	0.11	0.13 kWh/m <sup>2</sup>	0.45	0.07	+2.65 h	0.06	0.08	+0 h	0.30	-0.94
<b>WC#6</b>	0.10	0.19 kWh/m <sup>2</sup>	0.42	-0.04	+3.37 h	-0.06	-0.04	+0 h	0.18	1.18
<b>WC#7</b>	0.08	0.13 kWh/m <sup>2</sup>	0.56	-0.04	+3.04 h	-0.05	-0.04	+0 h	0.21	1.18
<b>WC#8</b>	0.10	0.23 kWh/m <sup>2</sup>	0.35	-0.04	+3.48 h	-0.06	-0.04	+0 h	0.16	1.25
<b>WC#9</b>	0.11	0.35 kWh/m <sup>2</sup>	0.45	0.07	+2.65 h	0.06	0.08	+0 h	0.30	-0.94
<b>WC#10</b>	0.10	0.40 kWh/m <sup>2</sup>	0.41	-0.04	+3.43 h	-0.06	-0.04	+0 h	0.18	1.18
<b>WC#11</b>	0.11	0.32 kWh/m <sup>2</sup>	0.62	-0.04	+3.02 h	-0.05	-0.04	+0 h	0.21	1.18
<b>WC#12</b>	0.08	0.39 kWh/m <sup>2</sup>	0.35	-0.04	+3.4 h	-0.06	-0.04	+0 h	0.16	1.25
<b>TB</b>	0.10	+0 kWh/m <sup>2</sup>	0.44	-0.01	+0 h	-0.01	0.01	+0 h	0.30	-0.94

Table 35: Effectiveness of the different control combinations (Winter) in function of the variation respect to SSF

## **5. Findings and conclusions**

In this section, the optimal control for both, summer and winter conditions, is selected, focusing on the results of the analysis performed in the previous chapter. This is the last step of the research method already illustrated in 3. For each season, the two aspects of the performance, energy consumption and indoor comfort for the occupants, in comparison with the two reference systems, are considered for the definition of the optimal control for the *DSF*.

### **5.1. Definition of the optimal control for the summer season**

In this section the evaluation of the results for the selection of the optimal control strategy for the summer season, considering the different domains of the performance, is reported.

#### **5.1.1. Energy Efficiency**

##### Energy need for heating

For the summer season, from the point of view of the energy need, the focus is of course the minimization of the energy need for cooling (both space and ventilation). Anyway, as mentioned in the part related to the results analysis, it is important to also consider the impact of the implemented control on the possible increasing of the energy consumption for space heating. Among the 20 proposed control strategies, the ones that have the worst impact on the space heating demand of the room are the ones which adopt the *SAC#5* control of the air flows. Indeed, *SC#17* is the worst under this point of view, with an energy requirement for space heating that is 20 times greater than the *SSF*. The control strategies which adopt the *SAC#3* and *SAC#4* are probably the best ones in terms of energy required for the heating, but there is anyway a worsening of the energy performance compared to the *SSF*.

##### Energy need for cooling

Considering the energy need for cooling, the strategies which implement *SAC#5* are the best solution for the minimization of the cooling energy need compared to the single system (the reduction is around 60% for all the four configurations of control). The best combinations indeed are *SC#19* and *SC#20*, which are on the other hand among the worst in terms of increasing of energy need for heating. This is a critical aspect related to the reduction of the overall energy need of the room during the summer season: the best solution in terms of cooling energy reduction is also the one with the worst performance under the point of view of the heating energy (and vice versa it is possible to say the same thing about the minimization of the increasing of the cooling requirements). For this reason, it is difficult to find a trade-off between the different domains of the energy performance (heating and cooling in particular).

A possible solution can be the one to find a balance between the two extreme situations, that is able to reduce of a certain extent the energy need for cooling, without compromising in a too critical way the energy performance for heating. The combinations which adopt *SAC#3* and *SAC#4* can be in this case a possible solution. Indeed, *SC#11* shows an overall reduction of the energy need for cooling compared to the *SSF* of about 8% and it is also the combination which causes the lowest increasing of heating energy need compared to the *SSF* (only 7.81 times with respect to it) among the proposed ones.

Energy need for artificial lighting

As mentioned in the energy analysis it is anyway necessary to consider also the energy need for artificial lighting, which is mainly influenced by the adoption of a certain control for the shading. The analysis performed during the summer season, shows that the temperature control (from *SSC#2* to *SSC#4*) is not good in summer if the air flow controls from *SAC#1* to *SAC#4* are applied, since the drawn mechanism of the blind is activated with a too high frequency, with a subsequent increasing of the related energy demand for artificial lighting. The adoption of a radiation (*SSC#1*) control is consequently preferred to reduce this energy need.

Keeping the *SAC#3* control for the air flow (the one implemented inside *SC#11*), it could be therefore possible to select *SC#9* as optimal solution of control in summer under the point of view of the energy performance. It incorporates the control *SSC#1* for the shading (with subsequent reduction of the energy requirements for artificial lighting), it is the second-best solution after *SC#11* in terms of energy for heating (with an increasing of only 7.93 times respect to the *SSF*) and the overall energy need for cooling is almost the same of the *SSF* (with an increasing of about 0.86% or 0.01 times). A schematic summary on the selection of *SC#9* as optimal control for the overall energy efficiency considering the different domains of the energy performance is reported in *Table 36*.

<b>Optimal control for the energy performance</b>	<b>Heating energy need</b>	<b>Cooling energy need</b>	<b>Artificial lighting energy need</b>
<b>SC#9</b>	Increase of only 7.93 times respect to <i>SSF</i> (2 <sup>nd</sup> best solution among the 20 possible control configurations)	Increase of just 0.86% respect to <i>SSF</i>	Adoption of <i>SSC#1</i> , more effective than the temperature control during the summer

*Table 36: Selection of the optimal control for the summer season in terms of energy efficiency*

**5.1.2. Indoor Environmental Quality**

Focusing on the indoor environmental quality evaluation, the selection of an optimal control is much more complex, since a greater number of domains and parameters should be considered (Fanger’s comfort indices, *CO<sub>2</sub>* concentrations, daylight levels, indoor operative temperatures).



### Indoor operative temperatures

Looking at the overheating prevention ability, based on the number of hours in which the limit of  $26^{\circ}\text{C}$  is reached, the best solutions are the ones which adopt *SAC#5* for the air flows control. Indeed, *SAC#5* coupled with the radiation control of the blind is the best solution under this point of view: *SC#17* is consequently the best control combination for overheating risk reduction compared to the *SSF* (with a lowering of about 45%).

### Indoor Air Quality

From the point of view of the indoor air quality, as mentioned before, all the implemented control strategies are not good and effective compared to a traditional *SSF* with openable window. It is therefore impossible to select in this case an optimal control under the point of view of the indoor air quality inside the room.

### Fanger's comfort indices

From the point of view of the Fanger's comfort indices in the indoor environment, as seen for the indoor operative temperature trends, the best solutions are the ones which implement the control *SAC#5* (but in any case, the traditional *SSF* shows a better performance compared to a ventilated cavity), especially in terms of number of occupied hours in which the *PMV* index is below  $-0.5$ .

### Indoor daylight

Considering finally the daylight in the room, in similar way to the energy need for artificial lighting, the best solutions are the ones which adopt the radiation control of the blind (*SSC#1*): the possible optimal solutions under this point of view are consequently *SC#1*, *SC#5*, *SC#9*, *SC#13* and *SC#17*. *SC#9* as said before is the possible optimal control strategy defined from the point of view of the energy consumption but is less effective in the prevention of the overheating risk (looking at the indoor operative temperature trends) than *SC#1*, *SC#5* and *SC#17*. This last one indeed can be assumed as possible optimal solution for the control of the *DSF* during the summer season considering the indoor environmental quality (thanks to the implementation of the *SAC#5* air flow control). A review on the selection of *SC#17* as optimal control for the indoor environmental quality considering the different domains of the indoor comfort is reported in *Table 37*, next page.

<i>Optimal control for IEQ</i>	<i>Overheating risk prevention</i>	<i>Fanger's comfort indices</i>	<i>Daylight</i>
<b>SC#17</b>	Reduction of 45% of the number of hours above 26°C compared to the <i>SSF</i>	Adoption of the <i>SAC#5</i> air flow control, that is the most effective under the point of view of the Fanger's comfort indices compared to <i>SAC#1</i> , #2, #3 and #4	Adoption of the <i>SSC#1</i> shading control, that is the most effective in summer conditions under the point of view of the daylight

Table 37: Selection of the optimal control for the summer season in terms of indoor environmental quality

The positive features and the negative aspects of the selected controls (from the point of view of the energy efficiency and the indoor environmental quality) are illustrated in Table 38: in the table the impact of the optimal control from the point of view of the energy efficiency on the indoor environmental quality is assessed and, in the same way, the impact of the optimal control from the point of view of the indoor environmental quality on the overall energy efficiency is evaluated. As it is possible to see, the optimal control selected from the point of view of the energy efficiency (in this case *SC#9*), has some positive features under the point of view of the indoor environmental quality, but also some consistent limitations in other domains of the *IEQ* performance. In similar way, the optimal control selected for the indoor environmental quality (in this case *SC#17*) shows positive features and negative aspects regarding the energy performance of the whole system. Therefore, it is impossible to fit inside the same control combination only optimal features for both the two domains (energy efficiency and indoor comfort) without any negative attribute.

<i>Optimal control</i>	<i>Positive features</i>	<i>Negative aspects</i>
<b>SC#9</b> (for the energy efficiency)	<ul style="list-style-type: none"> <li>• Effective for the prevention of the overheating risk in summer (-39% of occupied hours above 26°C compared to <i>SSF</i>).</li> <li>• Effective for the daylight in the indoor environment (smaller increase of the number of occupied hours below 500 lux with the adoption of the radiation control).</li> </ul>	<ul style="list-style-type: none"> <li>• High number of hours for PPD &gt; 10% (over 4 times the <i>SSF</i>)</li> </ul>
<b>SC#17</b> (for the indoor environmental quality)	<ul style="list-style-type: none"> <li>• Reduction of the energy need for cooling compared to the single skin system (about 60%)</li> <li>• Better solution for the artificial lighting energy need compared to the other forms of air flow and shading control.</li> </ul>	<ul style="list-style-type: none"> <li>• High increase of the energy need for heating (over 20 times the <i>SSF</i>)</li> </ul>

Table 38: Comparison between the optimal controls (for energy efficiency and *IEQ*) selected for the summer season

It is consequently necessary to understand which performance domain (indoor environmental quality or energy efficiency) should be preferred and optimized for the selection of a particular control: the designer must in this case set the priority need to follow in the control implementation (in this case making a preference between *SC#9* and *SC#17*).

## **5.2. Definition of the optimal control for the winter season**

In this section the evaluation of the results for the selection of the optimal control strategy for the winter season, considering the different domains of the performance, is reported, following the same path already defined for the summer season.

### **5.2.1. Energy Efficiency**

#### Energy need for heating

As mentioned before, during the winter season the focus for the control implementation, under the point of view of the energy need, is the reduction of the energy need for heating compared to the one in the *SSF*. In this case, the selection of an optimal combination for the reduction of the energy need for heating in winter is much more critical compared to the selection of the optimal control for the reduction of the cooling requirements in summer. This is because all the 12 implemented controls cause an increase of the energy need for heating. The *less bad* combination that produces the lowest increase (about 7.62% or 0.08 times) is in this case *WC#12*.

#### Energy need for cooling

The most critical aspect is anyway the fact that in all the combinations of control, there is a consistent increasing of the energy need for cooling (which is null in the single skin reference system). In this case, *WC#12* is the one that produces the highest increase of this energy demand. On the contrary, *WC#1* is the combination with the lowest increase of cooling demand, but also the worst under the point of view of the energy performance for heating (about 12%).

This is the same situation already observed in the summer season: the best combination in terms of energy need for heating is also the worst under the point of view of the energy need for cooling. The possible solution, as in the summer season, is consequently to find an intermediate alternative: indeed, *WC#7* is the 3<sup>rd</sup> best solution in the limitation of the increasing of the energy need for cooling (after *WC#1* and *WC#5*, about 0.13 kWh/m<sup>2</sup>) and it generates an increase of the heating demand of only 8.18% (2<sup>nd</sup> best solution under this point of view after *WC#12*), compared to the *SSF*.

Energy need for artificial lighting

Considering the energy requirements for artificial lighting, all the implemented controls are quite similar in their effectiveness (and in any case it is present a worsening compared to the *SSF*, as observed during the summer season). *WSC#4* shows the best results among the defined control logics for the shading system while *WSC#3* on the contrary is the one that causes the highest increase if coupled with all the different air flow control logics. Anyway, being the order of magnitude of the energy requirements for artificial lighting almost the same in all the combinations of control (between and 25 and 29 kWh for all the configurations), *WC#7* can be kept as optimal control from the point of view of the energy performance during the winter season, despite the use of *WSC#3* as control for the shading system.

A schematic summary on the selection of *WC#7* as optimal control for the energy overall energy efficiency considering the different domains of the energy performance is reported in *Table 39*.

<i>Optimal control for the energy performance</i>	<i>Heating energy need</i>	<i>Cooling energy need</i>	<i>Artificial lighting energy need</i>
<b>WC#7</b>	Increasing of the heating demand of 8.18% (2 <sup>nd</sup> best solution under this point of view after <i>WC#12</i> ), compared to <i>SSF</i>	3 <sup>rd</sup> best solution in the limitation of the increasing of the energy need for cooling (after <i>WC#1</i> and <i>WC#5</i> )	The increase in the energy need for artificial lighting is comparable to the other combinations with different forms of shading control ( <i>WSC#1</i> , <i>WSC#2</i> and <i>WSC#4</i> )

*Table 39: Selection of the optimal control for the winter season in terms of energy efficiency*

**5.2.2. Indoor Environmental Quality**

Considering the indoor environmental quality, the same parameters analyzed for the summer season should be of course considered.

Indoor operative temperatures and Fanger's comfort indices

Evaluating the operative temperatures, the radiation control is the worst to be applied in winter since it can significantly reduce the solar gains entering inside the indoor environment (with a subsequent worse performance compared to the *SSF*). The temperature control on the other hand allows a better indoor condition under the point of view of the operative temperatures. The same can be also assumed for the comfort indices (*PPD* and *PMV*): the temperature control reduces of about the 3.7% the number of hours above the limit of 10%, while in the for the radiation control the increase is around 7.5%. Consequently, the application of *WC#7* can be assumed good enough also under these points of view, since it adopts the temperature activation of the blind with regulation of the slat angle in function of the *cut-off* position (*WSC#3*).

### Indoor Air Quality

As seen for the summer season, the IAQ in the zone is not good for all the combinations of control implemented inside the room (in a more evident way compared to the summer). Anyway, for the winter season the comparison performance with the *SSF* is less critical, since also the room with the traditional single skin façade shows the same number of hours above the limit of  $CO_2$  concentrations.

### Indoor daylight and glare discomfort

For the evaluation of the daylight levels inside the zone, in the case of the winter season it is necessary to also consider the possibility to have glare discomfort for the occupants. In this case, *WSC#1* is the worst for the minimum illuminance levels to keep inside the zone (about 30% lower compared to the *SSF*), compared to the other forms of control for the shading. At the same time, anyway, it is also the best one to limit the glare discomfort risk during the occupied hours (with a reduction of about 94% of glare risk compared to the *SSF*). In the same way, *WSC#4* is the best one for the indoor illuminance levels (only 16% of reduction compared to the *SSF*) but also the worst solution for the glare prevention in the thermal zone (the number of hours above 3000 lux of horizontal illuminance levels is 1.25 greater than the reference *SSF*).

*WSC#3* is in this case an intermediate case in terms of indoor daylight levels (only 21% reduction compared to the single skin), but from the point of view of the glare discomfort prevention it is not so effective (it is anyway slightly better compared to *WSC#4*).

Consequently, giving the priority to the daylight levels in the zone (and not the glare risk prevention), *WC#7* (which adopts *WSC#3* for the shading control) can be assumed as optimal control strategy for the winter season also from the point of view of the indoor environmental quality. A review on the selection of *WC#7* as optimal control also for the indoor environmental quality considering the different domains of the indoor comfort is reported in *Table 40*.

<b><i>Optimal control for IEQ</i></b>	<b><i>Indoor operative temperatures</i></b>	<b><i>Fanger's comfort indices</i></b>	<b><i>Daylight and glare</i></b>
<b>WC#7</b>	Reduction of the number of hours below 20°C (-4%) compared to <i>SSF</i>	It adopts the temperature activation of the blind ( <i>WSC#3</i> ), reducing of about the 3.7% the number of hours above the maximum limit of <i>PPD</i>	Intermediate solution between the improvement of the indoor daylight levels and the glare risk limitation (with the adoption of <i>WSC#3</i> )

*Table 40: Selection of the optimal control for the winter season in terms of indoor environmental quality*

In *Table 41*, the same comparison performed for the summer season in *Table 38* is applied to *WC#7* (that is in this case the selected optimal control for both, energy and indoor comfort domains, differently from the summer season in which the selection underlined two different combinations of control).

In this case is consequently possible to select just one combination for the winter season considering both aspects of the performance (energy and indoor environmental quality): this is a better result compared to the summer season, in which basically it was not possible to select an optimal control for the both the 2 aspects of the *DSF* performance.

Anyway, as it is possible to see in the table, there are consistent limitations in both the domains of the performance, by selecting just this combination of control.

<i>Optimal control</i>	<i>Positive features</i>	<i>Negative aspects</i>
<b>WC#7</b> (for the energy efficiency and the indoor environmental quality)	Effective for the indoor operative temperatures trend (-4% of number of occupied hours below 20°C compared to single skin system) and for the daylight availability in the room (increase of 21% of the number of hours below 500 lux compared to SSF, but better than a radiation control of the blind)	Not so effective for the overall energy need of the room compared to SSF

*Table 41: Positive features and negative aspects of the selected optimal control logic for energy efficiency and indoor environmental quality in the winter season*

### **5.3. Critical points of the rule-based control effectiveness**

It is now possible to underline some conclusions regarding the application of the rule-based control for the *DSF* and its effectiveness in the optimization of the overall system performance, starting from the quantitative comparisons performed in 5.1 and 5.2.

#### *Energy performance optimization*

For what concerns the optimization of the performance of the *DSF* under the energy need point of view, the following conclusions and critical points in the application of the rule-based control can be underlined:

- 1) It is difficult to find an optimal control combination that can reduce at the same time the energy need for cooling and the energy need for heating: both in summer and in winter, the best performance in terms of heating energy need is associated to the worst one in terms of cooling energy need (and vice versa). It is consequently necessary to find a trade-off between these two aspects of the energy performance (as seen for the summer season).
- 2) In winter, with the adoption of the *DSF*, there is a worsening of both the performances (heating and cooling requirements), due to increased heat losses

and higher overheating risk. It is consequently more difficult to define which kind of control can be assumed as the best one. In addition, compared to the summer, in which the results produced by the different control logics are more variable, in winter the variations with respect the *SSF* in terms of energy need (especially for the heating) are of the same order of magnitude.

- 3) Considering the energy for artificial lighting, both in summer and winter conditions, the adoption of all the different control logics for the shading system in the *DSF* produces an increasing of this energy requirement. During the summer, indeed, the temperature control of the shading produces too high energy requirements for the artificial lighting in the room, due to a too frequent activation of the drawn mechanism. In addition, it is not visible a significant variation of the energy need for artificial lighting in function of the different controls of the blind slat angle (*fixed*, *cut-off* and *scheduled*) in case of temperature activation of the blind.

#### Indoor environmental quality improvement

On the other hand, considering the indoor environmental quality requirements in the room, the following conclusions can be observed:

- 1) The worst aspect of the performance is related to the indoor air quality in the zone. The adoption of the ventilated cavity in the free run configuration of the room is not good enough in the removal of the excess of  $CO_2$  concentrations. This situation is more evident in summer with the comparison with a traditional openable window in a *SSF*.
- 2) For the summer season, the implemented combinations of control are effective in the reduction of the overheating risk (looking at the trend of the indoor operative temperatures) compared to the *SSF*, but in the complex the values of *PPD* and *PMV* indices are largely better in the *SSF* system. Indeed, the number of hours below the limit of  $PMV = -0.5$  are significantly higher in the case of the adoption of the flexible *DSF*.
- 3) In the winter period, there is not a significant variation in the thermal comfort for the occupants (compared to the reference *SSF*), with all the different implemented controls for the air flows. The control combinations are not consequently so effective in the improvement of the indoor comfort during the heating season.
- 4) The daylight availability is compromised with all the different forms of shading control, both in summer and in winter, with an increasing of the number of occupied hours below the limit of  $500 \text{ lux}$  compared to the *SSF*. During the winter, in addition, the possibility to have a glare discomfort risk is higher, compared to the *SSF* with simple radiation control of the blind, if

the temperature control of the blind is activated (both in the case of fixed or variable slat angle). To this it is necessary to add the fact that the best shading control in terms of indoor daylight availability is also the worst in terms of glare discomfort risk prevention.

- 5) The optimal solution of control for the summer season under the point of view of the indoor environmental quality is at the same time the one which produces the highest increase of the energy requirements for heating. In similar way, during the winter season, the optimal control for the indoor climate is not so effective in terms of the overall energy need reduction in comparison with the *SSF*: consequently, it is difficult to find a control combination which is good for both the two aspects of the performance domain (energy need and comfort for the occupants).

From these final considerations, it is possible to introduce some important aspects related to possible further developments of the Thesis goals already defined in *1.5*.

Indeed, the crucial points to consider are in this case:

- The possibility to evaluate the control effectiveness in the optimization of the *DSF* performance in different boundary conditions: in this way, it could be possible to understand if the critical aspects emerged with the rule-based approach for a certain boundary condition are present also in other contexts (for example climate and façade orientations). This aspect can be linked with the goal illustrated in *1.5.1* about the simulation workflow development for *RBEs*, since different boundary conditions for the façade performance evaluation can be defined and analyzed.
- The necessity to apply more advanced forms of control for the *DSF* compared to the simpler rule-based approach: as illustrated in *1.4*, the rule-based approach has some intrinsic limitations and disadvantages, compared to other forms of control (as the model-based). To fully exploit the potentials offered by the flexibility of the *DSF* and its configurations, it could be therefore necessary to develop more complex control approaches for it. This aspect on the other hand is more linked with the goal illustrated in *1.5.2*, regarding the performance optimization of the *DSF* using more sophisticated forms of control.

The two final observations will be discussed more in detail in *6*.



## 6. Further developments of the Thesis work

Starting from the findings illustrated in 5.3 about the effectiveness of the rule-based control applied to a double skin façade system, some new concepts focused on the possible further developments of the Thesis methodology can be illustrated.

### 6.1. Analysis of different climates and different façade orientations

The analysis performed in 5 of the report have underlined the fact that some combinations of control produce very similar effects on the overall performance of the system, both in terms of energy efficiency and indoor comfort. It could be therefore interesting to see in which extent the proposed control logics are influenced by different boundary conditions (in particular, climate context and façade orientation): only in this way it could be possible to test the control efficacy under different boundary and operating conditions.



Figure 61: Location of the different climate conditions that can be analysed for the double skin performance evaluation (Frankfurt, Oslo and Madrid)

Different climates and locations (according to the *Kopper-Geiger* classification) for the evaluation of the *DSF* performance can be used for this performance evaluation. Possible examples of new climates to consider in the control implementation can be for example (Figure 61):

- Madrid, Spain (*Hot-summer Mediterranean Climate, Csa*)
- Oslo, Norway (*Humid-continental Climate, Dfb*)

These two are example of climates that are more similar and closer to the *Artic* (Oslo) and the *Saharan* ones (Madrid), therefore they can be considered as more “extreme” cases in which it could be possible to evaluate the double skin façade performance. Frankfurt, is exactly in the middle between the two other selected locations. For Madrid more extreme and critical summer conditions can be expected while for Oslo the worst season is of course the winter one, because of the higher latitude of the location ( $60.2^{\circ}N$ ). Anyway, in the case of Madrid, also possible problems with high incident solar radiation values on the façade can be present during the winter season, due to the lower latitude ( $40.45^{\circ}N$ ).

In the same way, different locations for the façade can be considered. Additional orientations of the façade can be the East and the West, characterized by higher values of incident solar radiation during the summer season, compared to the South one. In this way it will be possible to understand the influence of different orientations (and therefore different effects of the incident solar radiation) on the façade performance. In this way, considering two different seasons (winter and summer), three different locations (Oslo, Frankfurt, and Madrid) and three different façade orientations (South, East and West), the total number of boundary conditions for which evaluate the optimal control effectiveness is 18 (9 for the summer season and 9 for the winter season respectively). For each one of these control strategies, an optimal control combination should be selected and compared with the other ones (as done during this Thesis work for Frankfurt). In *Table 42* it is reported the total number of boundary conditions that can be evaluated: as it is possible to see, the performance evaluation made for Frankfurt, in summer and winter conditions, for a South orientation of the façade should be replicated for all the other 16 cases.

<i>Location</i>	<i>Season</i>	<i>Façade orientation</i>
<b>Frankfurt</b>	<b>Summer</b>	<b>South</b>
		East
		West
	<b>Winter</b>	<b>South</b>
		East
		West
Oslo	Summer	South
		East
		West
	Winter	South
		East
		West
Madrid	Summer	South
		East
		West
	Winter	South
		East
		West

*Table 42: Overall number of boundary conditions that can be considered for the performance evaluation of the double skin façade control (climate context, façade orientation and season).*

Using this approach, it is possible to define if the effect of a certain implemented control logic are the same in different boundary conditions, understanding if the same critical aspects of the rule-based control observed in Frankfurt for a South exposed façade are visible also in other climate contexts (Oslo and Madrid) and façade orientations (East and West).

## **6.2. Application of the model-based control**

As mentioned in 2.2.5, the innovative concept of the selected *DSF* model used in the Thesis work is the ability to change their configuration to ensure the best fit to a certain boundary condition. Anyway, traditional concepts of control as the rule-based have showed substantial limitations and criticalities in the fully exploitation of the façade flexibility. Consequently, more innovative forms of control are required for such a kind of envelope solutions.

Regarding the model-based approach for the control implementation of adaptive envelope systems, as mentioned before in 1.4, it is a more sophisticated form of control for the double skin façade since the optimal asset of the system is defined by means of the simulations carried out on the virtual model for different boundary conditions and time steps.

For the actuation of this control strategy, it is necessary to define a priori some criteria that will be used by the simulation environment to address the control of the façade and the definition of its optimal asset. These criteria correspond to the priority performance targets that the double skin façade must guarantee (already defined in the first step of the control implementation process in 2.2.1):

- *Guarantee thermal comfort for the occupants during the whole year*: this is equal to minimize as much as possible the number of occupied hours in which the Fanger's comfort indices are outside the optimal range (10% and  $\pm 0.5$ ).
- *Guarantee visual comfort for the occupants*: this corresponds to minimize the number of occupied hours in which the illuminance levels on the working plane are outside the range 500 lux – 3000 lux.
- *Guarantee good indoor air quality conditions*: this corresponds to minimize the number of occupied hours in which the  $CO_2$  concentrations are above the limit of 1000 ppm.
- *Guarantee energy savings for cooling, heating and artificial lighting*: this is equal to minimize the energy need for heating, cooling and artificial lighting in winter and summer conditions with respect to the *SSF* reference system.

For the application of the model-based approach, more complex forms of control than the Control Macros are required. Indeed, it is necessary to control the IDA ICE simulation environment externally, by means of an *API (Application Programming Interface)* written in the programming language Python and developed by EQUA. The API indeed enables the communication between the IDA ICE simulation environment and the user by means of an external interface (in this case *Virtual Studio Code*, a source-code editor that can be used with several programming languages, as, for example Python) [34]. A picture of the interface inside *VS Code* is showed in *Figure 62*.

```

util.py > ...
1  #function definition for the IDA API
2
3  import ctypes
4  import json
5  import time
6  from win32 import win32process
7  import sys
8  import os
9
10 # Define your path to the IDA ICE bin folder here
11 path_to_ice = "C:\\Program Files (x86)\\IDA50\\bin\\" #location of the IDA ICE application
12
13 #Start ida minimized to avoid user confusion when executing the script :D (The command open IDA ICE 4.9.9.)
14 command = path_to_ice + "ida-ice.exe \"" + path_to_ice + "ida.img" -G 1 -W icon"
15 startObj = win32process.STARTUPINFO()
16 #startObj.dwFlags=1
17 #startObj.wShowWindow=7
18 ret = win32process.CreateProcess(None,command,None,None,0,0,None,None,startObj)
19 pid = str(ret[2])
20 #print(pid)
21 time.sleep(5)
22 #Add path_to_ice to PATH variable, is removed when program finishes
23 os.environ['PATH'] = path_to_ice + os.pathsep + os.environ['PATH']
24
25 ida_lib = ctypes.CDLL( path_to_ice + "x64\\" + 'idaapi2.dll') #open the library file
26
27 ida_lib.connect_to_ida.restype = ctypes.c_bool
28 ida_lib.connect_to_ida.argtypes = [ctypes.c_char_p, ctypes.c_char_p]
29 ida_lib.switch_remote_connection.restype = ctypes.c_bool
30 ida_lib.switch_remote_connection.argtypes = [ctypes.c_char_p]
31 ida_lib.switch_api_version.restype = ctypes.c_bool
32 ida_lib.switch_api_version.argtypes = [ctypes.c_long]
33 ida_lib.call_ida_function.restype = ctypes.c_long
34 ida_lib.call_ida_function.argtypes = [ctypes.c_char_p, ctypes.c_char_p, ctypes.c_char_p, ctypes.c_int]
35 ida_lib.ida_disconnect.restype = ctypes.c_bool

```

Figure 62: IDA API script inside VS Code

Using the IDA API, it is possible to connect the source-code editor with the IDA simulation environment (corresponding to the *idm* file). In particular, by means of the script implemented inside the source-code editor, the user can launch the simulation inside the simulation environment, defining the main features and characteristics of this simulation.

After the launch of the simulation, the user can have access to the different outputs of the simulation using a specific tree structure, which starts from an *ancestor* node (in general the *idm* file in which the simulation is performed) that is then divided into

different *children's* nodes (all the elements that are defined inside the simulation IDA ICE environment).

With the same approach, it is possible to access to all the different parameters and variables of the objects inside the *idm* file (like for example a *DSF* object) using the hierarchical tree structure of the *children's* nodes, modifying them according to a specific control strategy.

The use of the model-based control for the definition of the optimal asset for the *DSF* can be applied using the IDA API, comparing in this way the results (in terms of overall performance of the system) with the ones given using the less-sophisticated rule-based approach, for the different boundary conditions already defined (climate contexts and façade orientations).



## **Appendix A: The use of BPS tools for the modelling of RBEs and IDA ICE features**

In this Appendix, the features related to the *BPS* tools and their use for the modelling of *RBEs* is illustrated to the reader.

The dynamic behavior of *RBEs* is the main reason of the intrinsic complexity which designers must deal with working on such kind of systems. If for conventional and static envelope systems it is always possible to use widespread simulation tools or standard key performance indicators, in the case of responsive building elements and adaptive façade systems, the evaluation of the performance is much more complex and difficult and consequently a successful design of proper control strategies is a challenging task [9].

Despite these initial obstacles, the performance evaluation of adaptive envelope systems is anyway a key element of their design process (if there is for example the need to understand the impact of these technologies on the overall building energy performance). Regarding this, the use of simulations carried on virtual models of the adaptive systems can be useful for the designers in this crucial phase.

Two are the main reasons for which a performance prediction by means of simulation tools of adaptive façades is crucial during the design phase:

- Simulation tools can be used for an investigation of the impact of the use of adaptive technologies on the whole building energy performance, understating the magnitude of the benefits generated using these solutions.
- Simulation tools can be also used for a further optimization of possible control strategies for such kind of elements, evaluating the effects of different control logics on the whole system efficiency.

Consequently, the prediction of the dynamic behavior of adaptive systems by means of computer models can be useful for the entire design and optimization process. It is anyway necessary to define which specific typology of simulation tools can be used to perform the previously listed tasks. In this field, the *Building Performance Simulation (BPS)* is defined as a computer based, multi-disciplinary and problem oriented mathematical model of given aspects of building performance based on fundamental physical principles and engineering models. BPS is nowadays a useful and well-established tool for the multi-domain performance assessments of buildings [35].

It is anyway necessary to say that *BPS* tools have been firstly developed without considering the adaptability capacity of building components [9]: indeed, these tools are used mainly to replicate convectional building envelope systems and it is difficult to predict how much they can be accurate in the description of transient heat and mass transfers that can occur through a *RBE* due to their responsivity and adaptability [36].

In addition, *BPS* tools in general do not focus on the description of the physical behavior behind each building component but on the evaluation of the energy loads of the entire building and on the interaction between its various parts [37].

Consequently, the performance prediction of adaptive façades in some cases can be a complex and difficult task, leading to possible errors and uncertainty. The main disadvantage linked to the use of *BPS* in the performance prediction of adaptive envelope systems is that modeling and replicating the behavior of adaptive systems is not a so common and diffused task, therefore scarce and fragmented information on this topic is present. *BPS* tools can be anyway a solution that can be adopted, on one side, to investigate the behavior of adaptive and dynamic envelope systems in the framework of the overall building energy concept and, on the other side, to test in a quick and efficient way different configurations and control possibilities for these kinds of elements [38].

Some advantages [9] offered by the adoption of *BPS* tools for the performance prediction are consequently:

- The capability to develop different control strategies for the façade performance optimization.
- The ability to simulate the dynamic interaction of the *RBEs* with the other building services (for example the *HVAC* system).
- The possibility to virtually test the robustness of the adaptive system with respect to occupant behavior and variable weather conditions.

To sum up, *BPS* tools, despite some limitations and difficulties in their use for advanced envelope solutions, are anyway the right solutions for the multi-domain performance evaluation of these systems, providing wider building performance indicators (such as the energy need of the building or the indoor environmental quality indexes) that can be used for the evaluation of the façade system efficiency instead of standardized façade performance metrics.

The *BPS* tool that has been used for this Thesis work for the control implementation and the performance evaluation, as already written, is *IDA ICE*. *IDA Indoor Climate and Energy* (*IDA ICE*) is a flexible, whole year detailed and dynamic multi-zone performance simulation tool that is mostly used in Nordic and Central European countries [9], such as Sweden, Finland, Germany and Norway.

It has been initially developed in 1998 by the Swedish company *EQUA Simulation AB* and now it reached the 5<sup>th</sup> release (used during this Thesis work as *beta* version). In the following sub-section, the main features and characteristics of the simulation environment will be analyzed.



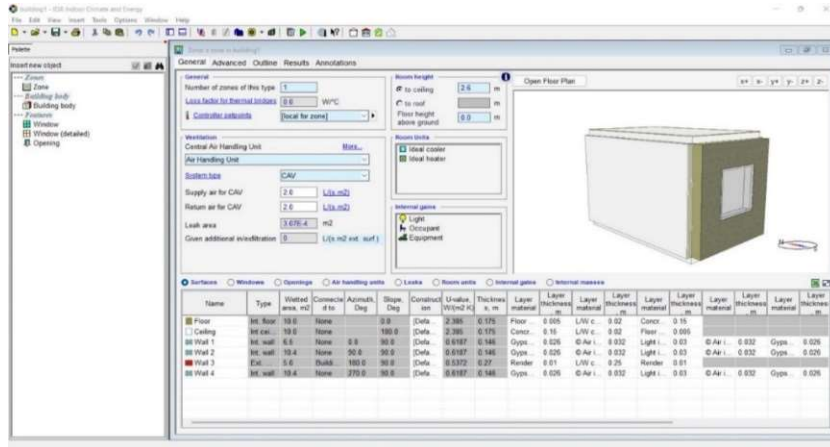


Figure 63: Graphic user interface of IDA ICE

Compared to other BPS tools, the IDA ICE user interface is designed to make it easy to build and simulate both simple and advanced cases, while still offering the advanced user full flexibility [39]. The simulation engine and the user interface are therefore already implemented inside the software, without the need to use external interfaces realized by other developers (as in the case of EnergyPlus and Design Builder, another widely diffused BPS tool). This is a clear advantage in terms of easiness of use for the designer (Figure 63).

IDA ICE is a *general-purpose* simulation environment: it manages the mathematical models of all the building components (envelope and technical building systems) as input data, allowing a user to simulate a wide range of system designs and configurations. Their main advantage is consequently the flexibility: almost anything that can be associated to mathematical modelling can be simulated. One of the most attractive features of the general-purpose simulation tools is that the user can build successively larger component model libraries and independent researchers can develop compatible models [40].

The different building components inside the simulation environment can be described using the so-called *text-based modelling languages* [41]: the *Neutral Model Format (NMF)* indeed is an example of this kind of standardized language. Using the *NMF* the mathematical models of the building components are expressed in separate modules that can be interconnected as desired, to define the customized system model [42]. In particular, the entire model library of IDA ICE is written using the *NMF*.

General	Outline	Code	Annotations	Name	Value	Start	Unit	Connected to	Logged to	Description
[-] Window_1 (DETWINDOW)										
[-] Interfaces				LAMBDA1	(1.0 1.0)		W			Pane thermal conductivity
[-] Variables				DPANE[1,2]	(0.00571...)		m			Pane thickness
[-] Parameters				WAVELENGT...	(9.0E-7)		m			wave lengths of solar radiation
				D[1-1]	(0.012)		m			Cavity thickness
				S[1-1]	(0.012)		m			Thickness of cavity
				H[1-1]	(1.436)		m			Height of cavity
				L[1-1]	(1.132)		m			Width of cavity
				MOLECMASS	(28.97)		di...			Molecular mass of gas fill
				ALAMBDA[1-1]	(0.002873)		di...			Thermal conductivity factor of ...
				BLAMBDA[1-1]	(7.8E-5)		di...			Thermal conductivity factor of ...
				AMYY[1-1]	(3.7E-6)		di...			Viscosity factor of gas see An...
				BMY[1-1]	(4.9E-8)		di...			Viscosity factor of gas see An...
				ACGP[1-1]	(1002.7)		di...			Specific heat capacity factor o...
				BCP[1-1]	(0.01232)		di...			Specific heat capacity factor o...
				TASIDE	20.0		°C	Tqwin_1.TWIN	[off]	Side A temp
				TBSIDE	20.0		°C	NMFZONE.opn.i...	[off]	Side B temp
				QABACKCV	0.0		W		[off]	Side A heat flux
				QBBACKCV	0.0		W	NMFZONE.opn...	[off]	Side B heat flux
				QASIDE	0.0		W	Tqwin_1.QIWIN	[off]	Side A heat flux
				QBSIDE	0.0		W	NMFZONE.opn.i...	[off]	Side B heat flux
				TAIR	20.0		°C	<-- Winshade...	[off]	Side A temp
				TBAIR	20.0		°C	NMFZONE.Ta[1]	[off]	Side B temp
				SCHEDSHADI	0.0	1.0	[0 ...	<-- Start value	[off]	shading control 0=OFF/1=ON
				CTRLHEAT	1.0	1.0	di...	<-- Start value	[off]	pane heating control signal
				AZIMUTSUN	97.0		Deg	<-- BUILDING...	[off]	sun's azimuth

Figure 64: Mathematical model of a window in IDA ICE: list of interfaces, variables and parameter in the Outline tab of the element.

More in detail, the standardized elements of a NMF model are the following ones (Figure 64) [43]:

- **Equations:** they describe the behavior of the physical system. They define in a mathematical way the interconnection between variables and parameters.
- **Links (or interfaces):** they are the interfaces with the other modules contained inside the whole system. They can be used for the information exchange between the different components of the building and the façade system.
- **Variables:** computed by the simulation environment for each defined time-step. They represent therefore the output of the simulation performed by the software.
- **Parameters:** given by the user as simulation input and used for the variable calculations.

In IDA ICE, expert users can implement adaptive features and control strategies directly into the mathematical model using the advanced level interface [9]. In general, there are two different typologies of advanced control that can be implemented inside the *BPS* tool:

- **Time-scheduled:** control actions are in this case pre-determined as a function of time, instead of being based on boundary conditions or simulation state variables. Time schedule control can be used successfully to represent the dynamic operations of building components, but the responsivity of the system to varying boundary conditions cannot be implemented. It is an easier form of control, but it can be efficiently used for example to distinguish between control strategies to be implemented in different periods of the day or week (occupied/unoccupied hours or working day/week-end days).

- Script-based: a script-based control can directly be coded by the user in the simulation tool. Script-based control gives consequently the possibility to test a specific control approach defined by the designer.

This form of advanced control can be applied in IDA ICE by means of user defined *Control Macros* (Figure 65). Using them, the users may implement custom control strategies for different devices and adaptive components in the building (for example the HVAC system) or in the façade element (openings, fans or shading systems).

The main elements of the control-macros are indeed the two interfaces that are used for the information exchange between the different model components:

- 1) Signal Sources: they can be used as input to the control algorithm (for example the outdoor air temperature or the incident solar radiation on the façade).
- 2) Control Targets: the output from control macros should relate to a control target object (for example a particular actuator of the façade).

Signal sources and control targets can be linked and managed in different ways according to the typology of control to be implemented and the actuator to which the control is focused. The IDA ICE *Control Macros* indeed have been used for the control implementation of the façade system in this Master Thesis work.

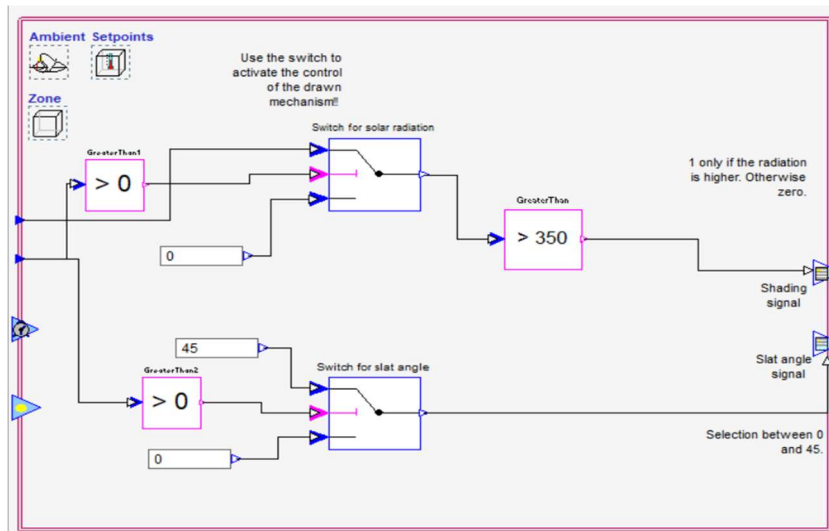


Figure 65: Control macro example from IDA ICE for the control of the shading system

The application of the *Control Macros* for the control implementation of adaptive façade will be discussed later more in detail in *Appendix D: Control implementation in IDA ICE*.

IDA ICE is indeed a simulation environment that can be used for the study of the indoor thermal climate as well as the energy consumption of the whole building [9]. Indeed, it is one of the few *BPS* tools nowadays developed that can cover all the different physical domains that constitute the whole building performance (*Figure 66*):

- Thermal comfort analysis
- Air-flows domain study
- Building services dynamic operations implementation
- Artificial and daylight models

For all these listed features, this *BPS* tools has been selected for the modelling of an adaptive envelope system and its subsequent multi-domain performance evaluation.

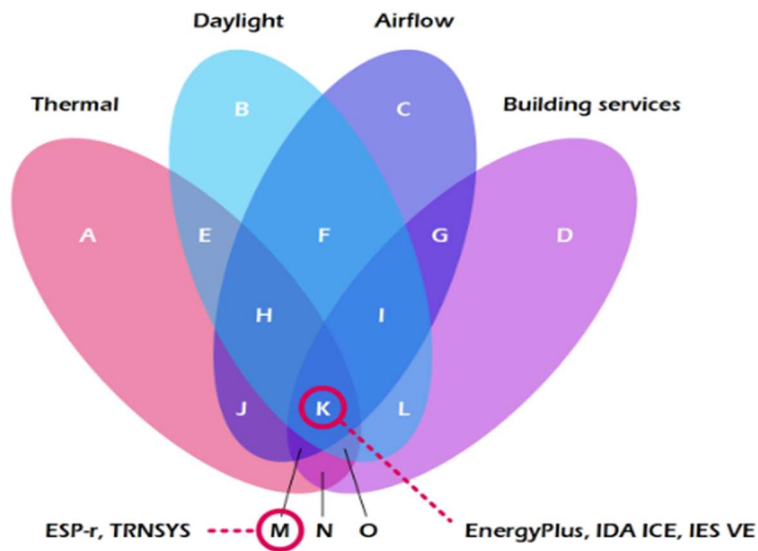


*Figure 66: Intersection of all the different domains for different BPS tools [9].*

## **Appendix B: The DSF system**

In this Appendix, the main features and characteristics of the *DSF* systems and its classification are reported.

Since the year of construction of the first glass architecture, the *Crystal Palace* in 1851, glazed façades in modern architecture have become the norm [44]. From the half of the 20<sup>th</sup> century, with the diffusion of the so-called *International Style* and the improvement of new technologies in the construction sector, the glass became one of the most iconic materials to be used in the new skyscraper façades [45].

Fully transparent building envelopes therefore have become widespread designed and realized since the 50s (especially among office and commercial buildings), with an increasing popularity of the industrialized curtain wall solution [4].

The two main reasons for the increased adoption of the glazed façades were the greater aesthetical appeal offered by this envelope solution compared to a traditional opaque one and the better indoor daylight conditions ensured by the glass transparency [46]. Anyway, some relevant disadvantages are related to the extensive use of glass in the building façade [47] [48]:

- Higher thermal transmittance compared to a traditional opaque partition, that can be cause of higher heat losses during the winter and possible thermal discomfort for the occupants.
- Higher passive solar heat gains, linked to the higher visible transmittance of the glass.
- Higher glare discomfort risk if the incoming solar radiation is not managed in the proper way.

As a result of these disadvantages, buildings with extensive use of glass in the façade usually were characterized by unacceptable indoor comfort conditions (due to the high energy loss in winter, the excessive thermal gain in summer and the visual discomfort caused by the absence of shading devices) complemented by relevant energy consumptions (mainly related to the *HVAC* system, which is necessary to provide suitable indoor conditions) [4].

Indeed, fully glazed façades tend to have higher space conditioning loads from heat transfer through the building envelope because windows have lower resistance to heat transfer than traditional insulated walls [49]. From these considerations, with the increasing need of a better energy performance within the building sector (as mentioned at the beginning of *I.I*), new solutions have been developed with the aim to overcome the gap between traditional opaque façades and fully glazed ones.

In particular, the introduction of the double skin systems in the contemporary architectural language from the 80s is a clear design effort in this direction.

## ***Explanation of the concept of double skin façade***

The *Double Skin Façade (DSF)* is an architectural trend (mainly diffused in European countries but anyway adopted all over the world) driven mostly by four reasons [12]:

- The aesthetic desire of architects and designers for an all-glass façade that leads to increased transparency of the building envelope.
- The practical need for improved indoor environment among buildings with fully glazed façades.
- The need for improving the acoustics and indoor air quality in buildings located in noise polluted areas.
- The reduction of the energy use during the occupation stage of the building.

Hence, the use of the *DSF* is mainly caused by the need to design a fully transparent envelope with a good performance from the point of view of both energy efficiency and comfort for the occupants [23]. Moreover, this improvement of the façade performance is also linked with the concept of dynamicity and responsivity of the building envelope: since outdoor weather and occupancy are dynamic boundary conditions, the façade solution must have the capacity to respond and adapt in a dynamic way to variable exterior conditions and to changing occupant needs [50].

According to this view, the *DSF* is based on the notion of exterior walls that respond dynamically to varying ambient conditions and that can incorporate a range of integrated sun-shading and natural ventilation devices or strategies [51].

Many different definitions of double skin façade systems have been defined in the decades within the scientific literature. One of the most complete is the following one, provided in [12]:

*“The double skin façade is a pair of glass skins separated by an air corridor (also called cavity or intermediate space) ranging in width from 20 cm to several meters. The glass skins may stretch over an entire structure or a portion of it. The main layer of glass, usually insulating, serves as part of a conventional structural wall or a curtain wall, while the additional layer, usually single glazing, is placed either in front of or behind the main glazing. The layers make the air space between them work to the building’s advantage primarily as insulation against temperature extremes and sound.”*

The functioning is therefore based on the doubling of the glass layer of a traditional fully glazed façade, with the purpose of using in an active way the air contained inside the gap between the two façade skins [8]. In addition, the cavity offers the possibility to insert shading devices for the control of the incident solar radiation (*Figure 67*).

To sum up, the main advantages provided by the double skin system are the reduction of the heat losses during the winter (thanks to the thermal buffer created by the still

air inside the cavity) and the reduction of the useless thermal gains in summer (thanks to the air circulating inside the cavity) [4]: this is therefore an example of the dynamicity required by adaptive envelope components, since different performance goals are achieved and optimized through the year.

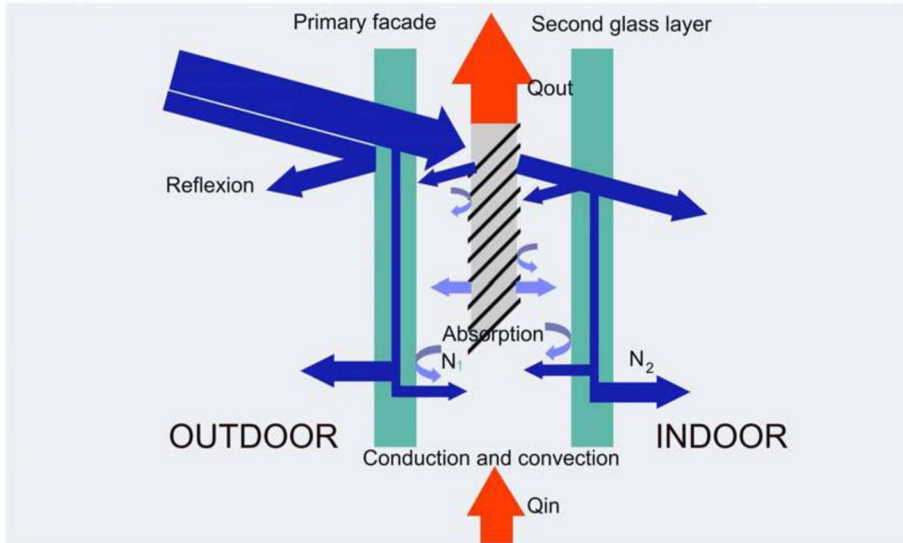


Figure 67: Structure of a double skin façade, with the different components of the system: primary façade (outer skin), second glass layer (inner skin), cavity and integrated solar shading device [52].

Probably, the first concept of double skin façade has been developed in the 1849, when Jean-Baptiste Jobard, at that time director of the *Industrial Museum* in Brussels (Belgium), described an early version of a mechanically ventilated multiple skin façade: in winter hot air should be circulated between two glazing skins to increase the insulation capability of the façade, while in summer it should be cold air for cooling purposes [53].

Anyway, little or no progress was made in *DSF* construction field until the early 80s of the 20th century when this type of façades started to acquire popularity in Western countries: the consciousness of the environmental costs of construction, the evidences of the relationship between inefficient façades and energy consumption and some practical problems determined an increased interest in this typology of advanced envelope. Consequently, it was during the 90s that this architectural system started to become more popular among high-rise commercial buildings in Europe [54].

Relevant examples of buildings with *DSF* system in Europe are:

- *SNAM Headquarters* (Milan, Italy), 1991, *Gabetti & Isola*
- *Helicon Building* (London, UK), 1996, *Sheppard Robson*
- *Citygate* (Dusseldorf, Germany), 1997, *Petzinka, Overdiek and Partners*

- *GSW Headquarter* (Berlin, Germany), 2000, *Matthias Sauerbruch, Lisa Hutton, ARUP*
- *Mercedes Building* (Berlin, Germany), 2000, *Renzo Piano*
- *AGBAR Tower* (Barcelona, Spain), 2004, *Jean Nouvel*
- *Gherkin Tower* (London, UK), 2004, *Norman Foster*
- *Intesa San Paolo Skyscraper* (Turin, Italy), 2015, *Renzo Piano*

Indeed, the use of this typology of façade, if well designed and integrated with the other building systems, can allow to some significant advantages, in particular [12]:

- Efficient use of the solar gains during the winter season.
- Acceptable thermal comfort during the whole year.
- Overall primary energy savings for heating, cooling, ventilation and lighting.
- Solar control and subsequent better visual comfort conditions thanks to the use of the integrated shading devices.

### ***The components of the double skin façade and their influence on the system functioning***

As said in the previous sub-section, double skin façades can allow a better performance than a traditional glazed façade. Anyway, this is possible only if the double skin façade is properly designed and operated by effective control strategies.

Otherwise, the potential benefits of this system can vanish. For this reason, the physical phenomena that can occur inside a double skin façade (and their relationship with the double skin façade components) must be well understood and predicted [20].

Starting from the double skin façade components, the main ones can be listed as:

- Exterior glazing skin, that can be both a single glazing unit and a double-glazing unit. In some case, the outer skin can be composed by movable transparent glass louvers.
- Interior glazing skin, that can be both a single glazing unit and a double-glazing unit.
- Air cavity, with a depth usually comprised between *4 cm* and *2 m*. It can be both, naturally or mechanically ventilated.
- Integrated solar shading devices, usually venetian blinds, or roller blinds. In general, roller blinds are more effective in blocking the light, but the venetian blinds usually are more flexible in the daylight management of the indoor environment, thanks to the variable slat angle.

The physics governing the behavior of a dynamic system as a double skin façade is not particularly easy to understand. Phenomena as transport of mass, momentum and thermal energy are highly dynamic and in constant interaction, influenced by indoor



and outdoor temperature fluctuations, wind speed and directions, solar radiation intensity and pressure difference between the cavity and the surrounding environments [20].

The main phenomena that can influence the performance of the façade system are:

- The heat transfers through the façade, both radiative and convective
- The air flows in the cavity, generated by natural or mechanical ventilation
- The optical properties of the façade

The heat transfers through the façade are the sum of both, convective and longwave radiative heat fluxes, that must be considered in separate way during the behavior analysis of the double skin façade. Indeed, the convective heat transfer coefficients are not easy to define, since a combination of forced and natural convection and laminar and turbulent flow can occur inside the cavity [38].

The presence of integrated shading devices inside the cavity can be an additional element of complexity in the *DSF* behavior prediction: shading systems are indeed able to absorb the direct short-wave solar radiation before it reaches the indoor environment, releasing in a second moment the absorbed heat to the cavity air, influencing in this way its temperature distribution [50]. The shading systems in addition divide the cavity in two separate sub-cavities, for each one it is necessary to define a flow regime and the corresponding convective heat transfer coefficient [12].

Regarding the ventilation, the calculation of the airflows between the two skins in case of naturally ventilated cavities is not an easy task, since it is influenced by the stack effect, pressure difference between the different environments and wind action [12]. In addition, the ventilation inside the cavity has an influence on the cavity heat transfers, since it influences the air velocity [20].

About the optical and solar properties of the façade system, they are highly influenced by the shape and the position of the shading system and by the solar and optical properties of the two glass skins [38]. All these elements influence the transmission and the absorption phenomena inside the *DSF* and consequently the heat transfers and the air flows.

Given these considerations, it is understandable how complex the behavior of this dynamic system is. The intercorrelation between the physical behavior of the *DSF* and the configuration of its components (for example the venetian blinds, the cavity openings or the ventilation fans) must be of course known if the designer has the task to set proper control strategies for the system.

A wrong implementation can indeed generate unwanted physical phenomena inside the façade (for example wrong ventilation paths or too high temperature increasing of the cavity air) leading to a worsening of the overall building performance.

### ***Possible classifications of the double skin façade***

Many different classifications for the *DSF* have been proposed in the last decades. Indeed, a correct understanding of them is crucial for a correct design process and a good control implementation for the façade actuators.

In function of the partitioning of the cavity space, there are four main possible configurations [54] (*Figure 68*):

- *Box window (a)*: in this case the façade is characterized by a simple window doubled inside or outside by a single glazing or by a second window itself.
- *Shaft-Box (b)*: the cavity is in this case closed in the horizontal direction, but not in the vertical one. Therefore, the cavity is designed as a vertical ventilation duct connecting different floors together.
- *Corridor façade (c)*: this is the opposite case of the shaft-box layout because the cavity is divided in the vertical direction only (usually at the level of each storey). Consequently, the cavities for each storey are independent.
- *Multi-storey façade (d)*: this case is characterized by a cavity which is not partitioned either horizontally or vertically. In some cases, the cavity can run all around the building without any interruption.

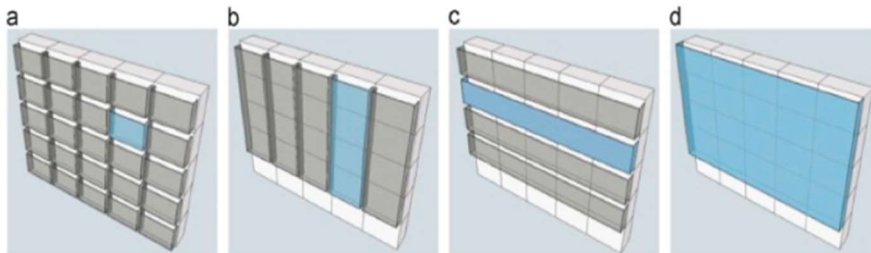


*Figure 68: Pictures of the DSF layouts: a) box window, b) shaft-box, c) corridor façade and d) multi-storey façade [20].*

Another important distinction, as said in the previous sub-section, is the one regarding the air driving force inside the cavity [6]:

- *Natural ventilation*: the driving force is the pressure difference generated by stack effect and wind action inside the cavity. Natural ventilation is preferred when the air temperature inside the cavity is not much high: for this reason, this type of double skin façade is a less recommendable choice for warm climates characterized by high irradiation levels.
- *Mechanical ventilation*: the air is forced into the cavity by means of mechanical devices, for example fans. It should be used when the required air

flow rate is higher due to the presence of high heat gains inside the cavity (typical summer conditions).

Finally, a crucial classification is the one regarding the ventilation mode (*Figure 69*), corresponding to the origin and the destination of the air flowing inside the ventilated cavity. The same ventilation mode can be implemented both in natural and mechanical way. The main ventilation modes for double skin façades are:

- *Outdoor Air Curtain (OAC)*: in this ventilation mode, the air introduced into the cavity comes from the outside and is immediately rejected towards the external environment. The ventilation of the cavity therefore forms an air curtain enveloping the outside façade. Usually, the inlet vent is located at the basis of the cavity, while the outlet one at the top of it: this configuration amplifies the cavity air flows and makes a more uniform rate inside the cavity, making this solution particular feasible for natural ventilation applications [38]. For the summer period it can be used for cooling the cavity air and remove in this way the excess of heat accumulated from the incident solar radiation [12]. To improve the air flow rates inside the cavity could be necessary to use the mechanical ventilation in the cavity, if the generated air flows are not large enough.
- *Indoor Air Curtain (IAC)*: the air comes from the inside of the room and is returned to the indoor environment. The ventilation of the cavity therefore forms an air curtain enveloping the indoor façade. This configuration can be used for the pre-heating of the air that is re-introduced inside the indoor environment. The application of this kind of façade is more cost effective in countries with a colder climate, since in milder conditions it can be cause of a significant increase of the cooling demand [55].
- *Air Supply (AS)*: the air is introduced in the cavity from the bottom opening. This air is then brought to the inside of the room. The ventilation of the façade thus makes it possible to supply the building with fresh air, that can be pre-heated by using the solar gains. This configuration is good for the winter days in which it is present a certain amount of incident solar radiation and the outdoor air temperature is not so low, but it can be applied also in summer if the cavity temperature is not high enough. It is also usually coupled with natural ventilation strategies [6].
- *Air Exhaust (AE)*: the air comes from the inside of the room and is evacuated towards the outside. The ventilation of the façade thus makes it possible to evacuate the air from the building, ensuring a good indoor air quality condition in the indoor environment. At the same time, the air movement can be used for removing the excess of heat inside the room and in the cavity. This feature can be useful especially during the summer season for night cooling purposes. In this case the cavity is used to extract and remove the heat

loads accumulated during the daytime, cooling down the thermal mass of the building [50].

- *Thermal Buffer (TB)*: in this configuration, all the openings of the cavity are closed, with the main aim to make the façade airtight. The cavity in this way forms a buffer zone between the indoor and outdoor environment thanks to the still air inside it. This configuration consequently is optimal for the winter days with very low outdoor temperature and low incident solar radiation on the façade or more in general for the night periods [6].
- *Climate Façade (CF)*: the configuration is similar to the one of the indoor air curtains, but in this case the air is returned to the HVAC system of the building. As seen for the AS configuration, air is preheated in the cavity but used in this case for the HVAC system, for the pre-heating of the ventilation air of the mechanical ventilation plant.

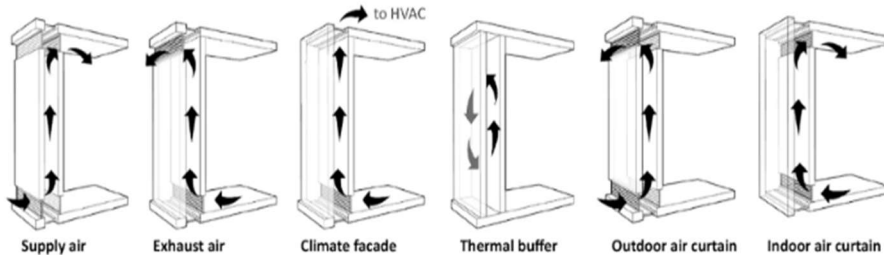


Figure 69: DSF ventilation modes classification [20].

All these ventilation modes can be implemented in the operations of the façade during the different seasons, ensuring dynamicity and flexibility features to the system, that can adapt to different weather and operational conditions.

All these ventilation modes have been implemented inside the flexible *DSF* model adopted during the Thesis work, as illustrated in 2.

## Appendix C: DSF modelling in IDA ICE

In this Appendix, the modelling of the *DSF* systems inside IDA ICE is illustrated.

After a general description of the double skin façade system, it is necessary to deal with the modelling of such kind of systems inside the *BPS* tools and with the IDA ICE simulation environment in detail.

Actually, *BPS* tools are widely used to assess the energy performance of buildings which are characterized by the presence of a double skin façade in their envelope [38] but anyway, there are several doubts about how accurately *BPS* tools can describe or not the transient heat and mass transfer that occur in the complex environment of a *DSF*, since these tools have been developed to replicate conventional building envelope components, not dynamic ones [37].

According to the existing scientific literature about this topic [9], the main issues that are faced by *BPS* tools in the performance evaluation of *DSF* are the following ones:

- Underestimation of the cavity air temperature
- Errors in the prediction of the natural air flows inside the cavity
- Underestimation of the solar radiation entering in the indoor environment

Therefore, all these problematics are mainly connected to the cases of peak solar loads conditions, that can influence in an extensive way the thermal and fluid dynamics domains of the *DSF*. Anyway, since this Thesis does not deal with the comparison of different *BPS* tools in the performance prediction of double skin façades, the focus of this sub-section is the description of the modelling capabilities that are implemented inside IDA ICE.

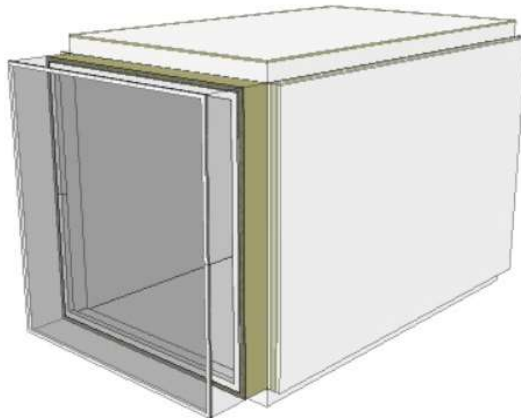
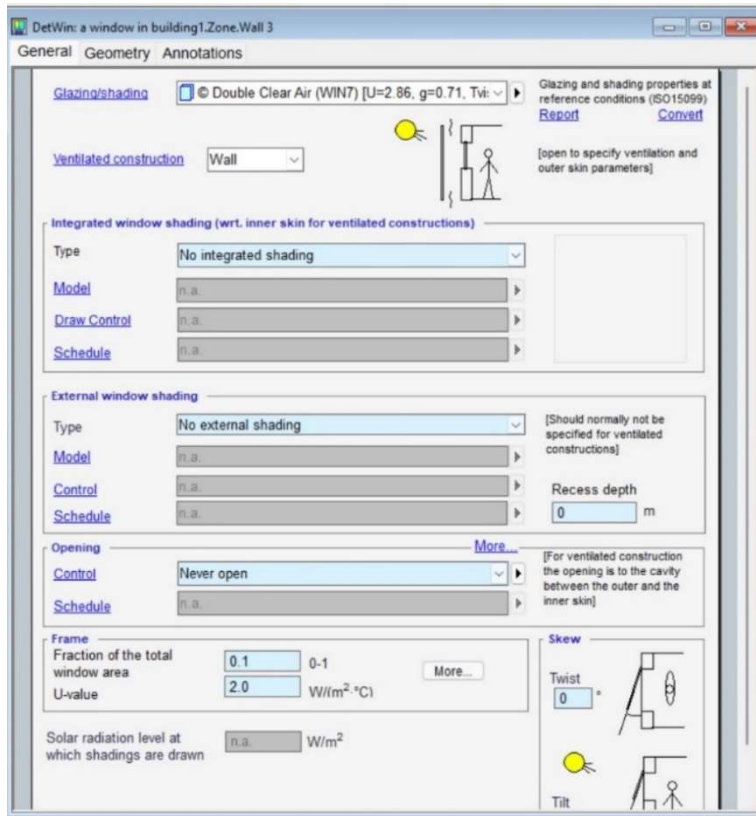


Figure 70: 3D view of the double skin façade in-built model from the IDA ICE graphic interface.

In particular, the *DSF* implemented inside IDA ICE (*Figure 70*) is an *in-built model*: whit this configuration the user can directly enter specific input information by means of the graphic user interface of the simulation environment. No additional modelling effort is therefore required from the user [38]. For this reason, IDA ICE has been selected as simulation environment for the modelling and the testing of the double skin façade system for this Thesis.

In IDA ICE, the double skin façade can be defined using the *Detailed Window* model and a custom additional component called *Double Glass Façade*. The user can define the properties of the inner skin (such as glazing configuration and frame fraction) using the *Detailed Window Form* already implemented inside the graphic user interface of the program (*Figure 71*). Using the *Opening* link in the same form, it is also possible to set the dimensions of the first opening that connects the cavity to the indoor environment, with the related control. The dimensions (length and width), in this case, are set in terms of percentage with respect to the overall dimensions of the inner skin.



*Figure 71: Detailed window form in IDA ICE. The glazing properties are referred to the inner skin of the double skin façade. In the “Ventilated construction” field the selection “Wall” enables the creation of the double skin façade model.*

On the other hand, in the field *Ventilated Construction* it is possible to specify the properties of the external skin and the cavity depth of the double skin façade: clicking on the field it is possible to open the *Double Glass Façade Form* (Figure 72).

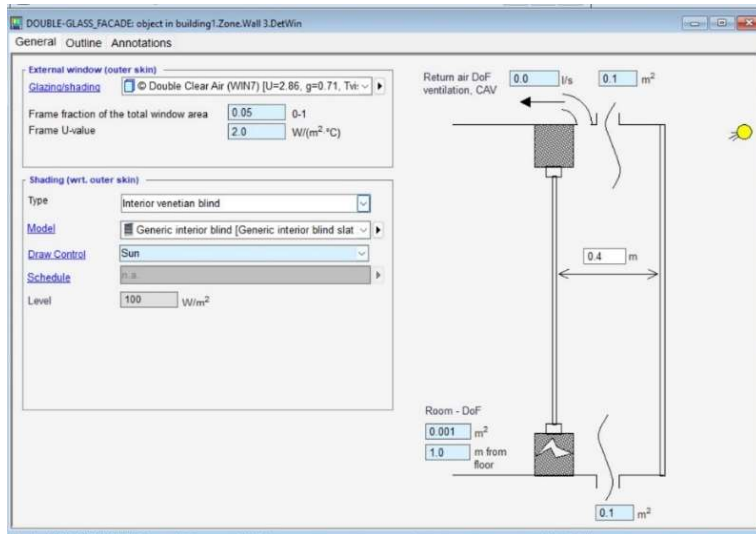


Figure 72: The form referred to the double glass façade component: here it is possible to define the properties of the external skin, the cavity and the integrated shading system.

Inside it the user can define the parameters related to:

- External skin glazing type
- Cavity depth
- Integrated shading (Venetian or roller blinds)
- Air paths between the different environments (Indoor environment, cavity and outdoor environment).

By default, 4 different air paths are considered inside the form:

- A leak at the floor level (bottom of the cavity) for the connection of the cavity itself with the outdoor environment.
- A leak at the ceiling level (top of the cavity) for the connection of the cavity itself with the outdoor environment.
- A leak between the room and the cavity, for which it is possible to set a given height. This leak represents the second connection between the indoor environment and the cavity of the double skin façade.
- A connection with the *HVAC* system of the linked thermal zone, assisted by a fan.

While the last opening can be directly expressed in terms of  $l/s$ , the first three air paths are expressed by default by means of the *equivalent* or *effective leakage area*  $A_{eff}$ . From this, it is possible to define the ventilation air flow through the opening using the following relation [32]:

$$Q = A_{eff} C_d \sqrt{\frac{2\Delta p}{\rho_{air}}}$$

Where:

- $C_d$  is the discharge coefficient, set equal to 1.
- $\Delta p$  is the pressure difference across the opening, set equal to 4 Pa.
- $\rho_{air}$  is the air density, set equal to 1.161 kg/m<sup>3</sup>.

Conventionally, the shading system of the double skin façade is defined as internal shading of the outer skin, using the *Shading* link in the *Double Glass Façade Form*. More details about the shading system can be defined in the dedicated section (Figure 73): slat material, spacing and width, ventilation gap, default slat angle and distance from the outer skin. The advanced control of the shading system (drawn mechanism and slat angle variation) can be implemented using the IDA ICE *Control Macro* in the *Drawn Control* link.

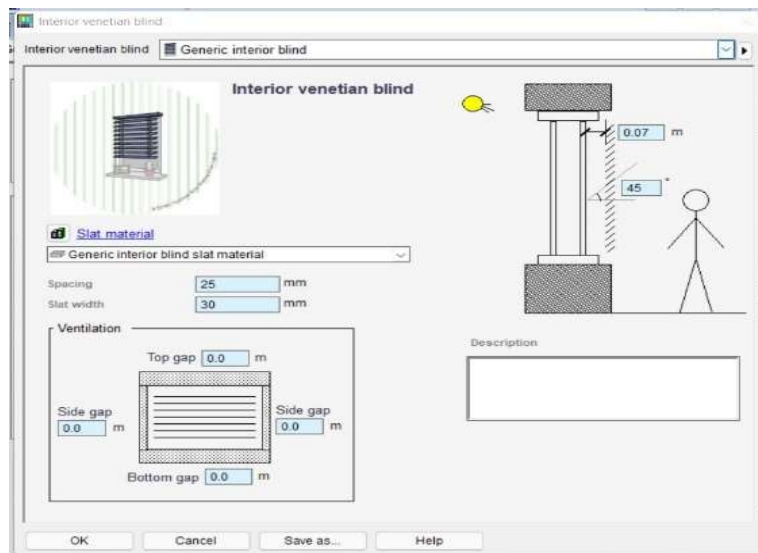


Figure 73: Definition of the shading system properties (in this case a venetian blind): materials, slat angle, distances.

Anyway, some additional modification of the standard *DSF* model in IDA ICE must be performed if more advanced control strategies must be implemented by the



designer (as in the case of this Master Thesis). The form dialog implemented in the graphic user interface, indeed, does not allow to specify more detailed information about the double skin characteristics.

For this reason, a more complex modelling approach is required. By creating the *Schematic* view of the double skin façade using the *Build Model* function in the *Simulation* tab of IDA ICE (Figure 74), it is therefore possible to view all the different modules that constitute the envelope and their connections with other building systems (for example the *HVAC* of the zone).

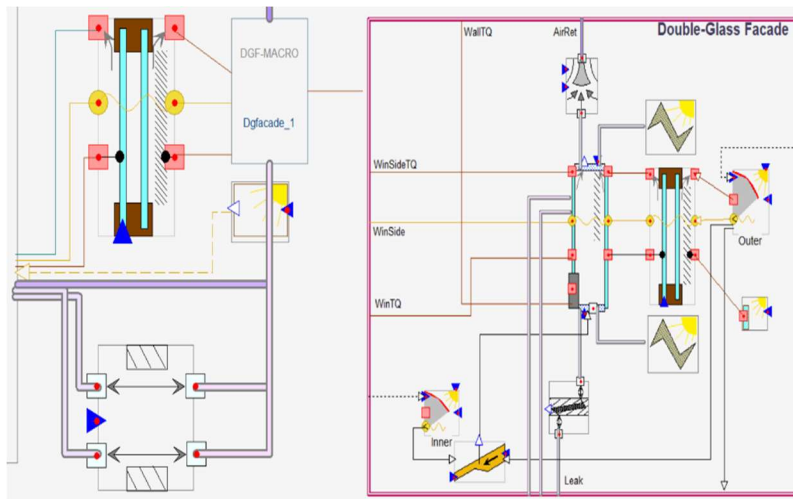


Figure 74: Schematic view of the double skin façade created on IDA ICE. On the left, it is visible the inner skin and the opening towards the zone, while on the right it is possible to see the ventilated cavity and the outer skin.

Whit this advanced interface, it is possible to customize the typologies and the interconnections of the different modules of the *DSF* according to the designer needs, enabling a more detailed modelling of the envelope system.

The most important modification, indeed, is the substitution of the leaks defined in the *Double Glass Façade Form* with some openings, that enable the possibility to implement an *open-closed* control using the IDA ICE *Control Macros* (Figure 75).

This approach has been developed and adopted by Elena Catto Lucchino in her PhD Thesis work and used also in this Master Thesis for the implementation of the rule-based control of the *DSF*.

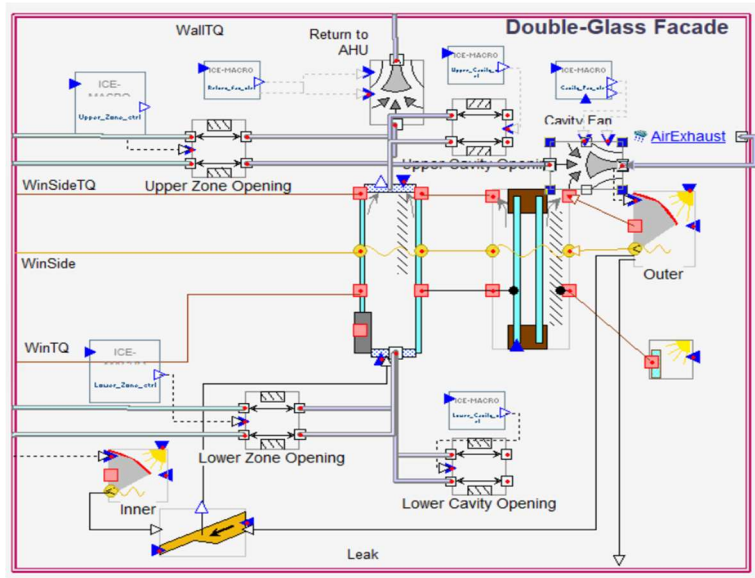


Figure 75: The modified configuration of the double skin façade system implemented inside IDA ICE

In this way, the connections of the cavity to the outdoor environment and the upper connection of the cavity to the linked zone can be assumed two different configurations (open and closed) according to the ventilation modes of the façade. The second step is the connection of the cavity with a fan that can be used for the implementation of the mechanical ventilation inside the cavity. As seen for the openings, the fan can be linked to a *Control Macro* that can manage its operations.

## Appendix D: Control implementation in IDA ICE

In this appendix, it is illustrated the implementation of the rule-based control inside the simulation environment IDA ICE. As illustrated in the *Appendix A*, IDA ICE offers advanced functionalities for the control implementation by using the so-called *Control Macros*. The Control Macros have been linked to the different actuators of the flexible *DSF* already described in *Appendix C*.

The *Control Macros* receive a certain input from an *interface*, linked to a specific variable of the model (for example, the indoor air temperature or the incident solar radiation), and defined a certain *output signal* (*On/Off* or *Open/Close* for example) that is send to an actuator.

Consequently, using the *Control Macros* it is possible to link a specific configuration of the double skin façade to a certain actuator state. Using the IDA ICE *Control Macros* it has been possible to define the decision trees illustrated in 2.3.1, 2.3.2 and 2.3.3: an example is reported in *Figure 76*.

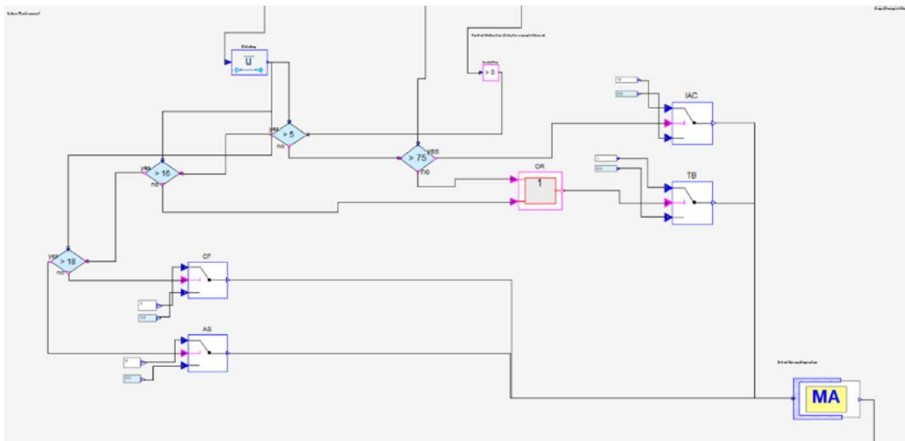


Figure 76: Example of decision tree for the cavity air flows built in IDA ICE

As explained in 2.2.4, the control targets of the façade system are 2:

- 1) Cavity air flows (openings and cavity fans)
- 2) Shading system (drawn mechanism of the blind and slat angle)

The 2 control targets are independent from each other and therefore their control is applied with the use of different *Control Macros* inside IDA ICE, as visible in *Figure 77*. Inside the two *Control Macros*, for the shading and the cavity air flows, the different decision trees of the control groups *SAC*, *WAC*, *SSC* and *WSC* have been defined.

In the *Control Macros* in particular it is possible to use a wide range of logical operators (*Modules*) that allow the construction of complex decision trees: the most largely used during the Thesis work are of course the *if-else* operators for the selection of the different configurations of the façade actuators.

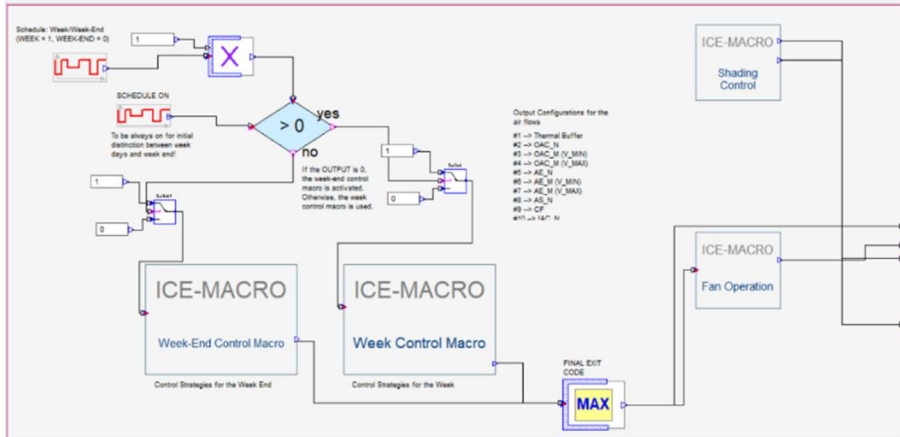


Figure 77: Control implementation for the cavity air flows (on the left) and the shading system (on the right) in the central Control Macro of the double skin façade

### Control Macros definition for the air flows

For the control of the cavity air flows, the involved actuators are:

- 1) The openings between the zone and the cavity
- 2) The openings between the cavity and the external environment
- 3) The return fan to the AHU
- 4) The cavity fan

The total number of involved actuators is consequently 6. To each one of the actuators, a certain state can be set in IDA ICE:

- 1) *Open* = 1, *Closed* = 0 for the openings
- 2) *On* = 1, *Off* = 0 for the fans
- 3) *VMIN* = 0, *VMAX* = 1 for the air flows generated by the fans if activated (respectively, a minimum and a maximum one).

As mentioned in 2.2.4 the total number of configurations for the double skin façade is 10 and to each one of them it is possible to assign a code from 1 to 10 (Table 43).

<i>Thermal buffer (CODE=1)</i>	<b>Facade actuator</b>	<b>State</b>
	Upper cavity opening	Closed
	Lower cavity opening	Closed
	Upper zone opening	Closed
	Lower zone opening	Closed
	Cavity fan	Off
	Return to the AHU	Off
<i>Outdoor Air Curtain (Natural) (CODE=2)</i>	<b>Facade actuator</b>	<b>State</b>
	Upper cavity opening	Open
	Lower cavity opening	Open
	Upper zone opening	Closed
	Lower zone opening	Closed
	Cavity fan	Off
	Return to the AHU	Off
<i>Outdoor Air Curtain (Mechanical) (CODE=3)</i>	<b>Facade actuator</b>	<b>State</b>
	Upper cavity opening	Open
	Lower cavity opening	Open
	Upper zone opening	Closed
	Lower zone opening	Closed
	Cavity fan	On (VMIN)
	Return to the AHU	Off
<i>Outdoor Air Curtain (Mechanical, increased air flow) (CODE=4)</i>	<b>Facade actuator</b>	<b>State</b>
	Upper cavity opening	Open
	Lower cavity opening	Open
	Upper zone opening	Closed
	Lower zone opening	Closed
	Cavity fan	On (VMAX)
	Return to the AHU	Off
<i>Air Exhaust (Natural) (CODE=5)</i>	<b>Facade actuator</b>	<b>State</b>
	Upper cavity opening	Open
	Lower cavity opening	Closed
	Upper zone opening	Closed
	Lower zone opening	Open
	Cavity fan	Off
	Return to the AHU	Off
<i>Air Exhaust (Mechanical) (CODE=6)</i>	<b>Facade actuator</b>	<b>State</b>
	Upper cavity opening	Open
	Lower cavity opening	Closed
	Upper zone opening	Closed
	Lower zone opening	Open
	Cavity fan	On (VMIN)
	Return to the AHU	Off
<i>Air Exhaust (Mechanical, increased air flow) (CODE=7)</i>	<b>Facade actuator</b>	<b>State</b>
	Upper cavity opening	Open
	Lower cavity opening	Closed
	Upper zone opening	Closed
	Lower zone opening	Open
	Cavity fan	On (VMAX)
	Return to the AHU	Off
<i>Air Supply (CODE=8)</i>	<b>Facade actuator</b>	<b>State</b>
	Upper cavity opening	Closed
	Lower cavity opening	Open
	Upper zone opening	Open
	Lower zone opening	Closed

<i>Climate Façade (CODE=9)</i>	Cavity fan	On
	Return to the AHU	Off
	<b>Facade actuator</b>	<b>State</b>
	Upper cavity opening	Closed
	Lower cavity opening	Closed
	Upper zone opening	Closed
	Lower zone opening	Open
	Cavity fan	Off
<i>Indoor Air Curtain (CODE =10)</i>	Return to the AHU	On
	<b>Facade actuator</b>	<b>State</b>
	Upper cavity opening	Closed
	Lower cavity opening	Closed
	Upper zone opening	Open
	Lower zone opening	Open
	Cavity fan	Off
	Return to the AHU	Off

Table 43: Exit codes for the DSF configurations and related actuators states

Therefore, to each actuator it is possible to associate a state in function of the number of the selected configuration (Table 44). The decision trees implemented inside IDA ICE provide some *exit codes* from 1 to 10, corresponding to the selected configuration for the double skin façade system.

The codes are then sent to the different façade actuators that in this way can change their state in accordance to the output of the decision tree.

Actuator	CODE	State	Actuator	CODE	State
Upper cavity opening	#1	Closed	Lower zone opening	#1	Closed
	#2	Open		#2	Closed
	#3	Open		#3	Closed
	#4	Open		#4	Closed
	#5	Open		#5	Open
	#6	Open		#6	Open
	#7	Open		#7	Open
	#8	Closed		#8	Closed
	#9	Closed		#9	Open
	#10	Closed		#10	Open
Lower cavity opening	#1	Closed	Cavity fan	#1	Off
	#2	Open		#2	Off
	#3	Open		#3	On (VMIN)
	#4	Open		#4	On (VMAX)
	#5	Closed		#5	Off
	#6	Closed		#6	On (VMIN)
	#7	Closed		#7	On (VMAX)
	#8	Open		#8	Off
	#9	Closed		#9	Off
	#10	Closed		#10	Off

<b>Upper zone opening</b>	#1	<i>Closed</i>	<b>Return to the AHU</b>	#1	<i>Off</i>
	#2	<i>Closed</i>		#2	<i>Off</i>
	#3	<i>Closed</i>		#3	<i>Off</i>
	#4	<i>Closed</i>		#4	<i>Off</i>
	#5	<i>Closed</i>		#5	<i>Off</i>
	#6	<i>Closed</i>		#6	<i>Off</i>
	#7	<i>Closed</i>		#7	<i>Off</i>
	#8	<i>Open</i>		#8	<i>Off</i>
	#9	<i>Closed</i>		#9	<i>On</i>
	#10	<i>Open</i>		#10	<i>Off</i>

Table 44: States of the different actuators in relation to each configuration code

The configuration number in each decision tree is define using the *Switch* module. If the conditions are respected, the number of the configuration is selected. In this way, each decision tree will have certain number of *exit codes*, but only one will be different from zero: it will be the selected configuration for the *DSF* system. In *Figure 78* it is visible the application of the *Switch* module inside the *SAC#1* decision tree. Only one code different from zero can be the output of the selected switch mechanisms: in this case the selection is between the codes 5, 6 and 7.

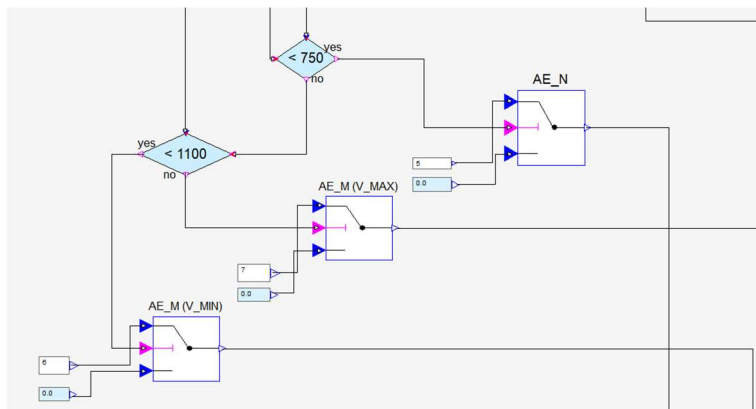


Figure 78: Example of switch modules at the end of a decision tree implemented in IDA ICE

For the selection of the code from the *Control Macro*, the *Max* module is adopted: being all the exit codes equal to zero except for the selected configuration, the final exit code will be always the greatest one. After the *Max* module, the *exit code* can be sent to the façade actuators.

In *Figure 79* it is showed the application of the *Max* module in the same decision tree: the *Max* modules receives all the exit codes sent by the *Switch* modules, defining in this way the output of the *Macro*.

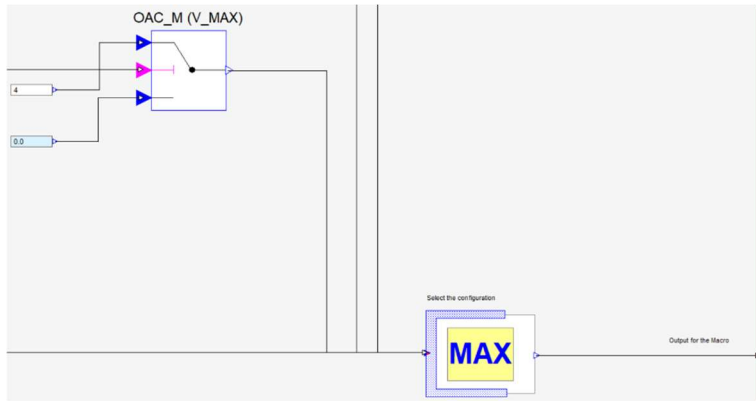


Figure 79: Application of the Max module for the definition of the output of the Macro

After the definition of the double skin façade configuration, it is necessary to associate the exit codes to a specific actuator state. For the definition of the related state, each actuator is associated with another *Control Macro*, which receives the exit code sent from the decision tree and by means of *Lessthan* and *GreaterEqual* modules define the related state of the façade actuator. In the case of the openings, the possible states defined by means of the *Control Macro* are 1 and 0, corresponding to the open and closed configurations.

The state also in this case is defined using a *Switch* module between 0 and 1. In *Figure 80* it is visible the application of this method in the case of the upper zone opening. Using the logical operators of IDA ICE the open state (corresponding to the number 1) is selected only if the exit code from the decision tree is 8 or 10. Otherwise, the opening is kept closed (corresponding to the number 0). For the fans in similar way the *On/Off* selection is performed using the codes 1 and 0 respectively.

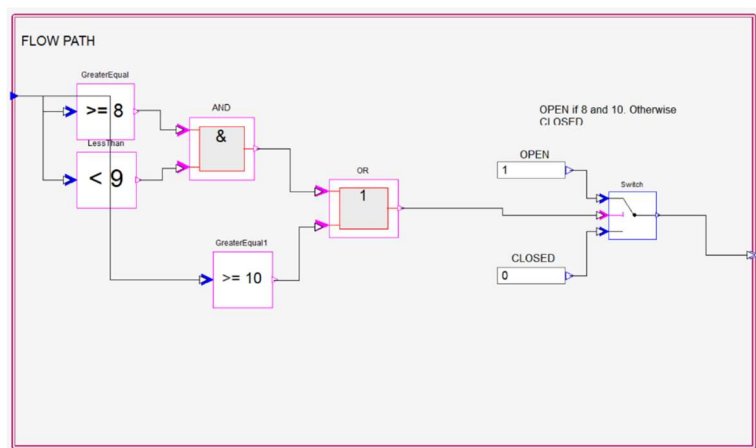


Figure 80: Definition of the actuators state in function of the decision tree



For the fans, an additional *Control Macro* defines the required air flow when the fan is on. In this way it is possible to also define the air flows in the cavity if the fan is in function. The selection of the air flows of the fan is sent to an additional *Switch* module that defines the velocity for the fan.

The *Multiplier* module in this case is used to consider a possible schedule of the fan: if the fan is turned off automatically because of a schedule, the code 1 is multiplied by zero and the resulting configuration of the fan is *Off*. In *Figure 81* it is showed the application of this system for the cavity fan activation.

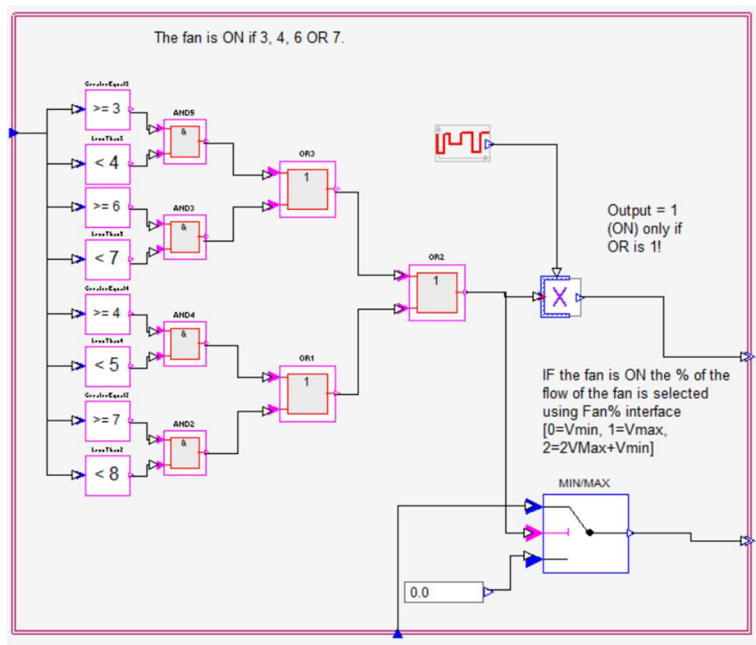


Figure 81: Definition of the fan configuration (on/off) and the related air flow (min/mx) inside the cavity fan Control Macro

### Control Macros definition for the shading system

As mentioned before, the control of the shading is focused on the drawn mechanism of the blind and the regulation of the slat angle.

Being the control of the shading system independent from the one of the cavity air flows, another *Control Macro* is adopted. The 2 outputs of the Control Macro are in this case the activation of the blind (1 for the drawn blind, 0 for the not drawn blind) and the slat angle (variable from  $0^\circ$  to  $90^\circ$ ). In *Figure 82* it is visible the implementation of the *WSC#3* control: the activation of the blind is performed by means of the temperature control, using the *Thermostat* module already present in IDA ICE.

If the blind is activated, the cut off position is implemented for the slats. The exact angle is calculated using the logical operators *Product* and *Add*, using the value of solar elevation angle for a given time step of the simulation. This variable is sent as input to the *Control Macro* using the *TAmb* link, related to the climate file of the selected location.

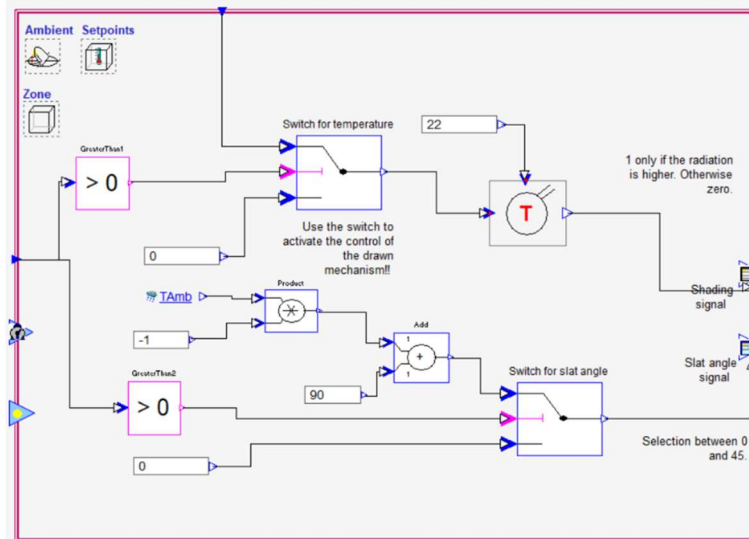


Figure 82: Use of the IDA ICE Control Macro for the application of the shading control

## Control of the AHU

Using the functionalities of the *Control Macros* it is also possible to connect the decision tree for the air flows control to the *AHU* components, in particular, the supply and return fans. When the façade is operating in *AE* configuration, the return fan can be switched off. On the other hand, when the façade is operating in *AS* configuration, the supply fan can be switched off. In the other configurations, the *AHU* can operate in accordance with the building operations. The control is implemented creating additional *Control Macros* in the standard one already implemented for the *AHU* in IDA. This additional control macro regulates the *On/Off* mechanism of the fans, in function of the exit code of the decision tree, and the required air flow (*VMIN* and *VMAX*).

To make the operations of the supply and the return fans independent, each fan is connected to a separate control macro, which defines the operations in function of the exit code of the decision tree. In *Figure 83* is reported the example for the return fan, for the summer configurations of the façade. The *On/Off* state is defined by means of a *Switch* module between 0 and 1. The presence of the occupancy schedule (0 for unoccupied periods, 1 for occupied ones) allows to consider the operational time of the fan during its control, using the *Multiplier* module.

When the façade is operating in the *AE* configurations, the supply fan is turned off, as it is possible to see from the selected exit codes (from 5 to 7). The velocity of the fans (*VMIN* and *VMAX*) is regulated using the occupancy schedule for the thermal zone.

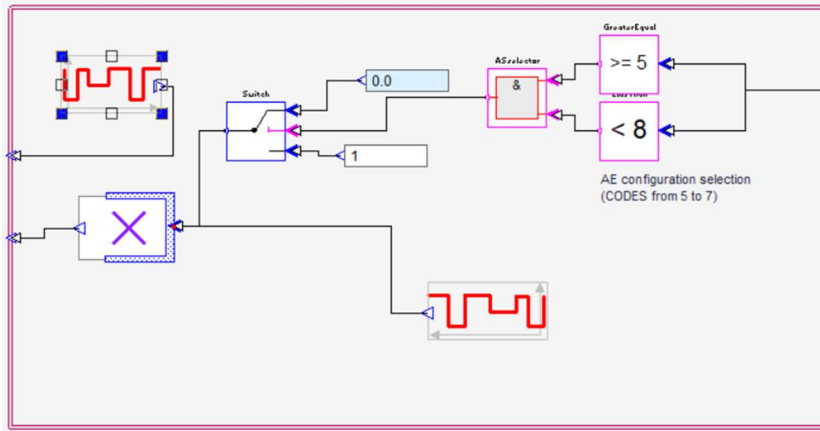


Figure 83: The Control Macro for the supply fan of the AHU

### Control Macros for the unoccupied hours

The distinction between control strategies for the occupied and unoccupied hours and for the working and weekend days is performed by means of schedules. Using the *Multiplier* module, it is possible to define if a given time step is inside an occupied time (code 1) or unoccupied one (code 0). Using the *If* module an activation signal (0 or 1) is sent to the control macros for the occupied and unoccupied hours. Only if the activation signal is positive, the control inside the *Control Macro* is activated and the blind state and the slat angle can be defined. Otherwise, the exit code for blind drawn mechanism and slat angle from the *Control Macro* is set null. In this way, using the *Max* module, it is possible to select the right configuration of the shading for a given time step. In *Figure 84* the application of this system is showed for the control of the shading during the working days in the winter season. The same approach has been adopted during the weekend to perform a distinction between night and daytime.

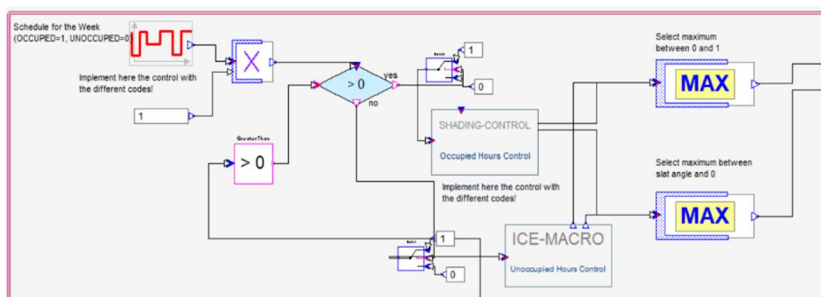


Figure 84: Distinction between the operating strategies for the shading system during the weekdays

## Resolution of possible numerical instabilities and too long simulation times

During the simulations of the control in IDA ICE, there could be possible problems caused by too long times required for the analysis. This can be caused by too frequent changes of the façade configurations, that modify the thermo-physical behavior of the system, increasing the computational effort required by the simulation environment. The main causes of a too frequent configuration change of the double skin façade are:

- High variability of the control variables during the simulation time (for example the cavity temperature of the *DSF*), that can increase the instability of the simulation
- Too narrow threshold limits of the control variables for the configuration switches of the façade actuators

The solution to the first problem is the use of the *Sliding Average* module (Figure 85): this module calculates the average of the selected control variable, referred to a previous period of time, defined by the user. The module has been used for example in the decision trees for the selection of the air flow configurations, for the calculation of the sliding average of the cavity air temperature used as control variable (both in summer and winter conditions). The selected time in this case is *900 sec (15 minutes)*. This solution can reduce in a significant way the time that is required for the simulation of the control decision tree, without affecting too much the results of the analysis performed on the model (the interval of time must be anyway short enough).

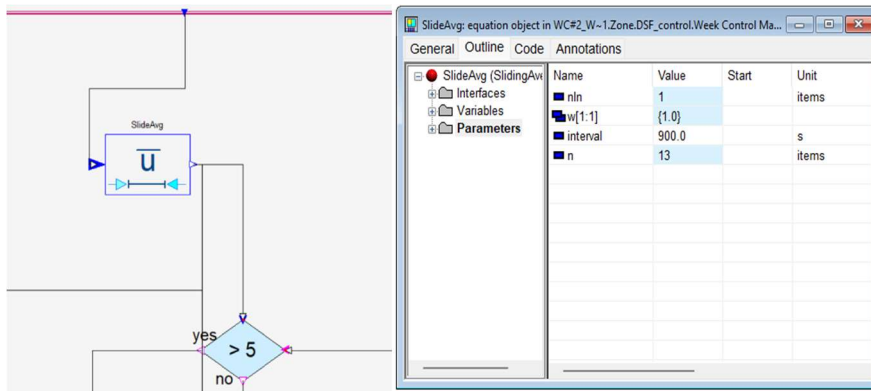


Figure 85: The Sliding Average module (left) and the definition of the interval parameter (right)

For the second problem, the only solution is the one to “enlarge” the distance between the different threshold limits of the control variables, avoiding in this way too fast changes in the façade configurations: also this option has been adopted, in case of too large simulation periods required by IDA ICE.

The *Sliding Average* operator have been used in other several cases during the definition of the *Control Macros*, the ensure proper simulation times for the different façade configurations.

### **Control Macros for the lighting system**

Following the same approach adopted for the other components of the model, also the control of the lighting can be defined (*Figure 86*): in this case, during the occupied hours, the light is turned off if the indoor illuminance levels on the working plane are below the limit of *500 lux*. Otherwise, during the unoccupied hours, the artificial lighting is turned off. Also in this case the *Sliding Average* operator have been used to calculate an average of the illuminance levels at the working plane, to reduce of a certain extent the required time for the different simulations.

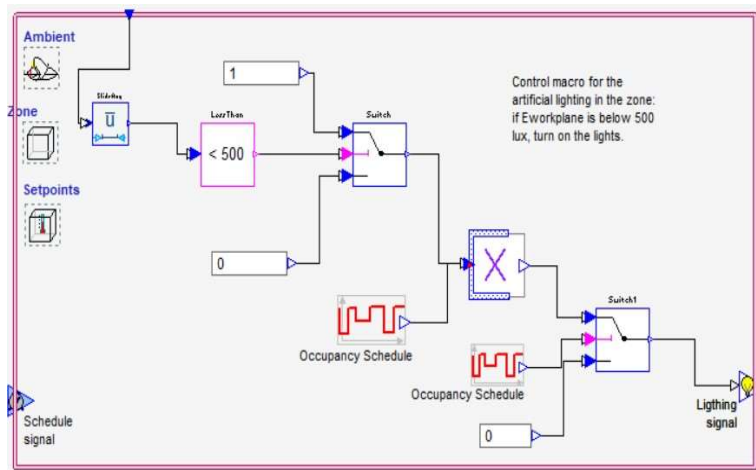


Figure 86: Definition of the control macro for the artificial lighting system of the room



## Sources and Bibliography

- [1] GABC, “Global Status Report for Building and Construction,” 2021.
- [2] GABC, “Global Status Report for Building and Construction,” 2016.
- [3] GABC, “Global Status Report for Building and Construction,” 2019.
- [4] F. Goia, “Towards an active, responsive and solar building envelope,” 2010.
- [5] A. Tabadkani, “A review of automatic control strategies based on simulations for adaptive facades,” 2020.
- [6] F. Favoino, “Experimental analysis of the energy performance of an Active, RESponsive and Solar (ACTRESS) façade module,” 2016.
- [7] F. Goia, *Energy efficient facades, Lecture from the course Integrtaed Energy Design, NTNU, Autumn 2021*, 2021.
- [8] F. Favoino, “Adaptive and responsive technologies, Lecture from the course Energy Performance Design and Indoor Environmental Quality, Politecnico di Torino, a.y. 2020/2021,” 2021.
- [9] F. Favoino, R. C. Loonen, M. Doya, F. Goia, C. Bedon and F. Babich, *Building Performance Simulation and Characterisation of Adaptive Facades*, 2018.
- [10] S.-H. Yoon, “Comparative study of static vs. dynamic controls of double-skin systems,” 2009.
- [11] C.-S. Park, “Integrated control strategies for double skin systems,” 2005.
- [12] H. Poirazis, “Double Skin Facades, a literature review,” 2006.
- [13] F. Favoino, «Quantifying performance of ABEs, Lecture from the course Energy Performance Design and Indoor Environmental Quality, Politecnico di Torino, a.y. 2020/2021,» 2021.
- [14] «EN ISO 7730:2005, Table A.5».
- [15] «EN 16798-1:2019, Table B.2».
- [16] «EN 12464-1:2011, Table 5.26».
- [17] «EN 17037:2018, Table E.1».

- [18] "TEK 17, Section 13.3".
- [19] "EN 16798-1:2019 Table B.10".
- [20] A. Jankovic og F. Goia, «Impact of double skin facade constructional features on heat transfer and,» 2021.
- [21] A. Gelesz, "Effects of shading control on the energy savings of an adaptable ventilation mode double skin facade," 2018.
- [22] W. Choi, "• Operation and control strategies for multi-storey double skin facades during the heating season," 2012.
- [23] C. Micono, "Double Skin Facades, Lecture from the course Energy Performance Design and Indoor Environmental Quality, Politecnico di Torino, a.y. 2020/2021," 2021.
- [24] S. B. Leigh, «A Study on Cooling Energy Savings Potential in High-Rise Residential Complex Using Cross Ventilated Double Skin Façade,» 2004.
- [25] S. Venosa, "Parametric simulation and dynamic control for a double skin facade," 2021.
- [26] "EN 16798-1:2019, Table B.9".
- [27] «EN 16798-1:2019, Appendix C».
- [28] "ISO 23045:2008, Annex C and D".
- [29] G. Pernigotto and A. Gasparella, "Classification of European Climates for Building," 2018.
- [30] «IDA ICE Climate File».
- [31] H.-P. Schettler-Köhler, "EPBD implementation in Germany," 2016.
- [32] EQUA, «IDA ICE User Guide».
- [33] ASHRAE, "Ventilation for Acceptable Indoor Air Quality," 2016.
- [34] EQUA, «IDA API User Manual».
- [35] M. Hamdy, Introducing Building performance simulations (BPS), Lecture from the course Building Performance Simulation, NTNU, Spring 2022.
- [36] E. C. Lucchino and F. Goia, "Reliability and Performance Gap of Whole-Building Energy Software Tools in Modelling Double Skin Façades," 2019.



- [37] E. C. Lucchino, "Modelling of double skin facades in whole-building energy simulation tools. A review of current practices and possibilities for future developments," 2019.
- [38] A. Gelesz, "Characteristics that matter in a climate façade: A sensitivity analysis with building energy simulation tools," 2020.
- [39] EQUA, "IDA Indoor Climate and Energy," 2022. [Online]. Available: <https://www.equa.se/en/ida-ice>. [Accessed 25 April 2022].
- [40] A. Bring, P. Sahlin and M. Vuolle, *Models for Building Indoor Climate and Energy Simulation*, Axel Bring, Per Sahlin, Mika Vuolle ((KTH Stockholm), 1999, 1999.
- [41] P. Sahlin, *NMF Handbook*, 1996.
- [42] P. Sahlin and A. Bring, *The NMF for BPS*, 1996.
- [43] M. Hamdy, "Getting started, IDA ICE Introduction, Lecture from the course Building Performance Simulation, NTNU, Spring 2022," 2022.
- [44] ARCHIVIBE, "Glass architecture: glazed facades in modern architecture," [Online]. Available: <https://www.archivibe.com/glass-architecture-glazed-facades-in-modern-architecture/>. [Accessed 28 04 2022].
- [45] *Encyclopaedia Britannica*, «International Style,» [Internet]. Available: <https://www.britannica.com/art/International-Style-architecture>. [Funnet 28 4 2022].
- [46] M. Roginska-Niesluchowska, "Use of Daylight and Aesthetic Image of Glass Facades in Contemporary Buildings," 2017.
- [47] J. Straube, «Can highly glazed building facades be green?,» 2008.
- [48] M. Abravesh, «A method to evaluate glare risk from operable fenestration systems throughout a year,» 2019.
- [49] K. Roth, T. Lawrence og J. Brodrick, «Emerging technologies: double skin façades,» 2007.
- [50] E. Lee, S. Selkowitz, V. Bazjanac, V. Inkarojrit and C. Kohler, "High-Performance Commercial Building Façades," 2022.
- [51] T. M. Boake, *Understanding the general principles of the double skin façade systems*, 2003.
- [52] F. Favoino, "Advanced Building Envelopes, lecture from the course Energy Performance Design and Indoor Environmental Quality, Politecnico di Torino, a.y. 2020-2021," 2021.

[53] *D. Saelens, "Energy performance assessment of single storey multiple-skin facades," 2002.*

[54] *W. Streicher, «Best practice for double skin facades: state of the art report,» 2005.*

[55] *A. Alberto, "Parametric study of double-skin facades performance in mild climate countries," 2017.*

[56] *E. Union, "EPBD – Directive 2002/91 – Recast – Directive 2018/844 and Regulation 2018/1999," 2018.*